ASSESSING THE IMPACTS OF CLIMATE CHANGE ON STREAMFLOW UNDER CMIP6 CLIMATE PROJECTION IN THE UPPER OMO GIBE RIVER BASIN, ETHIOPIA.

MSc THESIS

LEMLEM GETNET MOLA

HAWASSA UNIVERSITY, IOT,

HAWASSA, ETHIOPIA

MAY, 2023

ASSESSING THE IMPACTS OF CLIMATE CHANGE ON STREAMFLOW UNDER CMIP6 CLIMATE PROJECTION IN THE UPPER OMO GIBE RIVER BASIN, ETHIOPIA

LEMLEM GETNET MOLA

A THESIS SUBMITTED TO THE FACULTY OF BIO-SYSTEMS AND WATER RESOURCES ENGINEERING, DEPARTEMENT OF WATER RESOURCE AND IRRIGATION ENGINEERING

HAWASSA UNIVERSITY, INSTITUTE OF TECHNOLOGY
SCHOOL OF GRADUATE STUDIES
HAWASSA UNIVERSITY
HAWASSA, ETHIOPIA

IN PARTIAL FULFILLMENT OF THE REQUIREMENTS FOR THE DEGREE OF MASTERS OF SCIENCE IN WATER RESOURCE AND IRRIGATION ENGINEERING
(SPECIALIZATION: WATER RESOURCE ENGINEERING AND MANAGEMENT)

MAY, 2023

ADVISORS' APPROVAL SHEET

SCHOOL OF GRADUATE STUDIES

HAWASSA UNIVERSITY ADVISORS' APPROVAL SHEET

This is to certify that the thesis proposal entitled "Assessing THE IMPACTS OF CLIMATE CHANGE ON STREAMFLOW IN THE UPPER OMO RIVER BASIN, ETHIOPIA, UNDER CMIP6 RELEASE." submitted in partial fulfillment of the requirements for the degree of Master of "WATER RESOURCE ENGINEERING AND MANAGEMENT" the Graduate Program of the School of WATER RESOURCES AND IRRIGATON ENGINEERING and has been carried out by "LEMLEM GETNET MOLA" "ID.No. WREMR/0005/13", under our supervision. Therefore, we recommend that the student has fulfilled the requirements and hence here by can submit the proposal to the school of Water Resources And Irrigation Engineering.

Approved by:

Dr. Alemayehu Muluneh _____ _____

Name of the major advisor Signature Date

Dr. Tewodros Assefa _____ _____

Name of the co-advisor Signature Date

EXAMINER'S APPROVAL SHEET-I

HAWASSA UNIVERSITY

SCHOOL OF GRADUATE STUDIES

EXAMINERS' APPROVAL SHEET

As members of the Examining Board of the Final MSc Open Defense, we certify that we have read and evaluated the thesis prepared by Lemlem Getnet entitled "Assessing THE IMPACTS OF CLIMATE CHANGE ON STREAMFLOW IN THE UPPER OMO RIVER BASIN, ETHIOPIA, UNDER CMIP6 RELEASE.", and recommend that it be accepted as fulfilling the thesis requirement for the degree of Master′s of science in school of Water Resources and Irrigation Engineering with Specialization in Water Resource Engineering and Management.

Dr. Alemayehu Muluneh (Assist Prof)	_____	_____
Name of Major Advisor	Signature	Date
Mr. Teshale Tadesse (MSc)	_____	_____
Name of Internal Examiner II	Signature	Date
Dr. Ahmed Mohammed (Assist Prof)	_____	_____
Name of Internal Examiner I	Signature	Date
Dr. Sirak Tekleab (Assist Prof)	_____	_____
Name of External examiner	Signature	Date
_____	_____	_____
SGS Approval	Signature	Date

Declaration

I, Lemlem Getnet, declare that I am the author of the research paper titled "The Influence of Climate Change on Streamflow: A Case Study of the Upper Omo River Basin, Ethiopia, using the ARC SWAT Model." This work was conducted under the guidance of Dr. Alemayehu Muluneh and Dr. Tewodros Asseffa from the Department of Water Resource and Irrigation Engineering at Hawassa University Institute of Technology (IOT), as part of my Master's program. I confirm that this thesis is an authentic and original piece of work, and I have not previously presented it, nor will I present it, to any other university for a similar or any other degree.

Name: Lemlem Getnet Mola

Signature: _____

Date: _____

Acknowledgement

First and foremost, I would like to sincere thank the Almighty God, who made it possible, to begin and finish this work successfully. This day what God have done for me is really beyond what I can imagine.

I would like to extend my heartfelt appreciation to Dr. Alemayehu Muluneh, my main advisor, and Dr. Tewodros Asseffa, my co-advisor, for their unwavering guidance, encouragement, and motivation throughout the entire process, starting from the initial proposal writing to the final completion of my thesis. Numerous individuals have played a crucial role in the successful culmination of this study, and while it is difficult to acknowledge them all individually, their contributions are immensely valued. I am especially grateful to Nega Chalie for his invaluable guidance and support during the course of my thesis work.

I would like to express my gratitude and give special acknowledgment to the Ministry of Education (MoE) for awarding me a scholarship and providing financial assistance to complete my thesis.

I would like to express my gratitude to the National Meteorological Agency of Ethiopia (NMA) and the Ministry of Water, Irrigation, and Electricity (MoWIE), specifically the hydrology department, for generously providing me with the necessary data for my study, which included hydro-meteorological information, land use data, and soil shape files. Their assistance was invaluable, and I received this data without any financial obligation.

Lastly, but certainly not of lesser importance, I would like to express my sincere gratitude to all my relatives for their unwavering affection, support, and motivation, which acted as a wellspring of resilience during my time of academic pursuit.

Table of Contents

List of Tables

List of Figures

LIST OF Abbreviations and Acronyms

AOGCMS	Atmosphere Ocean General Circulation Model
AR4	Fourth Assessment Report
AR5	Fifth Assessment Report
AR6	Sixth Assessment Report
CC	Climate Change
CMIP3	Coupled Model Intercomparison Project Phase3
CMIP5	Coupled Model Intercomparison Project Phase5
CMIP6	Coupled Model Intercomparison Project Phase6
CRU	Climatic Research Unit
CORDEX	Coordinated Regional Climate Downscaling Experiment
DD	Dynamical Downscaling
DEM	Digital Elevation Model
EMIC	Earth system Models of Intermediate Complexity
EPA	Environmental Protection Agency
ESMs	Earth System Models
FAO	Food and Agriculture Organization
GCM	Global Climate Models
GHG	Green House Gas
HBV	Hydrological Byrans Valtenbalansavdelnng
HEC- HMS	Hydrologic Engineering Center- Hydrologic Modeling System
HRU	Hydrologic Response Units

IPCC	Intergovernmental Panel on Climate Change
LULC	Land Use/Land Cover
MoWE	Ministry of Water and Energy
NASA	National Aeronautics and Space Administration
RCM	Regional Climate Model
RCPs	Representative Concentration Pathways
SD	Statistical Downscaling
SHyFT	Statkraft Hydrologic Forecasting Toolbox
SRES	Special Report on Emissions Scenarios
SRTM	Shuttle Radar Topographic Mission
SSPs	Shared Socio-economic Pathways
SWAT	Soil and Water Assessment Tool
SWAT- CUP	Soil and Water Assessment Tool- Calibration and Uncertainty Program
TCFD	Task Force on Climate- Related Financial Disclosures
UNESCO	United Nations Educational, Scientific and Cultural Organization
UNFCCC	United Nations Framework Convention on Climate Change
USDA	United States Department of Agriculture
UTM	Universal Transverse Mercator
WXGEN	Weather Generator

Abstract

Climate Change is projected to have an impact on future streamflow in various watersheds. This study examined the impacts of climate change on streamflow in the Upper Omo River Basin using a Soil and Water Analysis Tool (SWAT). Projected climate variables (precipitation and temperature) ensemble of 5 Global Circulation Models (GCMs) were obtained from the World Climate Research Programme (WCRP), downscaled by the SDSM4.2 model and applied under the Shared Socioeconomic concentration pathways (SSP2-4.5) and (SSP5-8.5) scenarios. The downscaled SSPs data cannot be directly used to the hydrological model (SWAT) to simulate flow so, Distribution Mapping bias correction method was selected for this study. SWAT was calibrated and validated before it was used for simulation purpose. The performance measures R^2 and NSE for calibration (2000-2013) and validation (2014-2019) were 0.79 and 0.71 and 0.86 and 0.85 respectively. Mann-Kendall (MK) trend testing was used to determine if a change is statistically significant and to detect trends in temperature and precipitation. According to RCP4.5 and RCP8.5, the emission scenarios predicted significant increasing temperature, but significant decreasing precipitation. Streamflow was simulated for two consecutive periods from 2020 to 2045 and from 2046 to 2071 for both scenarios and compared with the base period from 2000 to 2019 to explore the impact of climate change on Streamflow. The results indicated that the basin is likely to experience increased temperatures and altered precipitation patterns, whereas overall annual flow was projected to be significantly decreasing under SSP2-4.5 and SSP5-8.5 emission scenarios in the mid and near future. These changes are likely to have major implications for water resources management in the region, particularly for agriculture, hydropower generation, and ecosystem services. The findings suggest the need for adaptive measures to address these impacts, including improved water management strategies and increased investment in climate-resilient infrastructure.

Key words: Climate Change, SSP, SWAT, Streamflow

1. INTRODUCTION

1.1. Background of the Study

Climate change refers to significant shift in the long-term mean values of weather variables that define Earth's local, regional, and global climates. These shifts are driven by a range of natural and human factors, including changes in solar radiation, volcanic activity, and greenhouse gas concentrations in the atmosphere. However, the overwhelming scientific evidence suggests that the primary cause of climate change in recent decades has been human activities, especially the burning of fossil fuels, deforestation, and other land-use changes (Melkamu *et al.* 2017). Climate change has a wide range of impacts on different natural and human systems, including changes in streamflow patterns(Abdo *et al*. 2009). The Intergovernmental Panel on Climate Change (IPCC), which is widely regarded as the leading authority on climate change, defines climate change as "a change in the state of the climate that can be identified (e.g., by using statistical tests) by changes in the mean and/or the variability of its properties and that persists for an extended period, typically decades or longer" (IPCC, 2014).

According to IPCC Fifth Assessment Report (AR5), the global mean temperature increases by 0.85^{o}c since1880 until 2012 (IPCC, 2014). These changes in global temperature have been accompanied by changes in climate in several ways. Change in precipitation implies greater risks of flooding and drought at many regions (Stocker, 2011). The changes in precipitation or melting snow and ice have most comprehensive impact on the hydrological system of many regions (Muluneh *et al,* 2019). The IPCC AR5 stated that if greenhouse gas emissions continued to rise at the current rate, global mean surface temperatures could increase by 2.6^{o}c to 4.8^{o}c by the end of the 21st century, compared to pre-industrial levels. This range was based on different scenarios of future greenhouse gas emissions and the associated climate sensitivity of the Earth's climate system.(IPCC, 2014).

Climate change can have significant impacts on streamflow patterns, affecting both the quantity and timing of water flow in streams and rivers. Changes in streamflow patterns due to climate change can have significant implications for water resources management. Water availability for agriculture, drinking water supplies, hydropower generation, and ecosystem maintenance can be affected (Ismail *et al*. 2020).

Nowadays, climate bring some changes on the hydrological cycle and its water balance. For instance, changes in temperature and precipitation that have direct impact on the processes of runoff production and Global warming increases heat waves, drought and change in rainfall pattern in which those changes will have a strong impact on availability and variability of fresh water. Accordingly, change in spatial and temporal availability of water resources that affects agricultural production, industry and urban development of the region. So, climate change is expected to have strong impacts on socio economic development in most continents of the world, particularly in developing countries where their economy is heavily dependent on agricultural production (Tigabu *et al*. 2021).

As African Development Report (2022) stated, climate change will have a strong impact on the function and operation of existing water infrastructures like hydropower, structural drainage, irrigation system and also on water management practices of river basins of Ethiopia. The water resource system of Ethiopia is highly affected by the population growth, deforestation, surface erosion, sediment transport and climate change impacts (UNDP *et al.* 2022).

According to the Ministry of Water Resource and Energy (2020), Omo Gibe River Basin is one of the main and important river basin in Ethiopia. The main river basins in which 80-90% of water resources of Ethiopia found are Abay (Blue Nile), Tekeze, Baro Akobo, and Omo Gibe in the west and south-western part of Ethiopia where the population is no more than 30 to 40 percent. On the other hand, the water resources available in the east and central river basins are only 10 to 20 percent whereas the population in these basins is over 60 percent (MoWE, 2020). The Upper Omo River Basin, a sub basin of Omo Gibe River Basin is experienced climate change which impacts streamflow of the basin. The objectives of this study were to assess future climate change trend and its impact on the streamflow using the most recent CMIP6 climate projection on the Upper Omo River Basin.

1.2. Statement of Problem

According to the Ministry of Water Resource and Energy (2020), climate change is the major problem in Omo Gibe river basin. The Omo Gibe River Basin holds significant importance as one of Ethiopia's main river basins. The Upper Omo River Basin, which is a part of the Omo Gibe River Basin, is currently dealing with a rising level of climate variability. This includes shifts in temperature and rainfall patterns that have the potential to cause changes in the flow of water within the basin. In essence, the region is experiencing the effects of climate change, which directly affects the streamflow in the basin. Climate change impacts, such as irregular rainfall patterns and temperature fluctuations, have a direct influence on the streamflow in the Upper Omo River Basin. These effects create difficulties for managing water resources, as the uneven distribution of rainfall can disrupt the availability of water for streamflow. Furthermore, changes in temperature can further impact the quantity of water accessible for streamflow. In areas that heavily depend on streamflow to fulfill their water needs, such as for irrigation or drinking water purposes, the fluctuations in streamflow can pose challenges in meeting the demands for water. Effective management of reservoirs, dams, and water diversions is necessary to address the impacts of erratic rainfall and guarantee an adequate water supply during dry periods (MoWE, 2020).

The majority of research conducted in the basin has involved combining hydrologic modeling with CMIP5 data from various Representative Concentration Pathways (RCPs) scenarios, in order to assess the impact of climate change on streamflow (Eromo *et al*. 2016; Yemsrach *et al.* 2012; Rafael *et al*. 2021). There was a noticeable absence of advanced climate models that belong to the new generation, which would have brought about substantial enhancements in our understanding of future climate variability and change. Additionally, the CMIP5 model had a coarse and lower spatial resolution, which didn't allow for a more detailed and better representation of regional climate features and processes. Moreover, the scenarios (RCP) used in CMIP5 rely on projections of future greenhouse gas concentrations, but they do not provide predictions on how climate change will specifically respond to socio-economic factors like population, economy, and energy alterations. As a result, studies that utilize hydrologic modelling integrated with the latest GCM dataset, Coupled Model Intercomparison Project Phase 6 (CMIP6), to fill in those gaps are crucial.(Worqlul et al., 2018).

1.3. Research Objective

1.3.1. General objective

The general objective of this study was to assess the impact of climate change on the stream flow of the upper Omo basin, under CMIP6 projections.

1.3.2. Specific objectives

The specific objectives of this study were:

- To assess the projected precipitation and temperature for two window periods (2020 – 2045 and 2046 – 2071) compared with a baseline period (1985-2019) under SSP2-4.5 and SSP5-8.5 scenario by using CMIP6 releases.
- To assess the historical and future climate trends of the Upper Omo river basin.
- To evaluate impacts of climate change on stream flow using SWAT hydrologic model.

1.4. Research Questions

- What are the projected changes in precipitation and temperature changes in the two window periods of 2020-2045 and 2046-2071?
- What are the climate change trends of temperature and precipitation in the Upper Omo river basin?
- What are the impacts of climate change on the stream flow under SSP2-4.5 and SSP5-8.5 in the near future (2020-2045) and mid future (2046-2071)?

1.5. Significance of the Research

Investigating climate change and its effects on hydrologic responses, specifically stream flow, is crucial in predicting the extent of changes in hydro-climatic conditions, which will ensure the sustainability of the river basin, proper management of the basin's water resources, and mitigation of potential damage caused by flooding and drought. This study utilize SWAT hydrologic model integrated with latest GCM dataset (CMIP6). The CMIP6 models provide data at much higher spatial resolutions than previous models, which is important for more detailed simulations and better representation of regional climate features and processes. This allows planners and decision makers to gain a deeper comprehension of the way climate change will impact particular regions, ecosystems, and communities. Additionally, CMIP6 incorporates new set socioeconomic scenarios called Shared Socioeconomic Pathways. These scenarios explore different potential future socioeconomic conditions including population growth, economic development and energy use. As a result, planners and decision makers can examine alternative futures and evaluate the potential consequences of different policy decisions. These investigations also aid in the implementation of suitable adaptations and mitigation measures to safeguard the water resources of the upper Omo river basin, taking into account potential climate change scenarios in the future.

1.6. Limitation of the Research

The impact of climate change on stream flow was assessed in this study, implying that land use or land cover will remain the same in the future. Regardless, land use or land cover in the basin is changing as a result of natural and human activities. Furthermore, the SSP scenarios are only used to calculate minimum, maximum, and precipitation values. As a result, the remaining climatic variables were assumed to be constant. Furthermore, the availability of data on the upper Omo basin is insufficient for the study, which reduces the accuracy of the results developed.

2. LITERATURE REVIEW

2.1. Global Climate Change Projection and trend

Climate is the synthesis of atmospheric conditions characteristic of a particular place in the long-term (Sead A., 2016). It is expressed by means of averages of the various elements of weather, and also the probabilities of other conditions, including extreme values. The United Nations Intergovernmental Panel on Climate Change (IPCC) is one of the international bodies that assess scientific, technical and socio-economic information concerning climate change, its potential effects and options for adaptation and mitigation. According to (IPCC, 2014) climate change is seen as a statistically significant variation in the mean state of the climate or in its variability persisting over an extended period, typically decades or longer. Therefore, climate change refers to a significant change in the average weather conditions experienced in a particular region or location. The changes could be seen with respect to a significant change in perceived temperature of the region, the amount of rainfall experienced in the region, duration of exposure of the ground to sunlight.

Globally, mean annual surface temperature has increased over the past century by 0.6° (IPCC, 2014). In the scientific community, there is a general consensus that this increase during the past 50 years can be attributed partly to Greenhouse Gas (GHG) emissions from human activity. Global Climate Models (GCMs), which are capable of providing credible projections of climate changes into the next 100 years, use a coarse global grid scale (IPCC, 2014). Temperature and precipitation trends, however, differ on a regional scale due to different feedbacks appearing from synoptic to local scales. This results in differing impacts at different regional scales. To date, impacts researchers have only had GCM scale output to help determine the impacts of climate change to species and ecosystems on a 50-100 year time scale.

As climate varies or changes because of human and other induced factors, several direct influences alter precipitation amount, intensity, frequency, and type (Trenberth, 2012). Warming accelerates land-surface drying as heat goes into evaporation of moisture, and this increases the potential incidence and severity of droughts, which has been observed in many places worldwide (Dai, 2011).

According to (IPCC, 2007) report eleven of the last twelve years (1995-2006) rank among the twelve warmest years in the instrumental record of global surface temperature (since

1850). The linear warming trend over the 50 years from 1956 to 2005 0.13ºc [0.10 to 0.16] ^{0}c per decade is nearly twice that for the 100 years from 1906 to 2005. Recently the temperature increase is widespread over the globe. Increases in sea level are consistent with warming. Global average sea level rose at an average rate of 1.8 [1.3 to 2.3] mm per year over 1961 to 2003 and at an average rate of about 3.1 [2.4 to 3.8] mm per year from 1993 to 2003 (IPCC, 2007). There is very high confidence, based on more evidence from a wider range of studies, that recent warming is strongly affecting hydrology, ecosystem and fresh water availability. With respect to Observational evidence's gained from all continents and most oceans shows that many natural systems are being affected by regional climate changes, especially temperature increases.

Climate change is caused by natural and anthropogenic processes including the chain from GHG emissions to atmospheric concentrations to radiative forcing to climate responses and effects. The GHG emissions resulting from the provision of energy services have contributed significantly to the historic increase in atmospheric GHG concentrations (IPCC, 2014). The IPCC Fourth Assessment Report (AR4) concluded that ―Most of the observed increase in global average temperature since the mid-20th century is very likely due to the observed increase in anthropogenic greenhouse gas concentrations. As very well know carbon dioxide (CO_2) is the most important anthropogenic GHG. Its annual emissions have grown between 1970 and 2004 by about 80%, from 21 to 38 Gigatonnes (Gt), and represented 77% of total anthropogenic GHG emissions in 2004. The rate of growth of CO_2 -eq emissions was much higher during the recent 10-year period of 1995-2004 (0.92 $GtCO_2$ -eq per year) than during the previous period of 1970-1994 (0.43 $GtCO_2$ -eq per year) (IPCC, 2007).

2.2. Climate Change Studies in Ethiopia

Ethiopia, like many African nations, has experienced increased temperatures in the last century. Furthermore, the impact of human-induced climate change is projected to cause even more warming in Ethiopia during the next century, at unprecedented rates (EPA, 2021). Over the last forty years, Ethiopia has experienced a gradual rise in its average annual temperature, with an increase of 0.37°C per decade. This rate is slightly lower compared to the average global temperature increase. According to Eromo, there is an overall increasing trend in future annual temperature and significant variation of monthly and seasonal precipitation from the base period 1985–2005. Also, the annual potential evapotranspiration

shown increasing trend for future climate change scenarios in the southern part of the country.(Eromo *et al*. 2016)

As, (Kassie *et al.*, 2014) stated, Ethiopia is experiencing a notable rise in its average annual temperature, which is resulting in increased evapotranspiration and higher water requirements for crops. This exacerbates the existing water stress that crops already face. Projections for the future indicate that the mean maximum temperature in Ethiopia will increase by approximately 2-2.3°C by 2030 and 2.2-2.7°C by 2050. Additionally, the mean minimum temperature is expected to rise by about 0.8-0.9°C by 2030 and 1.4-1.7°C by 2050. These temperature changes will coincide with more hot days and nights and a decrease in cold days and nights. The upcoming precipitation forecast indicates both an increase and a decrease. Climate change has been extensively studied in relation to the Ethiopian climate, especially due to the significant impact it has on rain-fed agriculture, which relies heavily on the quantity and consistent timing of seasonal rainfall (Bishaw, 2012). A study in East and West Hararghe zone that was done by Teshome *et al*., (2022) reported that A significant increasing trend in rainfall and temperature are projected compared to the baseline period for most of the districts studied. This implies a need to design climate-smart crop and livestock production strategies, as well as an early warning system to counter the drastic effects of climate change and variability on agricultural production and farmers' livelihood in the region. The importance of studies like this are important because rainfall and temperatures are the most fundamental climate parameters that determine the environmental condition of a particular region and a small mean change in those climate parameters threatens food production, especially in low-income and agriculture based economies (Kumar & Raj Gautam, 2014).

The IPCC findings indicate that developing countries, like Ethiopia, are likely to face greater susceptibility to the effects of climate change. This could have significant consequences for Ethiopia due to several factors, with a primary concern being the country's heavy reliance on agriculture as a key component of its economy. Given that a substantial portion of Ethiopia's population is highly vulnerable to climate change, it becomes especially important to prioritize the implementation of adaptation strategies within the overall program, particularly to address the challenges posed by inter-annual variations. (IPCC, 2014)

2.3. Climate Change impacts on Stream Flow

Water is involved in all components of the climate system. Climate change has a strong and comprehensive effect on water resource of the region particularly on stream flow. For instance an increase in the air temperature will cause water temperatures to increase as well. As water temperatures increase, water pollution problems will increase, and many aquatic habitats will be negatively affected. Moreover, it increases rates of evapotranspiration from water bodies, resulting in shrinking of some water bodies such as the Great Lakes and also it causes drought. Therefore, it is very important to make evaluations of the expected impact on the stream flow and water resources due to expected climate changes regardless of the direction of the change(Lai *et al*., 2012).

Changes in stream flow can directly influence the supply of drinking water and the amount of water available for irrigating crops, generating electricity and other needs. In addition, many plants and animals depend on stream flow for habitat and survival. Stream flow naturally varies over the course of a year. For example, rivers and streams in many parts of the country have their highest flow when snow melts in the spring and their lowest flow in late summer. The amount of stream flow is important because very high flows can cause erosion and damaging floods, while very low flows can diminish water quality, harm fish and reduce the amount of water available for people to use. The timing of high flow is important because it affects the ability of reservoir managers to store water to meet needs later in the year. In addition, some plants and animals (such as fish that migrate) depend on a particular pattern of stream flow as part of their life cycles (EPA, 2021).

The effects of climate change on stream flow vary depending on the unique characteristics of each watershed. Understanding how climate change impacts stream flows, soil moisture, groundwater, and other hydrological factors involves examining projections of global-scale climatic variables such as precipitation, temperature, humidity, and mean sea level pressure. Many climate change models for Ethiopia suggest minimal or slight increases in rainfall, although some models indicate both increases and decreases. Overall, climate change is unlikely to significantly affect average water availability. However, it is expected to lead to greater temporal variation in river flows in the future.(Bishaw, 2012)

2.3.1. Impacts of Climate Change on Streamflow in Ethiopia

Impact of climate change on streamflow has been carried out in several basins in Ethiopia. For example, a study of climate change impact in Omo Gibe basin by Bishaw, (2012)reported the existence of significant variation in the seasonal and monthly streamflow due to impact of future climate change projection. The study indicated that monthly streamflow is likely to decrease by up to 23.55% in the 2020s and increase by up to 33.43% in the 2050s. In the main rainy, season (June-September). However, the runoff will be reduced by 21.67% in the 2080s. Seasonal flow may show increase up to 18.72% in Bega and 12.87% in Belg. However, Kiremt season show decrease up to 17.59%. The result from different scenario also indicates that the catchment is sensitive to climate change. Similarly, Eromo *et al*., (2016) investigated the future impacts of climate change on surface hydrological processes of Omo-Gibe river basin and found out that an overall increasing trend in future annual temperature and significant variation of monthly and seasonal precipitation against the base period 1985–2005. The study also showed the annual potential evapotranspiration increase for future climate change scenarios. Similarly, the surface water decreases in terms of mean monthly discharge in the dry season and increases in the wet season. The percentage change in future seasonal and annual hydrological variables were shown increasing trends.

2.4. Climate Models in Climate Change Studies

Climate models are a mathematical representation of the climate system depend on physical, biological and chemical principles and they are an essential tool for assessing the response of the climate system to various forces(Kattsov *et al.,* 2013). As described by (Knutti and Hegerl, 2008), Climate models consist of a set of equations that are discretized on a grid and solved numerically on a large computer. Some equations are derived from first principles (e.g. equations of motion, and conservation of energy, mass and angular momentum), but many processes have to be parameterized in a simplified form. The equations derived from these laws are so complex that they must be solved numerically. For the parts of the model governed by fundamental equations (e.g. the equations of motion), increased computational capacity and thus finer resolution will improve the simulation (Masamba, 2018). Many climate models have been developed to understand the level of climate change in response to the emission of greenhouse gases (GHG). Population growth and living standards like, energy and land use are the main drivers of anthropogenic GHG emissions and the

representative concentration pathways (RCPs) are projections of GHG concentrations based on these factors. The RCP2.6 is for strict mitigation scenario, RCP4.5 and RCP6.0 are for two intermediate mitigation scenarios and RCP8.5 is for very high GHG emissions. (Jarraud and Steiner, 2012)

Modern climate models are composed of a system of interacting model components, each of which simulates a different part of the climate system. There are several climate models identified by IPCC for impact assessment studies (IPCC, 2014). But there is no single model which is appropriate for all purposes. Model used in climate research differ from simple energy balance models to complex earth system models (ESMs) (Goosse, 2019). The climate models stated below are models that are evaluated in the IPCC's Fifth Assessment Report (AR5).

2.5. Climate Model Downscaling

Downscaling is a method that derives regional to local- scale (10 to 100 km) information from larger-scale models or data analyses. By definition, downscaling of climate projections is the process of transferring general circulation model (GCM) output to a finer spatial scale that is more meaningful for analyzing local and regional climate conditions (Brekke *et al.,* 2009). Basically downscaling is a method to obtain high-resolution climate or climate change information from relatively coarse-resolution GCMs. Justification for downscaling is easy to find. Downscaling techniques have been designed to bridge the gap between the information that the climate modeling community can currently provide and that required by the impacts research community. Anthropogenic global climate change would lead to changes in large-scale atmospheric features. However, the effect of large scale feature changes on local surface climate cannot be resolved in the current generation of GCMs, which introduces the need for downscaling (Jain, 2012). Many impact models require information at scales of 50 km or less, so some method is needed to estimate the smaller-scale information. Downscaling tries to obtain observed small- scale (often station level) variables and using larger (GCM) scale variables, using either regional climate models, analogue methods (circulation typing), regression analysis, or neural network methods (Jain, 2012).

Two broad categories of downscaling procedures currently exist: Dynamical Downscaling (DD) techniques and statistical (or empirical) downscaling (SD) (Hewitson and Crane, 1996).

2.5.1. Dynamical downscaling

Dynamical downscaling relies on the use of a regional climate model (RCM), similar to a GCM in its principles but with high resolution. RCMs take the large-scale atmospheric information supplied by GCM output at the lateral boundaries and incorporate more complex topography, the land-sea contrast, surface heterogeneities, and detailed descriptions of physical processes in order to generate realistic climate information at a spatial resolution of approximately 20–50 kilometers (Schnarr, 2014).Since the RCM is nested in a GCM, the overall quality of dynamically downscaled RCM output is tied to the accuracy of the large-scale forcing of the GCM and its biases (Kidmose et al., 2013).

Regional climate models (RCMs)

A regional climate model is similar to a global climate model in that it simulates the physical processes in the climate system. Regional climate models cover a limited area of the globe and are run at much finer spatial resolution – 1-50 km grid spacing as opposed to 100-300 km grid spacing in a global model – thus they can simulate the interactions between large scale weather patterns and the local terrain. Global model output data are used to force the regional model at its boundaries and the regional model downscales the global model by producing fine-scale weather patterns consistent with the coarse-resolution features in the global model. The disadvantages of a regional climate model are that it is computationally expensive and cannot explicitly remove systematic differences (biases) between the global model and observations as statistical methods can. Thus, for many applications, some bias correction must be applied to the results, to remove the combined biases of the global and regional model.(Qian and Zhang, 2006) RCMs have become a critical component in the end-to-end assessment, or prediction system, where RCM bridges the spatial gaps between the GCM and other modeling components such as hydrological models that require regional climate information (Walthall *et al.*, 2013).

2.5.2. Statistical downscaling

Statistical downscaling involves the establishment of empirical relationships between historical and/or current large-scale atmospheric and local climate variables. Once a relationship has been determined and validated, future atmospheric variables that GCMs project are used to predict future local climate variables. Statistical downscaling can produce site-specific climate projections, which RCMs cannot provide since they are computationally limited to a 20–50 kilometers spatial resolution (Trzaska and Schnarr, 2014). However, this approach relies on the critical assumption that the relationship between present large scale circulation and local climate remains valid under different forcing conditions of possible future climates(Trzaska and Schnarr, 2014). It is unknown whether present-day statistical relationships between large- and regional-scale variables will be upheld in the future climate system. Since statistical downscaling methods rely on the assumption of an unchanged statistical relationship, they require long historical climate observation data for validation, which is not always available for every region (Anh and Taniguchi, 2018).

2.6. Bias Correction Method

The outputs of both Global and Regional Climate Models have a systematic error (biases). For instance, sometimes climate model have too many rainy days which underestimates rainfall extremes. Moreover, There can be errors in the timing of the monsoon or the amount of seasonal rainfall, or temperatures can be consistently too high or too low. Range of factors can cause an error in climate models. Errors or biases are caused by limited spatial resolution (large grid sizes), simplified thermodynamic processes and physics or incomplete understanding of the global climate system. Thus, the use of uncorrected outputs in impact models or climate impact assessments can often give unrealistic results. To overcome the large biases in climate models, a range of bias correction methods have been developed. For all methods it is important to realize that the quality of the observational datasets determines the quality of the bias correction. To do a good bias correction, it is important to have a good dataset of observations. If correcting extreme precipitation, then long-term data sets are needed (Copernicus, 2019).

2.6.1. Distribution mapping for bias correction

Distribution mapping adjusts the individual values of the model output such that their statistical distribution matches that of the observed data. This is accomplished by the method of Panofsky and Brier (1968), which constructs a transfer function that transforms modeled values into probabilities via the CDF (cumulative distribution function) of the model distribution and then transforms them back into data values using the inverse CDF (or quantile function) of the observational distribution (Panfosky, 1968):

$$X_{corrected} = \text{transfer}\ (x_{raw}) = CDF^{-1}\ \text{observed}\ (CDF\text{model}\ (x_{raw})).$$

2.6.2. Linear scaling for bias correction

Linear scaling method (Lenderink *et al.*, 2007) adjusts rainfall and temperature of RCM simulation using multiplicative and additive factors, respectively. The factors are developed by comparing the observed data with the corresponding historical RCM simulations. Linear scaling method corrects biases in mean but has limitations in correcting biases in probability of wet-days and intensities.

2.6.3. Power Transformation for bias correction

Power transformation method reproduce the standard deviation, coefficient of variation (CV), wet-day frequencies and intensities of rainfall based on observed data (Leander and Buishand 2007). In power transformation, daily rainfall of RCMs is changed into a corrected rainfall through fitting the CV of the corrected daily RCM rainfall with the CV of observed daily rainfall for each month. Parallel to power transformation, variance scaling was used to fit RCM simulation of temperature (Chen *et al.,* 2011).

2.7. Climate Scenario

Climate change scenario refers to a plausible future climate that has been constructed for explicit use in investigating the potential consequences of anthropogenic climate change. Such climate scenarios should represent future conditions that account for both human-induced climate change and natural climate variability. We distinguish a climate scenario from a climate projection, which refers to a description of the response of the climate system to a scenario of greenhouse gas and aerosol emissions, as simulated by a climate model. Climate projections alone rarely provide sufficient information to estimate future impacts of climate change. model outputs commonly have to be manipulated and combined with observed climate data to be usable, for example, as inputs to impact models (R.Leemans *et.al,* 2015).

The basis for all climate scenarios for use in adaptation assessments are projections of climate change from Global Climate Models (GCMs). (Clearly, this is not the same as saying that all adaptation studies require climate scenarios.) These climate projections depend upon the future changes in emissions or concentrations of greenhouse gases and other pollutants (e.g. Sulphur dioxide), which in turn are based on assumptions concerning, e.g., future socio-economic and technological developments, and are therefore subject to substantial uncertainty (Richard Jones *et.al,* 2003).

2.7.1. Shared Socio-economic Pathway emission scenarios

An important component (forcing) of the climate is the emission of greenhouse gases GHG) and consequently GHG forcing is also an important component of the numerical simulation of the climate. There are two sources of data for these emissions. First, for the past, emissions inputs come from observations made at different stations around the globe. Second, for the

future, the evolution of greenhouse gases is obtained from what are called emissions scenarios. Emissions scenarios describe plausible future releases of greenhouse gases, aerosols and other anthropogenic gases into the atmosphere. They are based on a coherent and internally consistent set of assumptions about driving forces, such as technological change, demographic and socioeconomic development and their key interactions (IPCC, 2014).

Emission scenario development is a process that occurs in parallel with the development of climate models. Teams of researchers are dedicated to evaluating how emissions will evolve in the future and these scenarios are then used to run climate models in order to produce simulations of future climate, each dependent upon a given emissions scenario. The Sixth Assessment Report (AR6) of the Intergovernmental Panel on Climate Change (IPCC), released in 2021, uses the new climate model in CMIP6, in which the new emission scenario driven by different socio-economic models, the shared socioeconomic pathways (SSPs), replaces the representative concentration pathways (RCPs) in CMIP5. As an important part of the new generation of climate change scenarios, SSPs look at five different development models of future economic and social system development, reflecting the relationship between radiation forcing and socioeconomic development. If SSPs are set from the perspective of mitigation and adaptation challenges faced by the future social economy, they can be divided into **five** paths (Sun *et al.* 2022).

1. **SSP1-2.6**

The SSP1-2.6 scenario describes a world with sustainable development and low climate change challenges. SSP1-2.6 is upgraded from RCP 2.6 in CMIP5 model. The SSP1-2.6 scenario in the CMIP6 is low-force, representing the combined effects of low social vulnerability, low mitigation pressure, and low radiative forcing (Sun *et al*. 2022).

2. **SSP2-4.5**

The SSP2-4.5 scenario looks at a middle of the road world, that is, social, economic, and technological trends do not deviate significantly from historical patterns and face moderate climate change challenges. The SSP2-4.5 scenario is intermediate, representing a combination of medium social vulnerability and medium radiation coercion. SSP2-4.5 is upgraded from RCP 4.5 in CMIP5 model (Sun *et al.* 2022).

3. **SSP3-7.0**

The SSP3-7.0 scenario is a medium-high reference scenario presents the worst development direction that society must avoid or prepare to deal with. SSP3-7.0 scenario is the one with the highest methane and air pollution precursor emissions (Sun *et al.* 2022).

4. **SSP4**

The SSP4 scenario involves intra-regional and external inequality, with low challenges to be mitigated but large challenges to be adapted (Sun *et al.* 2022).

5. **SSP5-8.5**

The SSP5-8.5 features a high-speed development pattern promoted at the cost of a large amount of fossil fuels. The SSP5-8.5 scenario is high-force, representing the combination of high social vulnerability and high radiative forcing, and it is the only path to achieve the man-made radiative forcing level of 8.5 W m−2 by 2100 (Sun *et al.* 2022).

2.7.2. Coupled Model Intercomparison Project Phase6 (CMIP6) Release

New simulations from the latest state-of-the-art climate models participating in phase 6 of the CMIP (CMIP6) are now available (V. EYRING *et al.* 2017). These simulations provide a new opportunity to evaluate the Earth system response to change in radiative forcing's during the twenty-first century. The CMIP6 models are typically enhanced versions of the models that participated in earlier phases of CMIP. Most have improved parameterizations of cloud microphysics and better representations of various Earth system processes, such as biogeochemical cycles and ice sheets. The average resolution of CMIP6 GCMs is also finer than that of CMIP5 GCMs (V. EYRING *et al.* 2017)

The sixth phase of the Coupled Model Intercomparison Project (CMIP6) dataset is used to examine projected changes in temperature and precipitation over the world. CMIP6 involves over 100GCMs. CMIP6 output includes historical climate projections or reference period for the years 1850-2014 and climate projections for three future window periods near term(out to about 2035), midterm(2035-2060) and long term(out to 2100 and beyond) under five Shared Socio-economic Pathways (SSPs). Some of the GCM models in CMIP6 are ACCESS-CM2, CESM2, CMCC-ESM2, MIROC6, CanESM5, EC-EARTH3, HadGEM3-GC31-HH, NESM3, MRI-ESM2-0, ARTS-2-3, BCC-CSM2-HR and others. The most appropriate models from those are selected based on resolution (the model with higher

resolution), validity (the GCM model that simulate the present day climate most faithfully) and representativeness (if more than one GCM applied in an impact assessment).

2.8. Current and Future Climate Trend Analysis

Climate change may lead to alterations in the dynamics of climatic variables. These changes can have tremendous effects for food, energy and water supply in particular in developing countries. The release of the Intergovernmental Panel on Climate Change (IPCC) Fourth Assessment Report has brought the issue of climate change and climate trends to the forefront of scientific and political communities. Investigations of regional and global climatic changes and variability and their impacts on the society have designed and operated based on the historical pattern of water availability, quality and demand assuming constant climatic behavior(Desalegn and Brook, 2019).

There are many studies analyzing the trends and the variability of meteorological variables in different parts of the world. For example, (Miller and Piechota, 2008)studied regional analysis of trend and step changes observed in meteorological variables around the Colorado River Basin. Their results indicated that temperature increased persistent throughout the year across the Colorado River Basin whereas rainfall only notably increased in a few climate divisions during February and remained relatively unchanged. Similarly Abdul Aziz and Burn studied trends and variability of the hydrological regime in the Mackenzie River Basin in northern Canada over different time periods. Their results indicated an increasing trend for temperature in winter and spring. Though, rainfall data exhibit a less well-defined trend (Burn *et.al*, 2004).

2.8.1. Current and Future Climate Trend Analysis Studies in Ethiopia

There are also some studies on the variability and trends of extreme rainfall events in different parts of Ethiopia. The study by Shang and Yan analyzed trends of rainy days and identified statistically significant declining trends for the wet day intensity and maximum consecutive five-day rain over eastern, southern and southwestern parts during Kiremt (main rainy season) and the Belg (small rainy season) but no significant changes for other parts of the country (Shang *et al.*, 2011). The study by Kebede and Bewket conducted in the southwestern part of Ethiopia, which is the wettest part of the country, identified generally a decreasing trend in annual rainfall (Kebede & Bewket, 2009). Similarly (Funk, *et al.*, 2012), indicated the presence of a weak rising rainfall trend in the arid lowlands of southern

and southeastern Ethiopia and declining trends over the southwestern highlands and Sudan border. A study in East and West Hararghe zone that was done by Teshome *et al*., (2022) reported that A significant increasing trend in rainfall and temperature are projected compared to the baseline period for most of the districts studied. This implies a need to design climate-smart crop and livestock production strategies, as well as an early warning system to counter the drastic effects of climate change and variability on agricultural production and farmers' livelihood in the region. The importance of studies like this are important because rainfall and temperatures are the most fundamental climate parameters that determine the environmental condition of a particular region and a small mean change in those climate parameters threatens food production, especially in low-income and agriculture based economies (Kumar and Raj Gautam 2014).

2.9. Climate Trend Analysis Methods

2.9.1. Mann-Kendall (MK) Test

The Mann–Kendall (MK) (non-parametric) test is usually used to detect an upward trend or downward (i.e. monotonic trends) in a series of hydro meteorological and environmental data. The null hypothesis for this test indicates no trend, whereas the alternative hypothesis indicates a trend in the two-sided test or a one-sided test as an upward trend or downward trend (Mann, 1945). There are two benefits of using this test. First, it does not require the data to be normally distributed since the test is non-parametric (distribution-free test) and second, the test has low sensitivity to abrupt breaks due to inhomogeneous time series. The data values are evaluated as an order time series and all subsequent data values are likened from each data value. The Sen's estimator is another non-parametric method used for the trend analysis of hydro climate data set. It is also used to identify the trend magnitude. Hence, this test computes the linear rate of change (slope) and the intercept as shown in Sen's method (Sen, 1968). The MK test is widely documented in various literature, as a powerful trend test for effective analysis of seasonal and annual trends in environmental data, hydrological data (climate data) and this test is preferred over other tests because of its applicability in time-series data, which does not follow the statistical distribution.

2.9.2. Mann-Whitney u-test

The Mann-Whitney U test (also known as Wilcoxon rank-sum test) has been introduced by Mann and Whitney (Mann and Whitney, 1947). and is a non-parametric test, in the sense

that no assumption is made concerning the distribution of the variables. The null hypothesis is that for randomly selected values X_k and Y_l from two populations, the probability of X_k being greater than Y_l is equal to the probability of Y_l being greater than X_k. It therefore does not test exactly the same property as the Student's t-test (means of two populations are equal), even though it is often compared to it (Zeman and Schär, 2021).

2.9.3. Z- Value test

In statistics, the Z-value test or Z-test can be used to compare a sample mean with a reference mean, where distribution of the test statistic is defined as a difference between the two means divided by the standard deviation (SD) of the observed and can be approximated by a normal distribution. This statistic is calculated under the null hypothesis (H_0) that there is no statistical significant difference between model and the observed mean, and the alternative hypothesis (H_1) that there is a significant difference between model and the observed mean (Jena *et.al.*, 2015).

2.10. Hydrological Model

According to (Singh, 2018), a model is a simplified representation of real world system. The best model is the one which give results close to reality with the use of least parameters and model complexity. Models are mainly used for predicting system behavior and understanding various hydrological processes. A model consists of various parameters that define the characteristics of the model. A runoff model can be defined as a set of equations that helps in the estimation of runoff as a function of various parameters used for describing watershed characteristics. The two important inputs required for all models are rainfall data and drainage area. Along with these, watershed characteristics like soil properties, vegetation cover, watershed topography, soil moisture content, characteristics of ground water aquifer are also considered. Hydrological models are now a day considered as an important and necessary tool for water and environment resource management (Ganasri, 2015). Hydrological models can be classified into three major types, lumped, distributed and semi – distributed models.

2.10.1. Introduction to SWAT model

Soil and Water Assessment Tool (SWAT) is a physically based distributed parameter model which has been developed to predict runoff, erosion, sediment and nutrient transport from

agricultural watersheds under different management practices. SWAT is capable of simulating hydrological processes with reasonable accuracy and can be applied to a large ungauged basin (Panhalkar, 2014). The Soil and Water Assessment Tool (SWAT) was developed to predict the effects of different management practices on water quality, sediment yield and pollution loading in watersheds (Adams, 2014).

The SWAT model is filled with hydro meteorological datasets, to simulate the flow of rivers, the sediment and the water quality. SWAT model proved to be an effective evidence to evaluate the land management practices in flood plain and agricultural chemicals and water resources (Wu *et al.,* 2021). In most countries, SWAT model has been extensively used as a river discharge estimator.

Soil and Water Assessment Tool (SWAT) is a river basin scale model that is developed to measure the impact of land management practices in large, complex reservoirs. It deals with the following elements with the hydrology model: Weather, surface waterway, return flow, water source, ventilation, transmission loss, pond and reservoir storage, crop growth and irrigation, underground flow, reaching path, nutrition and pesticide loading, and water transfers. SWAT uses Hydrological Response Unit (HRU), which describes local diversity, which constitutes the land cover, soil characteristics, and land slope characteristics of unique land use (Das *et al.,* 2019).

2.10.2. Hydrological Component of SWAT

Water balance is the driving force behind all the processes in the watershed because it has an effect on the growth of plants and the transportation of sediments, nutrients, pesticides, and pathogens. The land phase of watershed hydrology simulation regulates how much water, sediment, nutrients, and pesticides are loaded into each sub basin's main channel. The in-stream, or "routing" phase, on the other hand, controls how much water, sediment, nutrients, and pesticides are transported through the watershed's network of channels to the outlet. The brief description of the processes simulated by SWAT was clearly determined below.(S.L. Neitsch *et.al.,* 2005)

The Land Phase of the Hydrological Cycle

The hydrologic cycle as simulated by SWAT is based on the water balance equation;

$$S = SW_o + \sum_{i=1}^{t}\left(R_{day} - \left(Q_{surf} - E_a - W_{seep} - Q_{gw}\right)\right) \quad \text{.....1}$$

where SW_t is the final soil water content (mm H_2O), SW_0 is the initial soil water content on day i (mm H_2O), t is the time (days), R_{day} is the amount of precipitation on day i (mm H_2O), Q_{surf} is the amount of surface runoff on day i (mm H_2O), E_a is the amount of evapotranspiration on day i (mm H_2O), w_{seep} is the amount of water entering the vadose zone from the soil profile on day i (mm H_2O), and Q_{gw} is the amount of return flow on day i (mm H_2O). The potential pathways of water movement simulated by SWAT in the HRU are described below;

Infiltration is the entrance of water from the soil surface in to the soil profile. When infiltration increases, the wetting of soil increases which decreases the rate of infiltration until it reaches its steady state. The hydraulic conductivity of the soil is the same as the final infiltration rate. Curve number method enables the calculation of surface runoff that operates on a daily time step then we can model infiltration.

Evapotranspiration is a process in which water in the form of liquid or solid state at or near the earth surface changed in to atmospheric water vapor. It includes evaporation from water bodies like, rivers, lakes, from bare soil, from vegetative surfaces, from the leaves of plants (transpiration) and from ice and snow surfaces. In this study the amount of water Evaporated from river and Transpired from plant is **591.45mm**.

Potential Evapotranspiration is a term for the process in which evapotranspiration would occur from a large area that are uniformly and completely covered with growing vegetation in which unlimited supply of soil water is available. It is not affected by microclimatic processes like, advection or heat storage effects. The model provides three methods for estimating potential Evapotranspiration; Hargreaves(Hargreaves and Allen, 2003), Priestley – Taylor(Priestley and Taylor, 1972) and Penman – Monteith. (Monteith,J.L, 1965) Among those methods Penman – Monteith method is recommended for this study because of it determines the reference evapotranspiration when climate variables like, air temperature, relative humidity, wind speed and sunshine hour are available. In this study, the Potential Evapotranspiration is **632.92mm**. The formula for this method is determined below;

$$ET_O = \frac{0.408\Delta(R_n - G)}{\Delta + y(1 + o.34u_2)} + \frac{y}{\Delta + y(1 + o.34u_2)} \times \frac{900u_2(e_s - e_a)}{(T + 273)} \ldots\ldots\ldots\ldots\ldots\ldots\ldots\ldots\ldots\ldots\ldots\ldots\ldots\ldots 2$$

Where, ET_O …….. Reference evapotranspiration, mm/day

R_n …….. Net radiation, MJm- 2day- 1.

G …….. Soil heat flux, MJM- 2day- 1.

e_s ……. Saturated vapor pressure, KPa

e_a ……. Actual vapor pressure, KPa

$e_s - e_a$ …….. Saturated vapor pressure deficit, KPa

Δ …….. Slope of the saturation vapor pressure temperature relationship, KPa^{o}c

Y …… psychometric constant, KPaC-1

U_2 ..... Wind speed, ms^{-1}

T …….. Mean daily air temperature at 2m height (^{o}c)

Lateral Subsurface Flow is also called **interflow** that determines the contribution of stream flow originated below the surface but above the saturated zone in which rocks are saturated with water. The lateral sub surface flow in the soil profile with a dimension of 0 – 2m is calculated at the same time with redistribution. The model used to estimate lateral flow in each soil layer is called Kinematic storage model that accounts for variation in conductivity, slope and soil water content.

Surface Runoff is also called **Overland Flow** in which the water flows along a sloping surface. SWAT simulates peak runoff rates and surface runoff volumes for each HRU separately by using either daily or sub daily rainfall amounts. In this study the amount of water flows along a sloping surface (Surface Runoff) is **405.77mm.**

Surface Runoff volume is estimated with a modification of either the SCS curve number method (USDA, 1972) or Green and Ampt infiltration method (Green and Ampt, 1911).

Peak Runoff Rate is computed using a modification of the rational method. The modified rational method formula determines that the peak runoff is a function of the proportion of daily precipitation that falls during the sub basin t_c, the daily surface run off volume and the sub basin time of concentration. The proportion of rainfall occurring during the sub basin

t_c is estimated as a function of total daily rainfall using a stochastic technique. The sub basin time of concentration is estimated using Manning's Formula considering both overland and channel flow.

$$q_{peak} = \frac{a_{tc} \times Q_{surf} \times Area}{3.6 \times t_{concn}} \ldots\ldots\ldots\ldots\ldots\ldots\ldots\ldots 3$$

Where, q_{peak} ..... Is the peak runoff rate (m^3/s)

a_{tc} **.....** Is the fraction of daily rainfall that occurs during the time of concentration.

Q_{surf} **...** Is the surface runoff (mm).

$Area$ **....** Is the sub basin area (km^2).

t_{concn} **....** Is the time of concentration (hr) and **3.6 ......** is a conversion factor.

Ground water simulation is subdivided in to unconfined aquifer (shallow) and a deep confined aquifer in each sub basin. The unconfined aquifer flows toward the main channel or reach of the sub basin. deep confined aquifer provides to stream flow that is outside the watershed(Jha *et al.*, 2006). In this study, the amount of water percolated to shallow aquifer is **188.92mm** and the recharged water to deep aquifer is **9.45mm**.The water balance for unconfined aquifer is computed as follows

$$aq_{sh,i} = aq_{sh,i-1} + W_{rechrg} + Q_{gw} - W_{deep} - W_{pump,sh} \ldots\ldots\ldots\ldots 4$$

Where, $aq_{sh,i}$.......... the amount of water stored in the shallow aquifer on day i (mm)

$aq_{sh,i-1}$...... the amount of water stored in the shallow aquifer on day i-1 (mm)

Q_{gw}.......... Is the ground water flow or base flow in to the main channel on day i(mm) W_{deep}....... Is the amount of water percolating from the shallow aquifer in to the deep aquifer on the day i (mm) and $W_{pump,sh}$............Is the amount of water removed from the shallow aquifer by pumping on day i (mm)

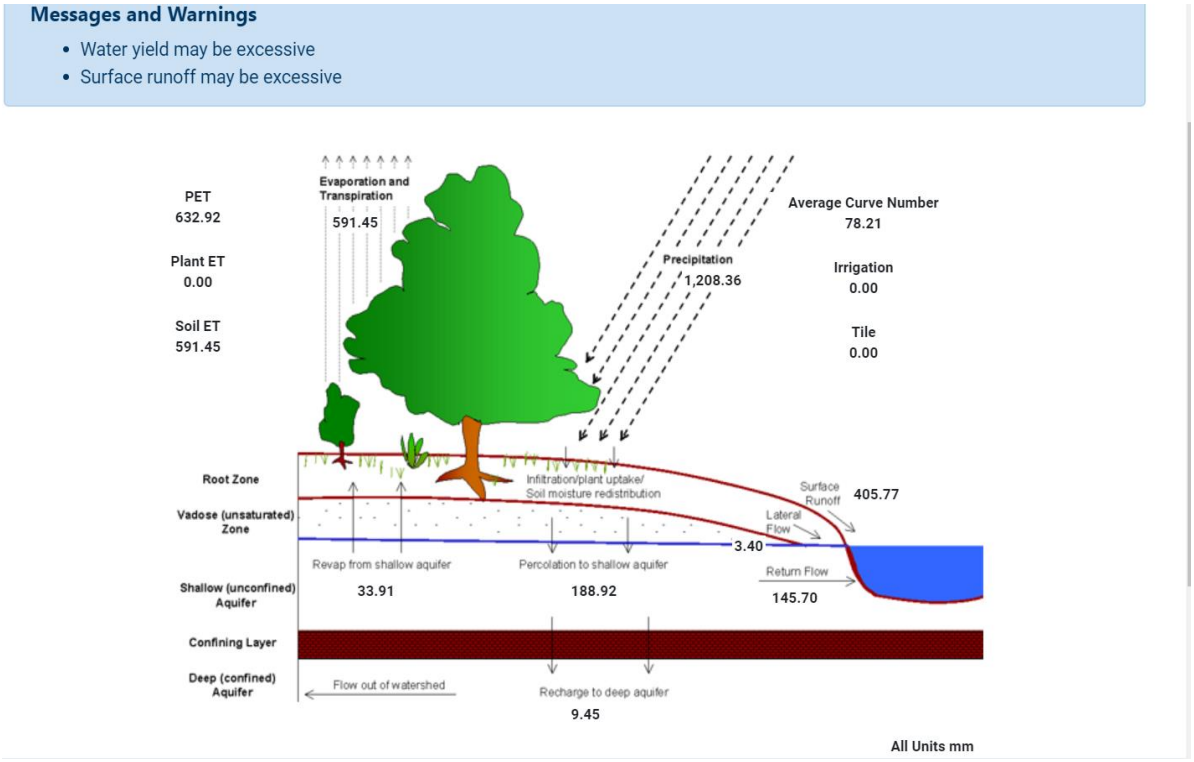

Figure 2.1: Land phase of the Hydrological Cycle

As shown in the previous figure, Streamflow is less than that of surface runoff. There is excess amount of rainwater but the highest amount of rainwater (precipitation) can no longer sufficiently rapidly infiltrate in the soil, therefore surface runoff increased while streamflow in the upper Omo river basin decreased.

Routing Phase of the Hydrologic Cycle

Next to land phase of the SWAT hydrologic simulation, SWAT determines the loadings of water to the main channel and the loadings are also routed through the stream network of the watershed that uses the structure the same as that of Hydrological modeling. (S.L. Neitch et.al., 2002)SWAT models keep the track of mass flow in the channel and the passage of chemicals in the stream and stream bed. There are four components in the routing of the main channel.

The flow rate and velocity are estimated by using Manning's equation. The shape of the main channels are assumed as a trapezoidal shape by the model. Flow is routed through the channel using a variable storage coefficient method or the Muskingum routing method. The storage method estimates the flow routed by using a simple continuity equation but the Muskingum routing method models the flow routed by the combination of wedge and prism storages and

also in this method when a flood wave advances in to the reach segment, outflow becomes higher than inflow in the reach segment and results a production of negative wedge. The variable storage method is using the equation below;

$\Delta V_{stored} = V_{in} - V_{out}$ ……5

Where, V_{in} …….. Is the volume of inflow during the time step (m^3 water)

V_{out} …….. Is the volume of outflow during the time step (m^3 water)

ΔV_{stored} … Is the change in volume of storage during the time step (m^3 water)

2.10.3. SWAT model performance

The performance/evaluation of the SWAT model outputs were assessed using several indices Nash–Sutcliffe efficiency (NSE), R^2 (square of Pearson's product), and percent bias (PBIAS) were the most commonly used indices. IA (index of agreement), RVE (relative volume error), r bias (relative bias) and VR (volume ratio) were the least used. Others used were RMSE (root mean square error), RSR (a standardized RMSE), KGE (Kling Gupta efficiency), IVF (index of volumetric fit), and bR^2 (a multiplication of the coefficient of determination by the coefficient of the regression line between measured and simulated data) (Akoko *et al*., 2021).

The **regression coefficient (R^2)** describes the proportion of the total variance in the observed data that can be explained by the model. The closer the value of r^2 to 1, the higher is the agreement between the simulated and the measured flow and is calculated as follow:

$$R^2 = \frac{(\sum[Qoi-Qoav][Qsi-Qsav])^2}{\sum[Qoi-Qoav]^2 \sum[Qsi-Qsav]^2} \quad \text{……6}$$

Where: X i is measured value, X av is average measured value, Y i is simulated value, Y av is average simulated value.

Nash and Sutcliffe simulation efficiency (NSE) indicates the degree of fitness of observed and simulated data are given by the following formula.

$$NSE = 1 - \frac{\sum(Qi-Qi)^2}{\sum(Qi-Qav)^2} \quad \text{……7}$$

The value of NSE ranges from 1 (best) to negative infinity. If the measured value is the same as all predictions, NSE is 1. If the NSE is between 0 and 1, it indicates deviations between measured and predicted values. If NSE is negative, predictions are very poor, and the average value of output is a better estimate than the model prediction (Nash, J. E. and Sutcliffe, J. V, 1970).

3. MATERIAL AND METHODS

3.1. Description of the Study Area

3.1.1 Location

The Upper Omo River Basin is part of the Omo Gibe River Basin. It is located in the south-western highlands of Ethiopia. It covers an area of 30,172km^2. Upper Omo River Basin is located between 3.75°N - 6.25°N latitude and 34.75°E - 37.25°E longitude (Figure 3.1). The basin is distinguished by a variety of topographic features. Some of the country's major rivers, including the Omo, Gilgel Gibe, and Gojeb, as well as their numerous tributaries, drain the area. As a result, the terrain has been dissected (Jaweso et al., 2019).

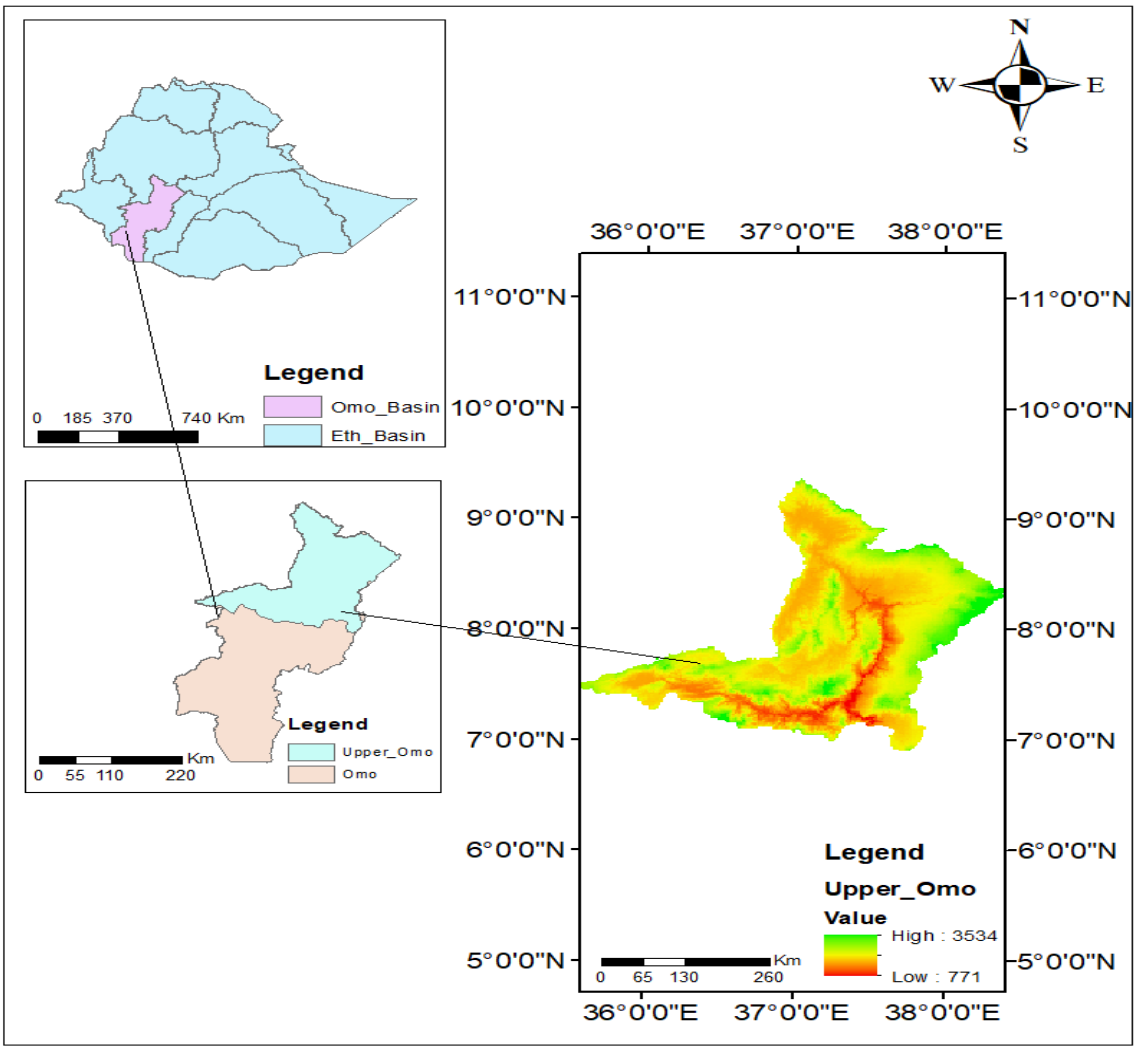

Figure 3. 1. Location Map of Upper Omo River Basin

3.1.2. Climate

Ethiopia's climate is divided into five climate zones based on altitude and temperature. Wurch (cold climate, altitude greater than 3000 m), Dega (highland temperate climate, altitude between 2500 and 3000 m), Woina-Dega (warm climate, altitude between 1500 and 2500 m), Kola (hot and arid climate, altitude less than 1500 m), and Bereha (hot and hyper-arid type of climate) According to this, the upper Omo river basin's climate in the southern and northern highlands is Kola and Wurch, respectively. (NMSA, 2020). The study area's elevations ranged from 746 meters above sea level in the south to 3522 meters above sea level in the north.

A. Rainfall

The rainfall pattern in the basin is monomodal. The major rainfall occurs from March to October with peak flow in July. The mean annual rainfall (1985-2019) of the study area was 1425 mm, with the wet season (March–October) receiving 92% of the annual rainfall and the dry season (November–February) receiving only 8%. (NMSA, 2020)

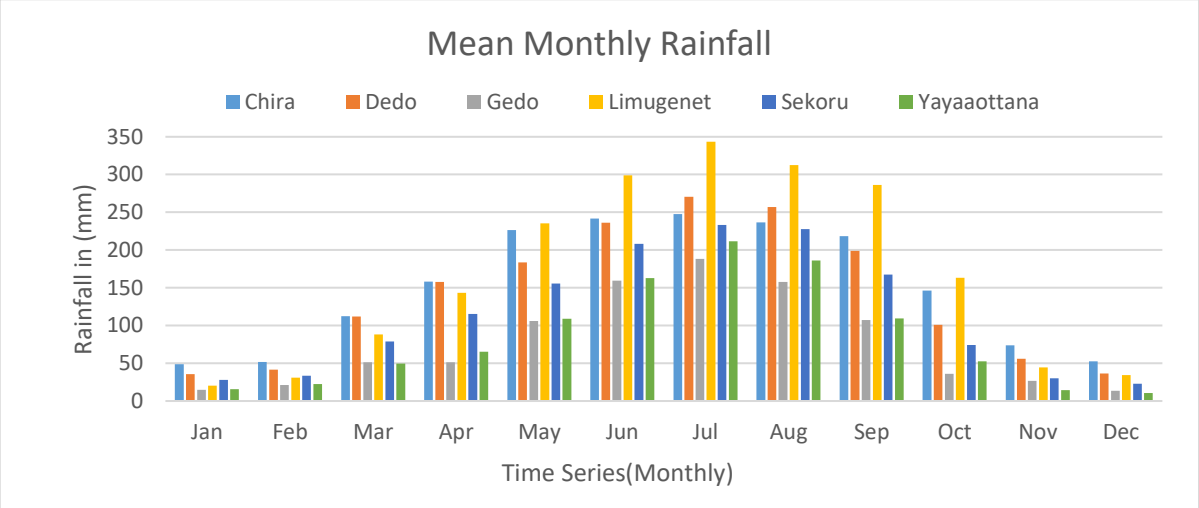

Figure 3.2. Mean Monthly Rainfall Distribution for Selected Stations (1985-2019)

B. Temperature

The mean annual minimum and maximum temperature of the Upper Omo river basin were ranging from 12.3^{o}c-25.6^{o}c. The mean annual temperature is 19.2^{o}c.

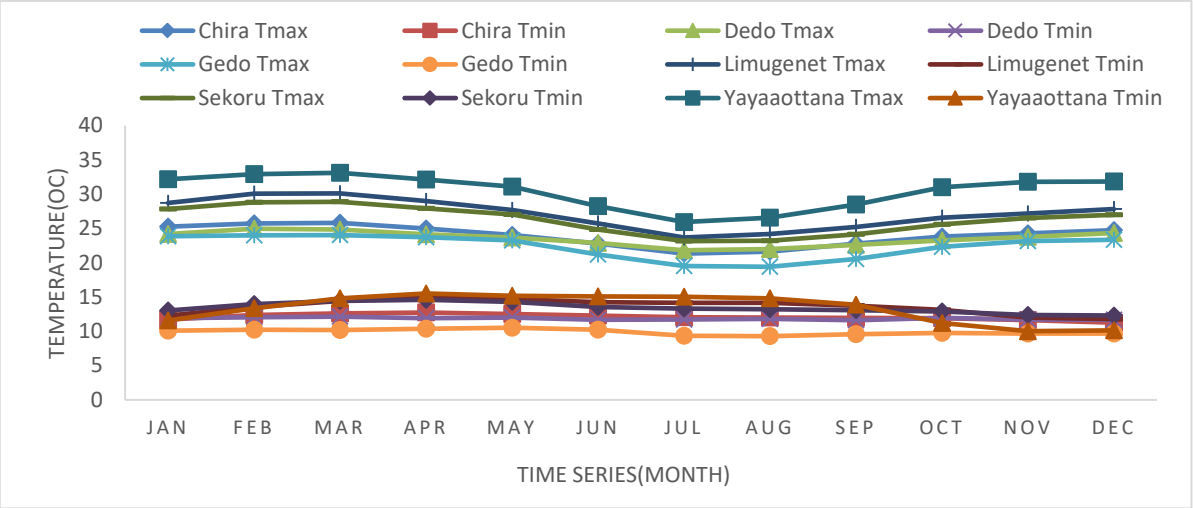

Figure 3.3. Mean Monthly Max and Min Temp for selected Stations (1985-2019)

3.1.3. Land cover/Land use

The Upper Omo River Basin is distinguished by extensive agriculture and increased land pressure. Forest areas are confined to areas too steep and inaccessible to farm. Generally, the central and western parts of the basin boundary area have extensive tracts of high forest. The Gibe, Gojeb, and Omo gorges are relatively unpopulated and support a cover of shrub land and grass land through inaccessible areas, such as where the Addis Ababa to Jimma road crosses the Gibe Gorge. The eastern catchment boundary has some of the most densely populated and intensively farmed areas in the basin. The south of the basin is more sparsely populated, with a greater population of natural vegetation. (MoWE, 2020)

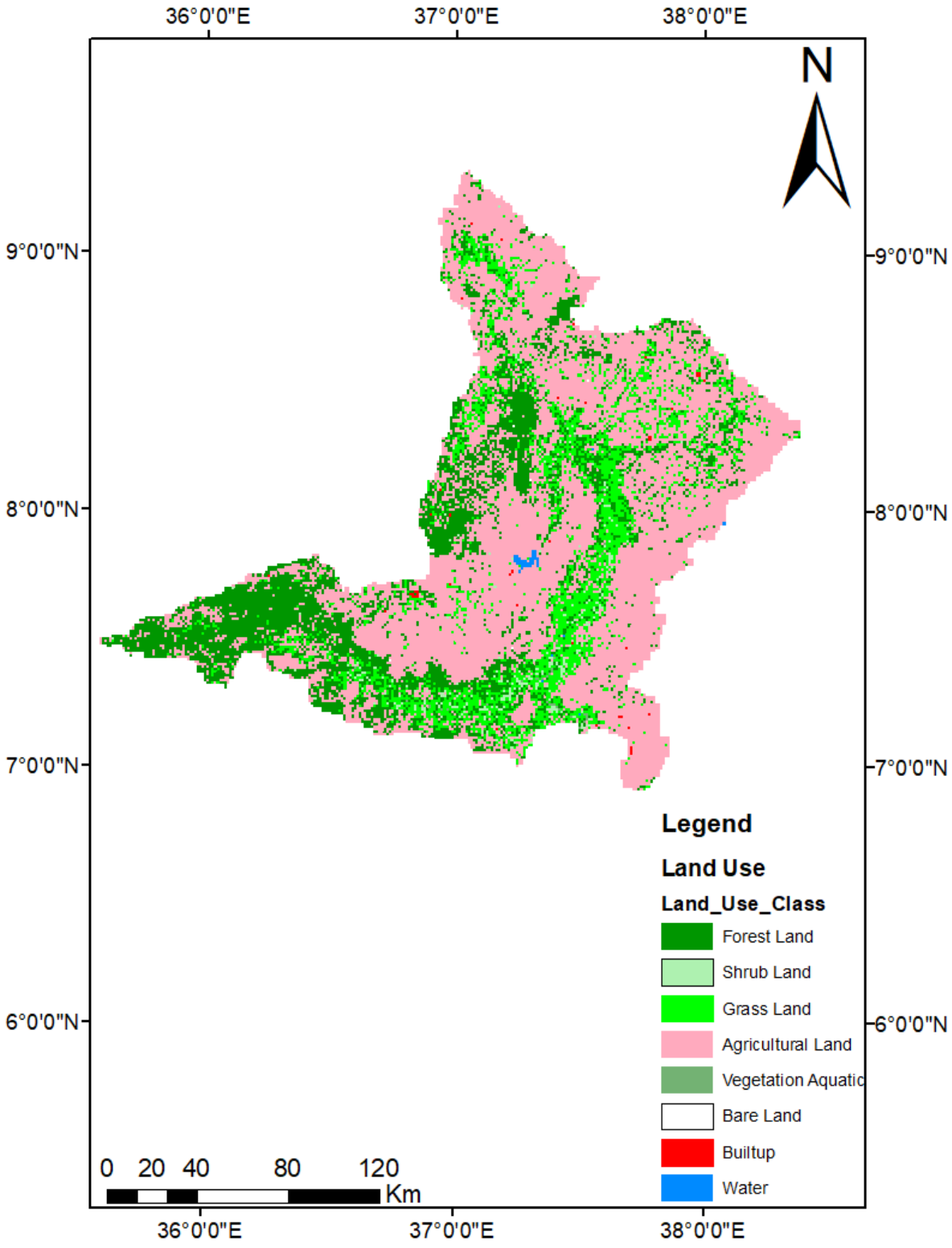

Figure 3. 4. Land use/Land cover map of Upper Omo River basin

3.1.4. Soil

The Upper Omo Basin soil is predominantly composed of clay, with some areas having sandy loam soils. The soils in this region have been classified as Humic Nitisols, Humic Alisols, Eutric Vertisols, Dystric Vertisols, Chromic Luvisols, Rendzic Leptosols and Lithic Leptosols. Humic Nitisols, Humic Alisols and Eutric Vertisols are the dominant soil type in the basin. Rendzic Leptosols are found in smaller areas within the basin (FAO, 2020).

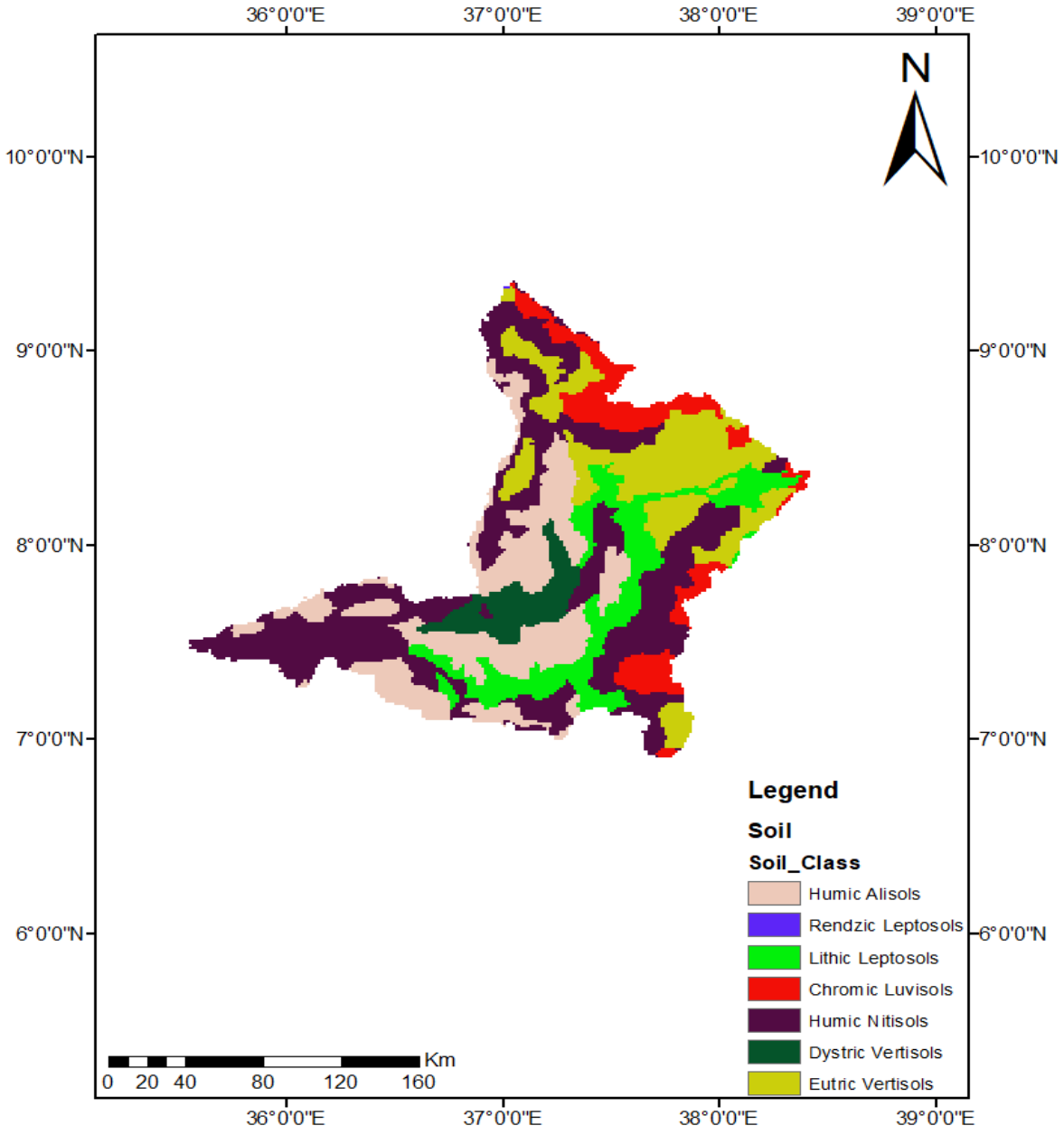

Figure 3.5. Soil Map of Upper Omo River Basin.

3.1.5. Infrastructure

The infrastructure in Upper Omo river basin includes both natural and man-made features that are essential for the region's social, economic, and environmental well-being. In terms of natural infrastructure, the Upper Omo River Basin is characterized by a network of rivers and lakes that provide water for drinking, irrigation, and hydropower generation. The region also contains several forests, wetlands, and grasslands that support biodiversity, soil conservation, and carbon sequestration. Man-made infrastructure in the Upper Omo River Basin includes roads, bridges, dams, and other structures that have been built for transportation, energy generation, and water management. For example, the Gilgel Gibe III dam is one of the largest hydroelectric power plants in Africa, and it generates electricity for Ethiopia and neighboring countries. Additionally, several roads and bridges have been constructed to improve access to markets and services for local communities.(Atinafu, 2015)

3.1.6. Socio-economic status

Agriculture is the main economic activity. The socio-economic status of the region is characterized by high levels of poverty, low educational attainment, and limited access to basic services such as healthcare and clean water. Poverty is pervasive in the region, with more than 60% of the population living below the national poverty line. The study also found that the region has a low level of educational attainment, with only 23% of the population having completed primary education, and less than 1% having completed tertiary education. (Atinafu, 2015)

3.2. DATA COLLECTION AND ANALYSIS

3.2.1. Climate Data

In this study, observed (1985-2019) and projected (2020-2071) climate data (precipitation, maximum and minimum temperatures) were collected from the National Meteorological Agency (NMA) and were downloaded from the World Climate Research Program (WCRP) respectively. These climate data are needed to assess the future impact of climate change and are needed for the SWAT hydrological model to simulate streamflow for the reference period. It is also important to compare production in future periods.

3.2.1.1 Baseline climate data

In this study, observed daily climate data (precipitation, maximum and minimum temperatures) for six stations in the study basin from 1985 to 2019 were collected from the Ethiopian National Meteorological Agency (NMSA, 2020). These climate data are needed to assess the future impact of climate change and are needed for the SWAT hydrological model to simulate streamflow for the reference period.

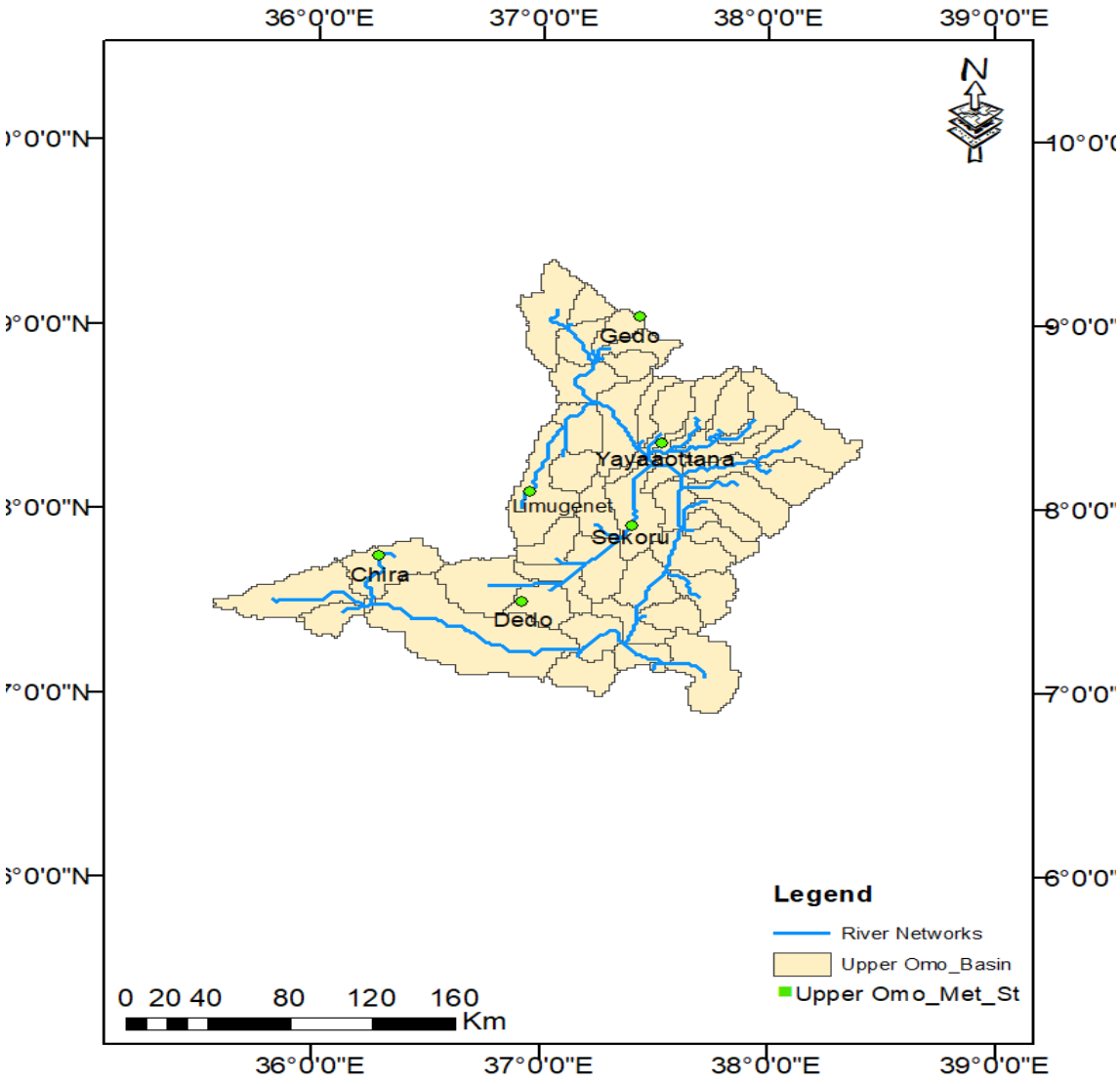

Figure 3.6. Meteorological stations at Upper Omo river basin

3.2.1.1.1. Precipitation data quality

Filling of missed data

The best method for estimating missing rainfall data can differ for different areas based on their rainfall patterns and spatial distributions. According to this, the arithmetic mean method is used when the normal annual rainfalls at surrounding gauges are within 10% of the normal annual precipitation at the stations concerned. The arithmetic procedure could then be adopted to estimate the missing data.

In contrast to the arithmetic mean method, the normal ratio method is used when the normal annual precipitation of any nearby gauges exceeds 10% of the gauge under consideration. This calculates the effect of each nearby station.

The inverse distance weighting method, on the other hand, estimates missed data weighting by assuming that the weight for each station is inversely proportional to the target station's squared distance from the neighboring station with data. However, this method does not take into account the spatial distribution of variables and is not recommended if the stations are close together. Because of its simplicity and the fact that the annual average rainfall at the target station exceeded 10% of the normal annual precipitation of its surrounding stations. so, the normal ratio method was used to fill in the missing data.

The general formula for this method is;

$$\boldsymbol{P} = \frac{\boldsymbol{Nx}}{\boldsymbol{M}}\left[\frac{\boldsymbol{P1}}{\boldsymbol{N1}} + \frac{\boldsymbol{P2}}{\boldsymbol{N2}} + \frac{\boldsymbol{P3}}{\boldsymbol{N3}} + \cdots\cdots + \frac{\boldsymbol{Pm}}{\boldsymbol{Nm}}\right] \ldots\ldots\ldots\ldots\ldots\ldots\ldots\ldots\ldots\ldots\ldots 8 .$$

Where, **M**…..Total no of stations considered/ target stations.

Nx…. Average annual rainfall of station at the missing data.

N1, N2, N3….**Nm**… Average annual rainfall at the adjoining /surrounding/ stations.

Consistency test

The consistency of precipitation and temperature data from individual stations was checked using a double mass analysis. When using a double mass spectrometry technique, it is critical to include a sufficient number of stations; otherwise, inconsistencies in individual stations will have no significant effect on the consistency of the computed group average. When

performing data analysis for an entire river basin, there are usually more than enough stations. For instance, in this study, six stations were provided, and those stations require slope adjustment. Based on the theory that the precipitation data recorded is said to be consistent over time if the relationship between the cumulative rainfall of the station and the cumulative rainfall of a group of stations plots generally as a straight line, However, there is a lot of variability in nature, such that the relationship between a single station and a group of stations will not be perfectly straight.

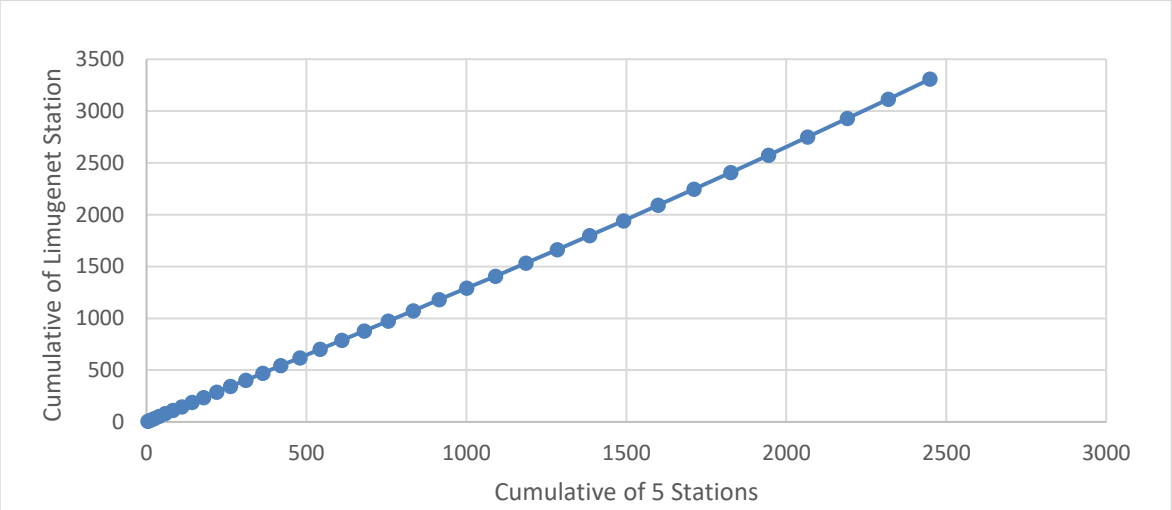

Figure 3.7. Annual Rainfall Double Mass Curve

As long as the general trend line is straight and there are no significant deviations from the general trend line, the data are consistent. The records of these stations did not reveal inconsistency since the graph was found to follow fairly straight line and therefore, these stations had no recording problems or subjected to any external factors during the study period.

Homogeneity Test

The homogeneity of precipitation was tested using RAINBOW. In RAINBOW the test for homogeneity is based on the adjusted partial sums or cumulative deviations from the mean (Buishand, 1982).

$S_K = \sum_i (xi - \bar{x}), K = 1, \ldots n$ 9

Where, Xi the records of the partial duration series X1, X2….Xn and $\bar{X}$ the mean

For a homogeneous record one may expect that the SK's fluctuate around zero since there is no systematic pattern in the deviations of the Xi's from their average value. In RAINBOW the rescaled cumulative deviations, obtained by dividing the SK's by the sample standard deviation value (α_x). A statistic which is sensitive to departures from homogeneity is,

$$Q = max\left|\frac{S_k}{\alpha_x}\right|, k = 0, \dots, n \quad \text{.....10}$$

High values of Q are an indication for a change in the mean level. Another statistic which is used for homogeneity is the range, given as below

$$R = max\left(\frac{S_k}{\alpha_x}\right) - min\left(\frac{S_k}{\alpha_x}\right), K = 0, \dots, n \quad \text{.....11}$$

In RAINBOW the maximum cumulative deviation (Q) and the range (R) are used to decide whether or not to reject the homogeneity of the data. According to the test the flow is homogeneous.

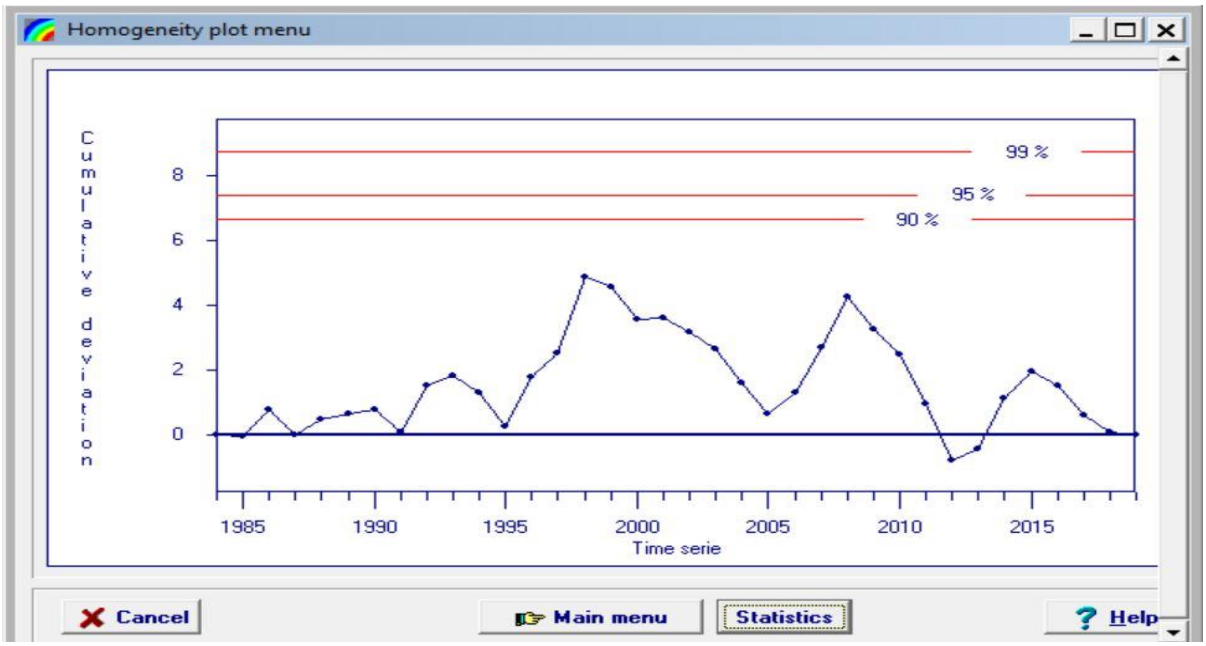

Figure 3.8. Graph of Homogeneity Test

3.2.1.1.2. Estimation of areal precipitation

There are several methods that are used for the estimation of actual precipitation. The best method for estimation of area-wide precipitation can differ for different areas based on the station's area coverage. According to this, the Theissen polygon method was used in this study to calculate the area average precipitation by weighting the area ratio of the Theissen

polygons enclosing the watershed stations that observe the rainfall.(Yang and Kang, 2019) The general formula for this method is;

$$\mathbf{P_m} = \frac{A_1P_1 + A_2P_2 + \cdots\cdots\cdots + A_nP_n}{A_1 + A_2 + \cdots\cdots\cdots + A_n} \quad \ldots\ldots\ldots\ldots\ldots\ldots\ldots\ldots\ldots\ldots\ldots\ldots\ldots\ldots\ldots\ldots\ldots\ldots\ldots\ldots\ldots\ldots 12$$

Where, $\mathbf{P_m}$ ..... is the average precipitation in the watershed,

$\mathbf{P_1}$,…,$\mathbf{P_n}$….the rainfall observed at **n**-stations in the watershed, and

$\mathbf{A_1}$,….**An**….the areas of each observation point.

The Theissen polygon method obtains the average precipitation by weighting the area of each station. This method takes into account the relative locations of the rainfall stations in the watershed and the relative density of the observation network. As a result, the method performs better than the arithmetic average method, so this method was used in this study area in order to estimate the actual precipitation. However, it does not consider changes in precipitation due to altitude. The respective rain gauge stations (Chira, Dedo, Gedo, Limugenet, Sekoru and Yayaaottana) were considered to determine their corresponding Areal Rainfall. The Theissen coefficient of each gauging station for the watershed was determined.

Table 3.1. Rainfall Stations and their corresponding Area

Station Number	Rainfall Stations	Areal Rainfall in mm	Area in KM^2
1	Chira	1833.66	3637
2	Dedo	1686.1	7137
3	Gedo	933.5	3545
4	Limugenet	2001.4	2367
5	Sekoru	1374.6	7563
6	Yayaaottana	1009.9	7905

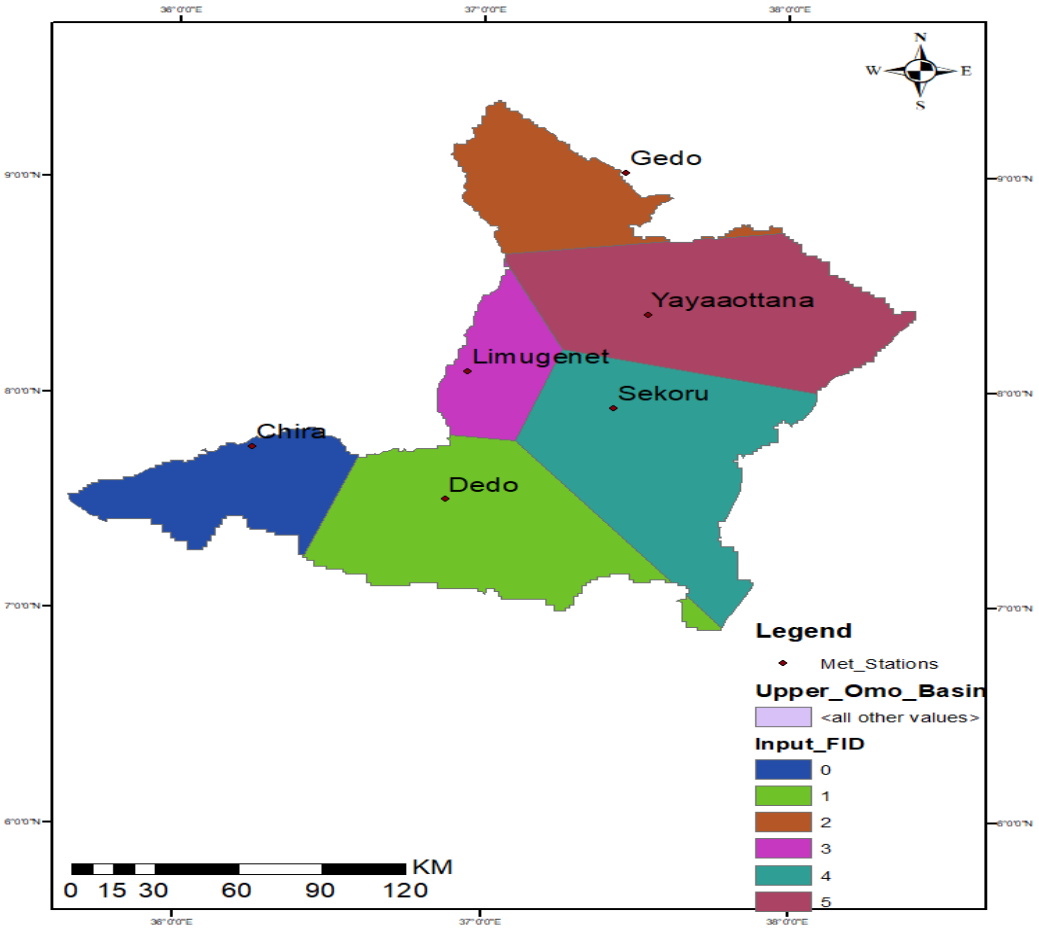

Figure 3.9. Theissen Polygon for Upper Omo river basin

3.2.1.2. Projected climate data

3.2.1.2.1. Climate data period

The window periods for the projection of future climate data (precipitation, minimum temperature, and maximum temperature) are the near future from 2020 to 2045 and the mid-future from 2046 to 2071.

3.2.1.2.2. Global Climate model (CMIP6 model)

The projection of future change in precipitation and maximum and minimum temperature were modeled from the compilations of the Coupled Model Inter-comparison Projects (CMIPs), overseen by the World Climate Research Program. Data were presented in CMIP6, derived from the sixth phase of the CMIPs. The CMIP6 climate model outputs can be downloaded from https://esgf-node.llnl.gov/search/cmip6/. Five GCM models from CMIP6

used are ACCESS-CM2, CMCC-ESM2, MIROC6, EC-EARTH3 and NESM3. Those models are selected based on resolution (the model with higher resolution), validity (the GCM model that simulate the present day climate most faithfully) and representativeness (if more than one GCM applied in an impact assessment).CMIP6 supports the IPCC's sixth Assessment Report. The data's projected at a resolution of 10 km * 10 km.

3.2.1.2.3. Criteria for Global Climate Model Selection

In this study, all models in the ESGF holdings for the CMIP6 Scenario were assessed. The models selected based on the four objective criteria, listed below.

Criterion 1. Mean daily minimum temperature (Tmin) and mean daily maximum temperature (Tmax) are the directly measured elements of the long term temperature record, and are the fundamental temperature elements in many climate change impact analyses.

Criterion 2. Models need to have at least one simulation for three of the four major SSP marker scenarios (SSP1-2.6, SSP2-4.5, SSP3-7.0, and SSP5-8.5).

Criterion 3. One model per institution: This criterion is a widely applied best practice in ensemble selection (Leduc, 2016) as one measure to increase independence among ensemble members. For the purposes of this criterion, different physics or forcing schemes of the same model were considered different models.

Criterion 4. No large biases: Bias is the degree to which a model simulation differs from the observed climate over a reference period (1985-2019 in this case). Models with large biases relative to the rest of the ensemble in one or more variables were excluded.

3.2.1.2.4. Climate scenario (SSPs) data

In order to reflect such differences as well as model variability, which is representative of all SSPs, the study used two future scenarios. The first scenario considers what the future climate will be under conditions with a Shared Socio-economic Path (SSP) that assumes the radiative forcing will reach 8.5 w/m2 in the 2060s (SSP5-8.5), which is the extreme climate scenario, and the second scenario considers that the radiative forcing will stabilize at 4.5 w/m2 in 2060 (SSP2- 4.5).

The ensemble of rainfall, minimum and maximum temperatures of 5 GCMs based on the four objective criteria for the period 1985–2100 was collected from the World Climate

Research Programme (WCRP) dataset. The data referred to five SSP scenarios: SSP5-8.5, SSP4, SSP3-7.0, SSP2-4.5, and SSP1-2.6. But from those five SSP scenarios, only two of them—SSP2-4.5 and SSP5-8.5—were selected because they are suitable for CMIP6 projections for the period of 2020–2071 for six stations.

3.2.1.2.5. Downscaling technique (DST)

Statistical Downscaling Model (SDM)

SDSM 4.2 Statistical Downscaling Method was selected for this study. SDSM 4.2 is selected because of it is stochastic model, it can reproduce the unique meteorological characteristics of the individual stations, it's less data intensive than dynamical methods and it develops quantitative relationships between predictors and predictands. The predictors are GCM variables and predictands are temperature and precipitation. The procedures used in SDSM 4.2 Statistical Downscaling are;

1. **Pre-processing**

The predictors are standardized before downscaling in order to minimize biases in the mean and variance of GCM atmospheric fields relative to observations or reanalysis data. The data is regridded to conform to the spacing of the GCM model grid.

2. **Statistical Downscaling**

Statistical downscaling establishes empirical relationships between GCM resolution climate variables and local hydrological variables:

$$R = F(L) \quad \text{.....13}$$

R: Predictand (a local climate variable)

L: Predictor (a set of large scale climate variable)

F: Deterministic/Stochastic function (conditioned by predictor L and determined empirically from historical data and observations.)

3.2.1.2.6. Bias correction using Distribution Mapping

The downscaled SSPs data cannot be directly used for impact assessment so, Distribution Mapping bias correction method was selected for this study. Distribution Mapping is

selected because of it showed better performance in adjusting wet day probability and percentiles of rainfall and temperature, it is a powerful and flexible method for correcting biases in machine learning models, It can improve the accuracy of predictions, is easy to interpret, and can be applied to a wide range of data types and models (Teutschbein C and Seibert J, 2018).

$$\mathbf{P_{d,\,cor}} = \boldsymbol{P}_{\boldsymbol{d,raw}\left(\frac{\mu\left(P_{m,obs}\right)}{\mu\left(P_{m,row}\right)}\right)} \quad \text{.....14}$$

Where, **Pd, cor ……** is the corrected daily precipitation and

P d, raw…… is the daily raw precipitation data from CFSR. In this case,

P m, obs ……..is the long-term mean monthly rainfall of observed data, and

P m, raw …… is the long-term mean value of the monthly/yearly raw rainfall data.

The bias correction approaches in this investigation were carried out using the CMhyd tool (Rathjens et al. 2016) The tool compares raw GCM output to observed data, computes the difference between observed and simulated data, and applies several bias correction approaches to rectify past and future climate model output. For the bias correction of future GCM simulations, bias correction algorithms derived from historical GCM simulation and observed data were used.

3.2.2. Current and Future Climate Trend Analysis

The Mann–Kendall trend test is a non-parametric test usually used to detect an upward or downward trend (i.e. monotonic trends) in a series meteorological data (Mann, 1945). In this study, the rainfall and temperature trend analysis was undertaken, monthly, annual and seasonal for the baseline and future data series. For baseline period (1985-2019) the trend test was analyzed for each station, as well as for the mean of the stations whereas, for the future period, the trend test was analyzed for the mean of the stations. The MK trend test is based on two hypothesis; one is null (H_o) and the other is the alternative (H_a) hypotheses. Based on the 5% significance level, if the P value is $\leq \alpha = 0.05$, then the alternative hypothesis is accepted; which signifies the presence of a trend in the data and if the P value $\geq \alpha = 0.05$ then Ho will be accepted; that denotes the absence of a trend in the data. The

mathematical equations used for the standardized calculation of Z-test statistics and Mann Kendall statistics(S) are calculated as follows;

$$S = \sum_{i=1}^{n-1} \sum_{j=i+1}^{n} sgn(xj - xi) \quad \text{.....15}$$

Where n is the number of data points, xi and xj are the data values in time series i and j (j>i), respectively and sign (xj-xi) is the sign function.

$$Z_s \begin{cases} \frac{S-1}{\sqrt{VAR(S)}}, if\ S > 1 \\ 0, if\ S = 0 \\ \frac{S+1}{\sqrt{VAR(S)}}, if\ S < 1 \end{cases} \quad \text{.....16}$$

The significance is rejected when the absolute value of Z is less 1.96 and the significance should be accepted (significant) when the absolute value of Z is greater than 1.96.

3.2.3. Hydrological Modeling with SWAT

3.2.3.1. SWAT model data input and preparation

SWAT model was applied for simulating streamflow of Upper Omo River Basin. The model requires data such as digital elevation model (DEM), soil-map and land use-map of the region under consideration. Others include rainfall, temperature, relative humidity, wind-speed and solar-radiation. The spatial data was processed with Arc-Hydro tool and ArcGIS Program. Daily archives of the streamflow data from 2000-2019 were obtained from the hydrology department of the Ministry of Water, Irrigation, and Electricity.

3.2.3.1.1. Digital Elevation Model

DEM describes the elevation of any point in a given area at a specific spatial resolution as a digital file. DEM is an essential input for the SWAT model, which is used to delineate the basins into several sub-basins and analyze the drainage pattern of the basin, including slope, stream length, and the width of the channel within the basin. The DEM is obtained from the NASA Shuttle Radar Topographic Mission (SRTM) with a resolution of 30 m by 30 m.

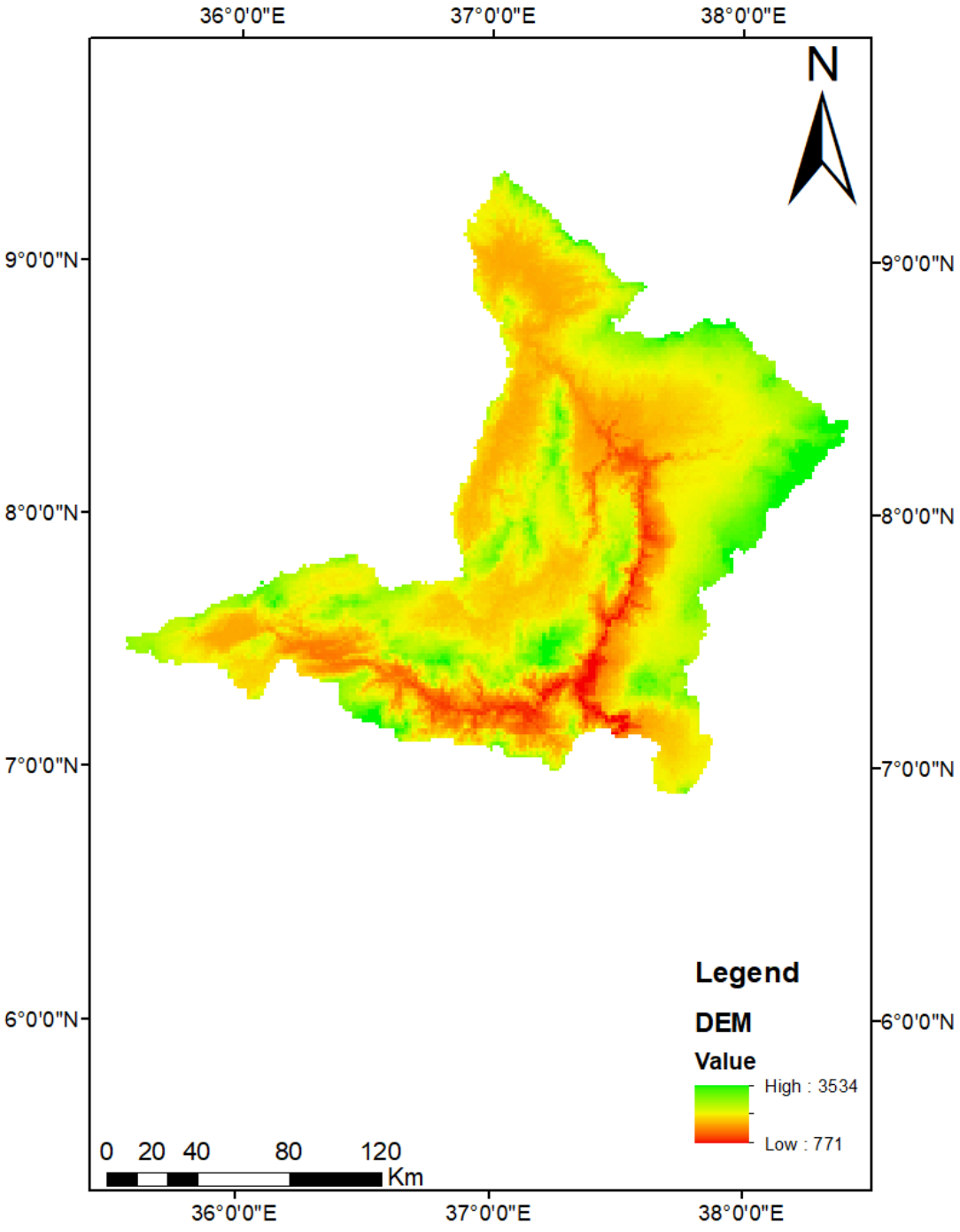

Figure 3.10. Digital Elevation Model of Upper Omo River Basin

3.2.3.1.2. Soil

Soils in the study watershed were classified on the basis of the revised FAO/UNESCO-ISWC. The spatial distribution of several soil types was the most important factor affecting the whole hydrology of a watershed. Soil data is the most important input for the SWAT

model in order to define lumped land areas and HRUs. The soil data is extracted from the 1:250,000 scale soil map developed by the Ministry of Water and Energy (MoWE). (MoWE, 2020). The SWAT soil database requires all physio-chemical properties of each soil type in the river basin, so the basic physio-chemical properties of major soil types in the watershed were mainly obtained from the following sources: the Omo River Basin Integrated Resources Master Plan, the SWAT soil database, and the digital soil map from the MoWE. In addition to these sources, some soil properties were estimated based on available soil parameters.

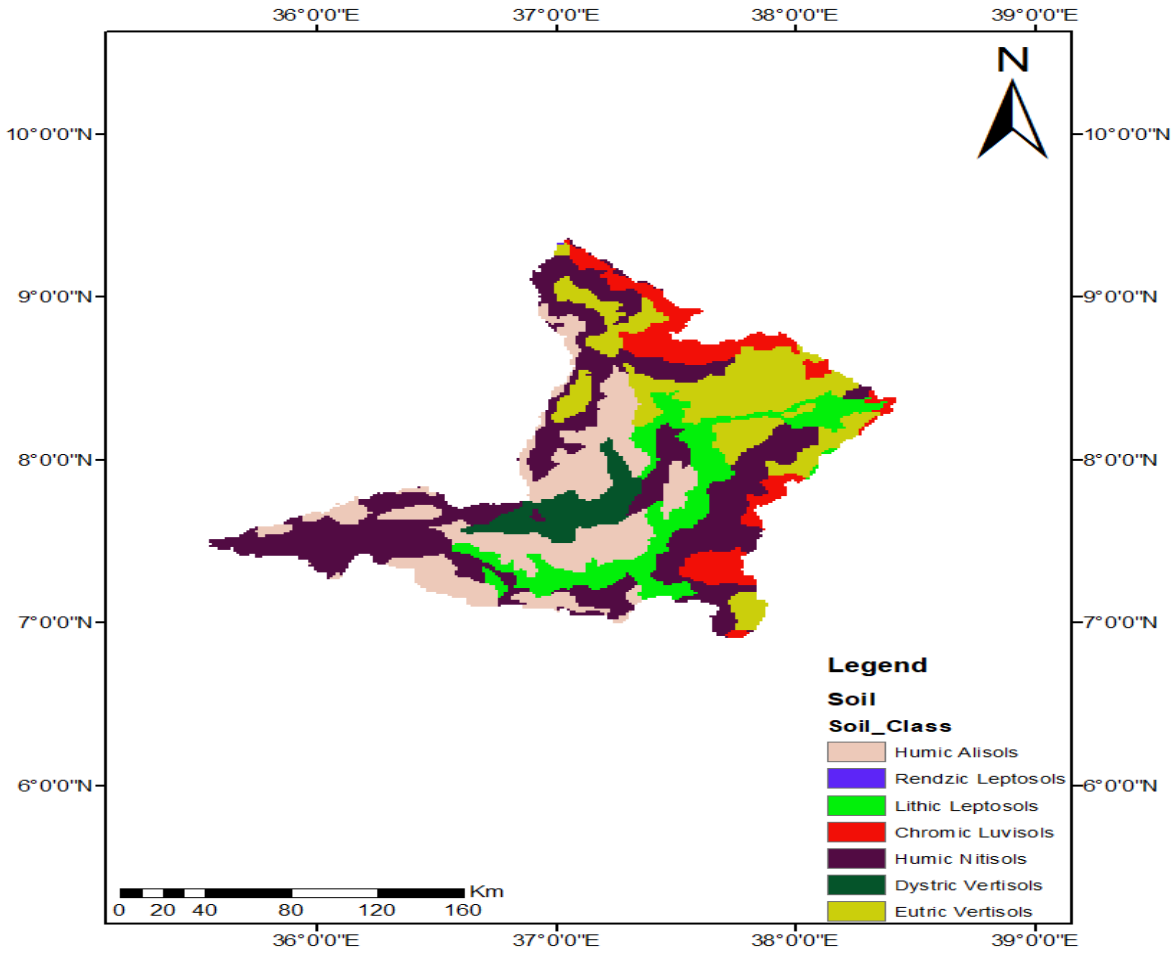

Figure 3.11. SWAT Soil Map of Upper Omo River Basin

3.2.3.1.3. Land use/ Land cover

Land use and land cover have either a direct or indirect effect on surface erosion, runoff, and evapotranspiration in a watershed. The land use/land cover map was obtained from the

Ministry of Water and Energy. (MoWE, 2020). The spatial data is obtained from either satellite imagery (Landsat) or from collected field data. The most current and detailed LULC data is available for the study watershed or for the upper Omo basin. In order to assign the land use according to the specific LULC types and the respective crop parameters for the SWAT database, reclassification of the land use map has to be done.

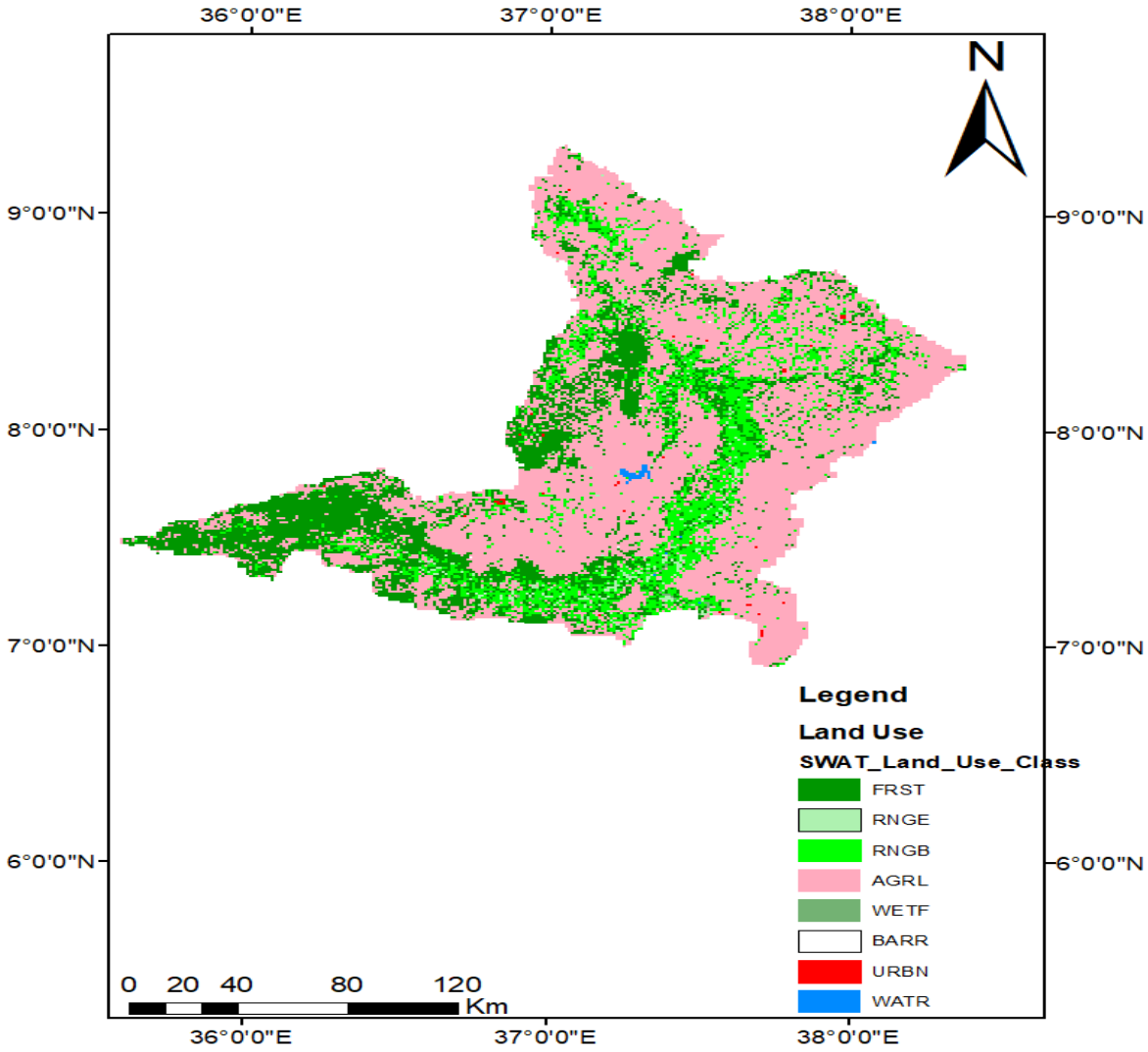

Figure 3.12. SWAT Land use Map of Upper Omo River Basin

3.2.3.1.4. Weather Data

The weather data definition is divided into six tabs: weather generator data, rainfall data, temperature data, solar radiation data, wind speed data and relative humidity data. The data collected from the meteorological stations have a missing value. Therefore, using weather generator solves such types of problem by generating data from the observed one. The

SWAT model requires daily hydro meteorological data from measured data or generated from values using monthly average data over a number of years. In this study measured data were used for all climatic variables. Since the climatic data collected from stations in the Upper Omo river basin had missing values, the SWAT weather generator was used to fill the missing parameters.

3.2.3.2. SWAT model set up

Arc SWAT version 2012.10_4.21 was downloaded from SWAT website and its toolbar was added to Arc GIS10.4.1 for modeling process. The modeling procedure includes SWAT project setup, Watershed delineation, and HRU Analysis, Write Input Tables, Edit SWAT Input and SWAT simulation.

3.2.3.2.1. Watershed Delineation

The first step in generating SWAT model is watershed delineation. The soil map, Land use map and the DEM were projected using ARCGIS 10.4.1 to the same projection prior to watershed delineation. This was done to overlap the three maps during SWAT modeling. The watershed and sub watershed delineation was performed using 30m by 30m resolution of DEM data and using Arc SWAT model watershed delineation function. The DEM was loaded and its projection was defined. There are two options for stream definition: the user can import predefined stream network in shape file format (it can be used if the location of the streams in the catchment area is known) and DEM based (Can be used if the exact location of the streams in the catchment is not known). In this study since the exact location of the streams in the watershed were not known, the DEM based option was chosen. Since the location of gauging station was known the outlet generated by model was modified at the gauging location for later calibration purposes. The location of the stream flow gauging station (Abelti) was manually added during the model set up process. Once the DEM set up was completed and the location of outlet was specified on the DEM, the model automatically calculates the flow direction and flow accumulation. Finally stream networks, sub watersheds and topographic parameters were calculated using the respective tools. The stream definition and the size of sub basins were determined by selecting the threshold area. The Upper Omo river basin was delineated into 23 sub basins having an estimated total area of 30,172.9km^2. During the watershed delineation process the topographic parameters such as elevation and slopes of watershed and its sub watershed were generated from the DEM

data. The elevation of the watershed ranges from771m to 3361m above mean sea level. The slope of the watershed was classified into four classes as shown in Table 3.3.

Table 3.2. The Slope Class of Upper Omo River Basin

Slope	Area(ha)	%Wat.Area
0-5	1599361.6	53.01%
5-10	850629.9	28.19%
10-15	370251.9	12.27%
>15	197045.7	6.53%

3.2.3.2.2. Spatial data projection

In order to use Arc SWAT, all the data to be used must be in the same projection, and GIS processing can take place. UTM projection is appropriate because of It is commonly used for larger areas in GIS. The DEM was used for the delineation of the watershed and for the analysis of the drainage patterns of the land surface terrain. DEM derived sub basin parameters such as terrain slope gradient and slope length, as well as stream network characteristics such as channel slope, length, and width.

3.2.3.2.3. HRU definition

HRU is considered in determining the total effect of different land covers, crops, and soils. The total runoff varies with regard to the variation in actual hydrologic conditions of each land cover, crop, and soil present in the watershed. In order to estimate runoff in the basin, the impact of each type of land use was determined in this modeling. HRU analysis in SWAT included reclassification of HRUs by slope classes, land use, and soil types. After reclassification of the land use, soil, and slope in the SWAT database, the land-use, soil, and slope maps and overlays that are used for the distributions of the Hydrological Response Units (HRUs) were determined As the SWAT manual recommends, when the study considered four classes of slope, 0-5%, 5-10%, 10-15%, and > 15%, the multiple HRU definition criteria were performed for most applications using the default values for land use threshold (20%), soil threshold (10%), and slope threshold (20%). In this study, the HRU distribution was determined by assigning multiple HRU to each sub-basin. Due to this upper

Omo river basin was divided into 159 HRUs, each has a unique land use and soil combinations.

3.2.3.2.4. Weather generator

Daily precipitation and maximum and minimum temperatures are vital for SWAT. Those inputs, or weather data, were generated from monthly average data. The model generated some sort of weather data for each sub basin. The weather values were determined individually, and there was no spatial relation between the generated values of each sub basin.

WXGEN is a weather generator model included in SWAT. (Sharpley, A.N. and Williams, J.R., 1990) It is used for generating climate data or for filling gaps in measured data. WXGEN was developed for the contiguous U.S. If other weather generators are more suitable than WXGEN, then daily input values for various weather parameters are generated with the more suitable model and formatted for input to SWAT.

The amount of rain that occurs in a given area within a given day has a great impact on the relative humidity, temperature, and solar radiation for the day. Firstly, the weather generator generates precipitation (the total amount of rainfall) for the day, and then the distribution of rainfall within the day for the sub basin is determined. In addition to this, infiltration was calculated by the Green and Ampt method, and maximum temperature, minimum temperature, solar radiation, and relative humidity were computed depending on the presence or absence of rain during the day, but wind speed was determined independently.

3.2.3.2.5. Sensitivity analysis

Sensitivity analysis is used to determine the amount of change in model output with regard to changes in model inputs. The identification of key parameters and the precision of those parameters are important for the calibration process (Mendelsohn 2007). Topography, geomorphology of the landscape, size of the watershed, land use variations, and human impacts affect the sensitivity of several parameters. For the determination of sensitive parameters, the model had to run for both the warm-up and calibration periods.

3.2.3.2.6. Calibration

Testing a model is done with model calibration, and observed data can be tuned with model calibration. Model calibration is important for the successful use of hydrologic and water quality simulations. Calibration could be done either manually or automatically. Using both methods is important for better calculation of sediment transport and runoff. Firstly, the model was automatically calibrated for hydrology, and then the model was calibrated for sediment transport. The model calibration was done for 14 years, from 2000 to 2013. The first two years were used to prime the model. The model requires at least two years for better calculation of results through priming (Moriasi et al., 2015).

3.2.3.2.7. Validation

Stream flow data from six years, from 2014 to 2019, was used for validation. The three statistical model performance measures used in the calibration procedure were also used in validating stream flow. The statistical criteria that were used in the calibration process were also examined in order to make sure that the simulated stream flow was within the accuracy limit or not.

3.2.3.2.8. SWAT model performance evaluation

The performance/evaluation of the SWAT model outputs were assessed using several indices Nash–Sutcliffe efficiency (NSE), R^2 (Coefficient of Determination), and percent bias (PBIAS) were the most commonly used indices. IA (index of agreement), RVE (relative volume error), r bias (relative bias) and VR (volume ratio) were the least used. Others used were RMSE (root mean square error), RSR (a standardized RMSE), KGE (Kling Gupta efficiency), IVF (index of volumetric fit), and bR^2 (a multiplication of the coefficient of determination by the coefficient of the regression line between measured and simulated data)(Akoko et al., 2021).

The **Coefficient of Determination (R^2)** describes the proportion of the total variance in the observed data that can be explained by the model. The closer the value of R^2 to 1, the higher is the agreement between the simulated and the measured flow and is calculated as follow:

$$R^2 = \frac{(\sum[Qoi-Qoav][Qsi-Qsav])^2}{\sum[Qoi-Qoav]^2 \sum[Qsi-Qsav]^2} \quad \text{.....17}$$

Where: Qo i is measured value, Qo av is average measured value, Qs i is simulated value, Qs av is average simulated value.

Nash and Sutcliffe simulation efficiency (NSE) indicates the degree of fitness of observed and simulated data and given by the following formula.

$$NSE = 1 - \frac{\sum(Qi - Qi)^2}{\sum(Qi - Qav)^2} \quad \text{.....18}$$

The value of NSE ranges from 1 (best) to negative infinity. If the measured value is the same as all predictions, NSE is 1. If the NSE is between 0 and 1, it indicates deviations between measured and predicted values. If NSE is negative, predictions are very poor, and the average value of output is a better estimate than the model prediction (Nash, J., Sutcliffe, J., 1970)

3.2.3.3. Impacts of Climate Change on Streamflow

The main goal of this study is to assess impacts of climate change on stream flow in case of Upper Omo River Basin. As explained above, Upper Omo River Basin has experienced climate changes in the period of 2000-2019 due to population growth rate which lead to resource competition. These changes of climate have an influence on stream flow. The daily observed stream flow data at the outlet of the basin (Abelti gauging station) in the upper Omo-Gibe river basin from 2000–2019 was collected from the hydrology department of the Ministry of Water, Irrigation, and Electricity. The stream flow data was used for calibrating and validating the SWAT model simulation.

Table 3.3. Gauging Stations at Upper Omo river basin

Station name	Longitude	Latitude
Nr. ABELTI	$8^0$14'N	$37^0$35'E

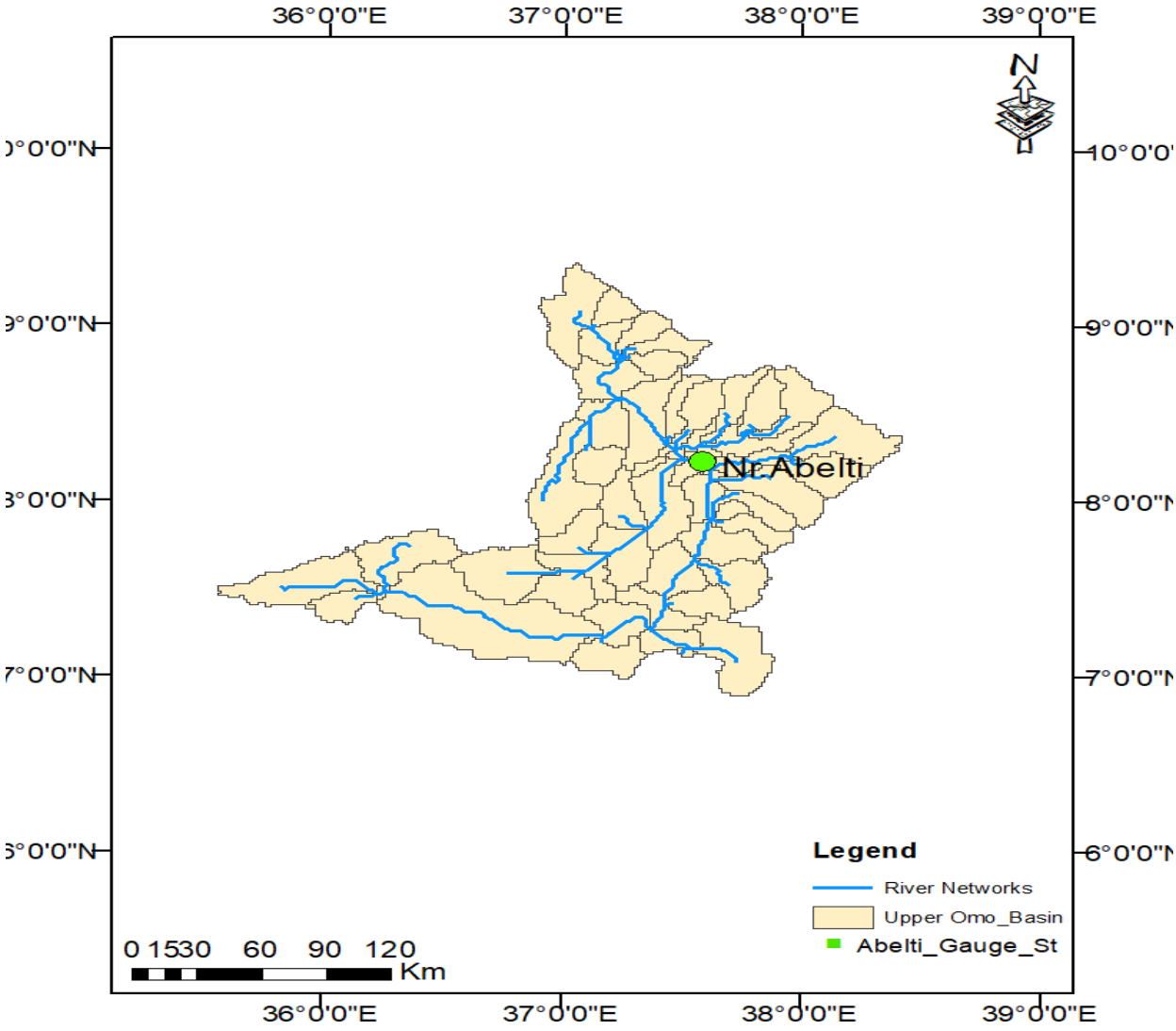

Figure 3.13. Gauging Stations at Upper Omo river basin

Table 3.4. Materials used in the study

Name	Description and Purpose
Arc – GIS 10.3	• Used for spatial analysis of hydrological and physical parameters.
SWAT	• Soil and Water Assessment Tool used for simulation.
SWAT - CUP	• A sensitivity analysis program interface of SWAT. • Used for calibration, sensitivity analysis, uncertainty measure and validation.
Distribution Mapping	• A climate data analysis tool. • Used to extract and bias correct data obtained from Global and Regional climate models.
Weather Generator	• For weather generator data preparation
EXCEL	• For hydro meteorological data homogeneity test.
XLSTAT	• Is an EXCEL add – in tool. • Used to prepare, describe, visualize and analyze hydro meteorological data.
DEM 30m * 3om	• Digital Elevation Model (30m*30m) spatial resolution for stream delineation.
Soil map (MoWE)	• The soil map of the study area is taken from the soil maps prepared by MoWE. • An input data for SWAT model simulation.
WCRP	• Coordinated Regional Climate Downscaling Experiment. • To obtain a downscaled historical and future climate data for Ethiopia and then extracted to upper Omo basin.
Meteorological data	• Rainfall, Temperature, Solar radiation, Wind speed and Relative humidity. • Used as an input data for SWAT simulation.
Hydrological data	• Stream flow data. • Used for model calibration and validation

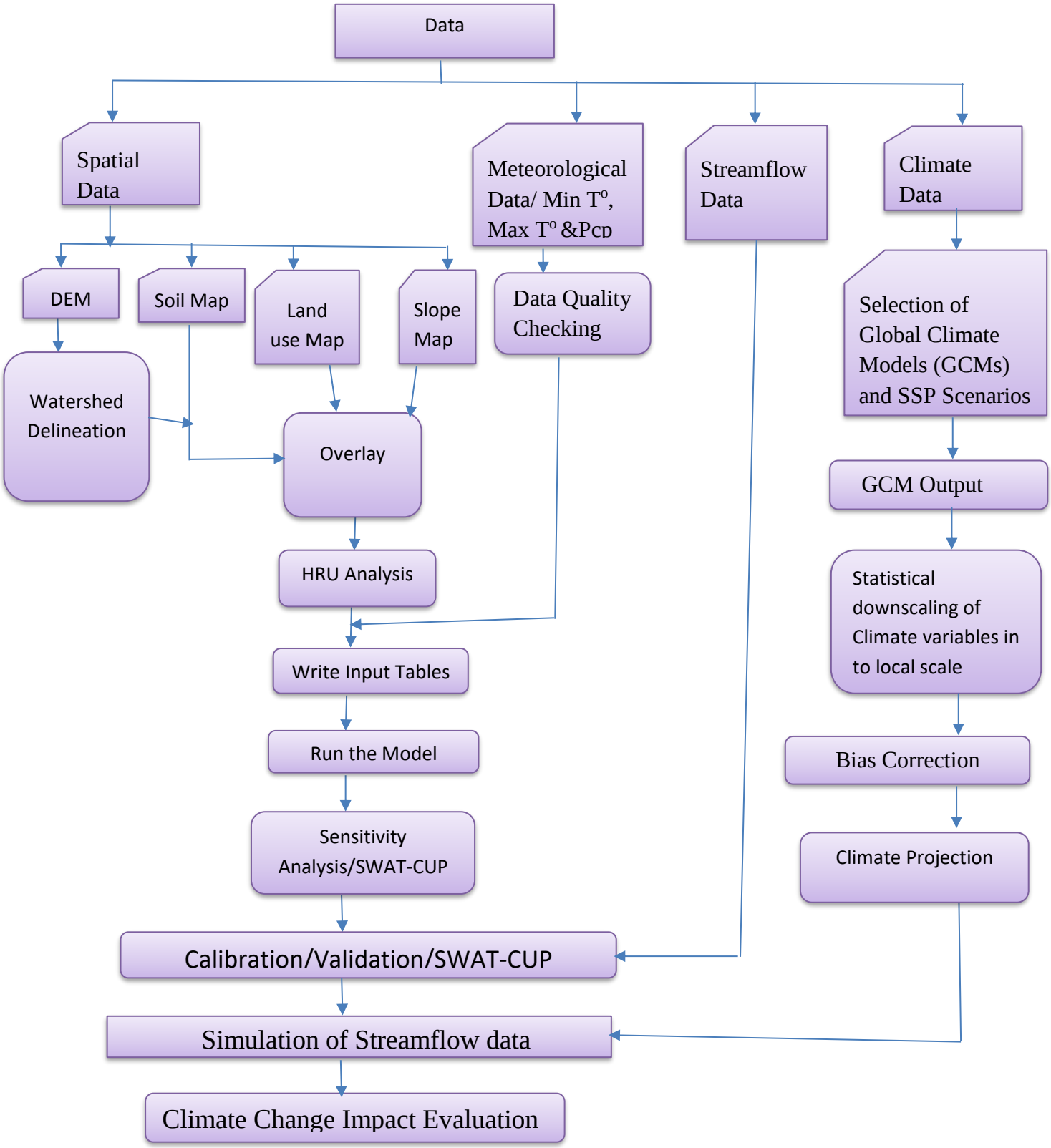

Figure 3.14. Flow chart for the general frame work of the study

4. Result and Discussion

4.1. Bias Correction of Precipitation and Temperature

The ensemble average monthly distribution of precipitation for five GCMs before and after bias correction against the observed data is shown in figure 4.1. All the five GCMs overestimated the historical uncorrected precipitation data at all months except in Jan. The maximum overestimation in the monthly precipitation was seen in Aug, while the minimum overestimation was in Dec. In Aug, the monthly precipitation was 226.49mm, while the ensemble GCM model was overestimated to be 304.88mm, which was found to be 213.55mm after bias correction. Similarly, in Dec, the observed precipitation was 29.24mm, but the ensemble GCM model overestimated it to be 32mm. After applying the bias correction, monthly precipitation was found to be 23.8mm. Similar tendencies were observed at other months when using those ensemble GCM models.

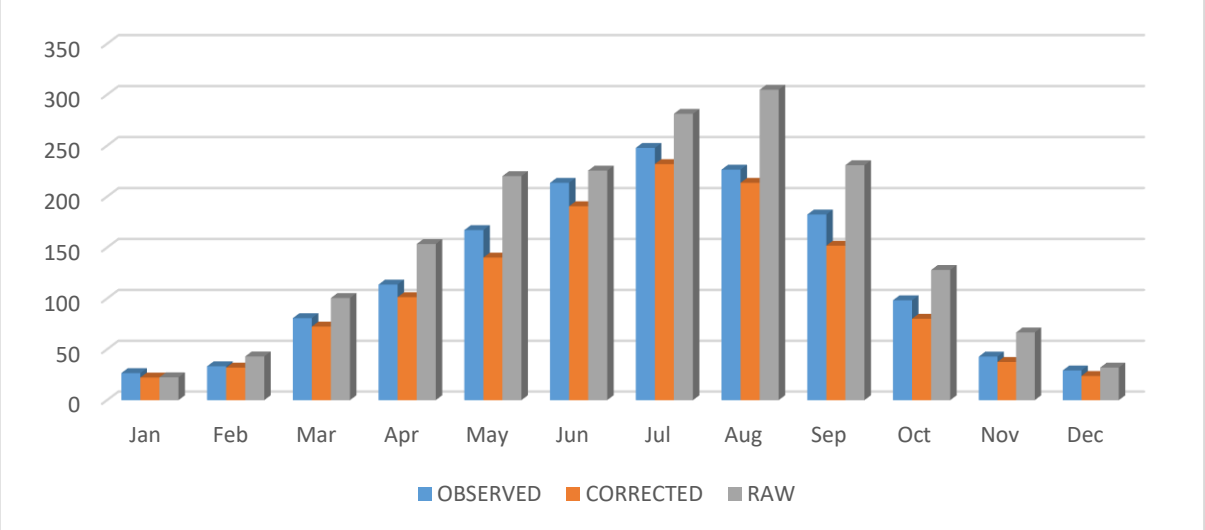

Figure 4.1. Comparison of observed and corrected rainfall for Upper Omo River Basin (1985-2019)

The ensemble mean monthly distribution of temperature for five GCMs before and after bias correction against the observed data is shown in figure 4.2. All the five GCMs overestimated the historical uncorrected temperature data at all months. The maximum overestimation in the monthly temperature was seen in Mar, while the minimum overestimation was in Jul. in Mar, the monthly precipitation was 20.4^{o}c, while the ensemble GCM model was overestimated to be 22.7^{o}c, which was found to be 20.36^{o}c after bias correction. Similarly, in Jul, the observed temperature was 17.6^{o}c, but the ensemble GCM model overestimated it

to be 18.6^{o}c. After applying the bias correction monthly precipitation was found to be 17.9^{o}c. Similar tendencies were observed at other months when using those ensemble GCM models.

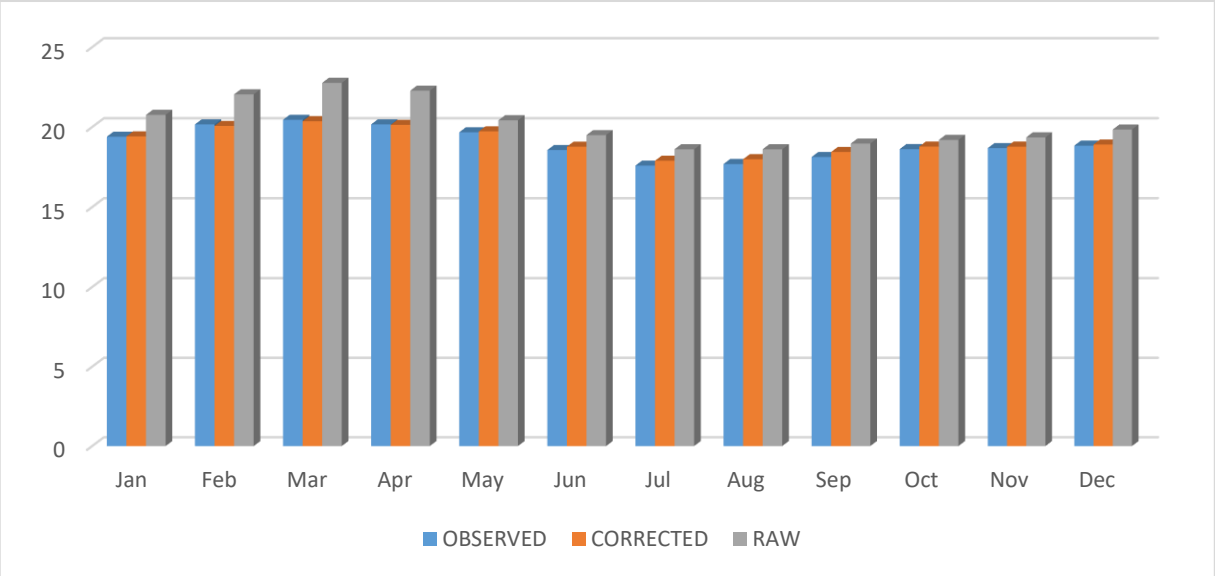

Figure 4.2. Comparison of observed and corrected mean monthly temperature for Upper Omo River Basin

4.2. Projected Changes in Annual and Seasonal Precipitation

The annual total and average annual precipitation of the river basin were assessed to be 8,819 mm and 1,469 mm, respectively, at the current count of the reference period (1985–2019) (Table 4.1). The future precipitation projection did not manifest the same increase or decrease all over the time horizons. However, future projection has shown considerable change. Annual precipitation amounts were projected under SSP2-4.5 and SSP5-8.5 emission scenarios for two future study periods. Projected annual precipitation under SSP2-4.5 and SSP5-8.5 emission scenarios for near study period show a significantly decreasing trend and an increasing trend for mid future, as shown in Table 4.1 and Figure 4.3.

Table 4.1. Annual precipitation projected

Years	Baseline and Projected total Annual Precipitation in (mm)	Projected change average annual precipitation in (mm)
PR_ Baseline period 1985-2019	8,819	1469
PR_SSP2-4.5_2020-2045	8,420	1403
PR_SSP2-4.5_2046-2071	8,873	1478
PR_SSP5-8.5_2020-2045	8,512	1418
PR_SSP5-8.5_2046-2071	10,174	1695

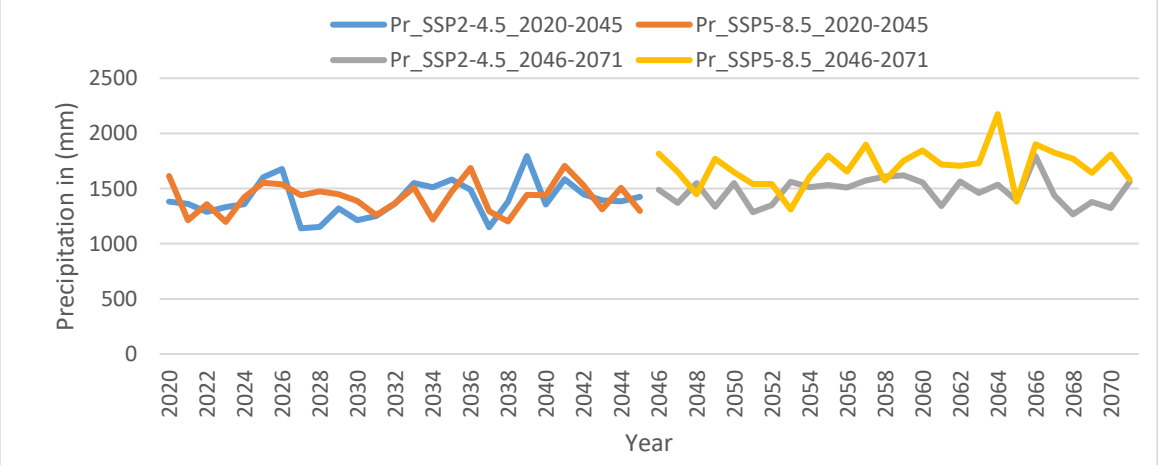

Figure 4.3. Projected annual precipitation change under SSP5-8.5 and SSP2-4.5 emission scenarios over (2020–2071).

The summer main rainy season (June–August) and spring (Feb-May) erratic rainy season precipitation projected under SSP2-4.5 and SSP5-8.5 emission scenarios assessed increasing and decreasing trend respectively as shown in Table 4.2. For the period of 2020–2045, the percentage change under SSP2-4.5 and SSP5-8.5 scenarios is projected to increase by 24.3% and 29.9% in the spring season, respectively and show a decrease by 0.03% and 0.68% in the summer season, respectively (Figure 4.4 and Figure 4.5). Similarly, for the period of 2046–2071, the percentage change under SSP2-4.5 and SSP5-8.5 scenarios is projected to increase by 24.8% and 21.96% in the spring season, respectively and show a decrease by 5.3% and 16.06% in the summer season, respectively (Figure 4.4 and Figure 4.5)

Table 4.2. Seasonal precipitation projected

Years	Projected change average precipitation during the main rainy season in (mm)	Percentage change projected average precipitation in the main rainy season (%)	Projected change average precipitation during the erratic rainy season in (mm)	Percentage change projected average precipitation in the erratic rainy season (%)
PR_SSP2-4.5_2020-2045	697.7	-0.03	329	24.3
PR_SSP2-4.5_2046-2071	748.6	-5.3	321.4	24.8
PR_SSP5-8.5_2020-2045	703.4	-0.68	319.1	29.9
PR_SSP5-8.5_2046-2071	848.4	-16.06	342.7	21.96

Projected precipitation changes in annual amount and seasonal distribution for two future periods were assessed and compared to the basin's reference period under SSP2-4.5 and SSP5-8.5 emissions scenarios. The results in (mm) indicate that the annual quantity and seasonal distribution of the main rainy seasons during the summer from June to August will increase but, the erratic rainy season(spring) from March to May will decrease expectedly compared to the reference periods (Tables 4.1 and 4.2).

In 2020, the SSP2-4.5 scenario showed a monthly mean precipitation decrease up to 12.2% and monthly mean precipitation increase reach up to 43.66%. On the same fashion SSP5-8.5 scenario shows a monthly decrease up to 32.23% and percentage increment up to 9.51% in different months. In 2046, the SSP2-4.5 scenario showed a monthly mean precipitation decrease up to 21.01% and monthly mean precipitation increase reach up to 42.35%. And also, SSP5-8.5 scenario shows a monthly decrease up to 54.89% and percentage increment up to 51.25% in different months.

In general, for near term the annual precipitation increase by 4.5% and 3.8% for SSP2-4.5 and SSP5-8.5 respectively. For midterm the annual precipitation decrease by 0.6% and 15% for SSP2-4.5 and SSP5-8.5 respectively.

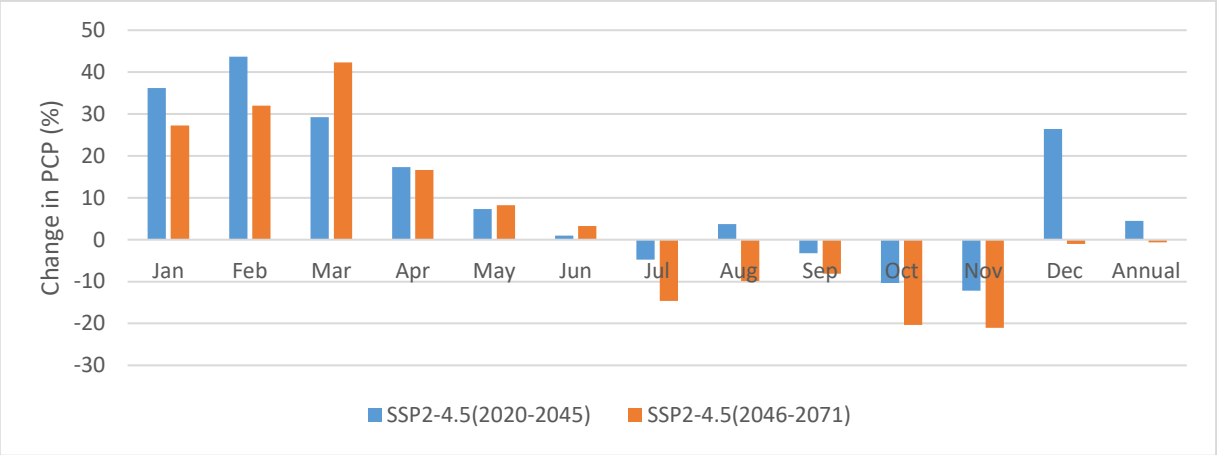

Figure 4.4. Mean monthly Precipitation change under SSP2-4.5 scenario

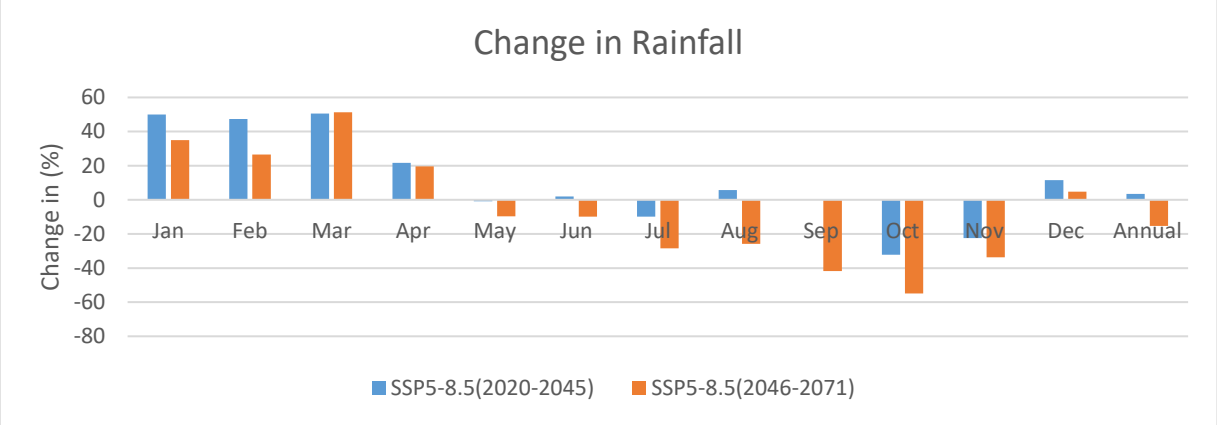

Figure 4.5. Mean monthly Precipitation change under SSP5-8.5 scenario

4.3. Trend Analysis of Annual and Seasonal Precipitation

Based on the Mann Kendall trend test trend Changes in annual and seasonal precipitation were assessed. The results of the trend test revealed decreasing trends in the baseline and projected annual and seasonal (Kiremt and Belg) precipitation. In the average annual precipitation at six weather gauging stations in the upper Omo River Basin were analyzed. The annual average precipitation change results showed a decreasing trend at the four meteorological gauging stations. (Fig.4.6)

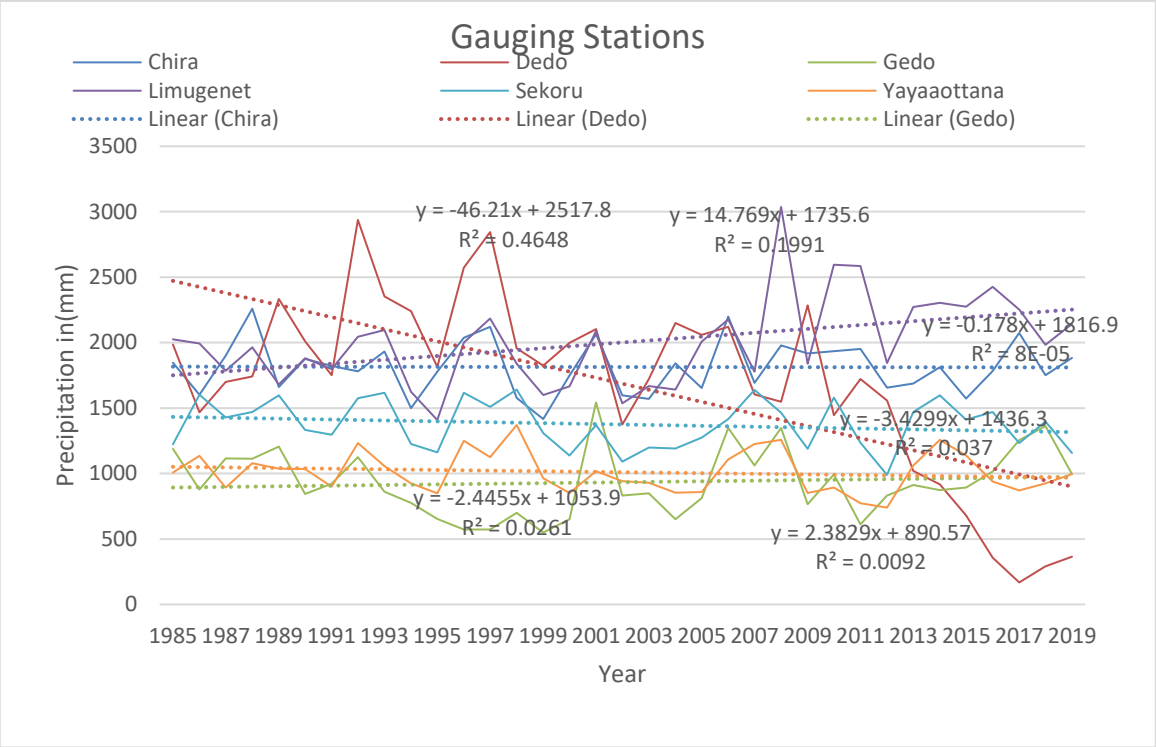

Figure 4.6. Observed annual precipitation changes in Upper Omo River Basin over the period (1985–2019).

Based on the Mann Kendall trend test, the mean annual rainfall showed a decreasing trend in four out of six stations. However, only two stations (Limugenet and Dedo) have experienced statistically significant changes evaluated at a 0.05 significance value ($P<0.05$). The rainfall decreased at Dedo with $Z=-2.49$ where as it increased at Limugenet with $Z=2.21$. The Seasonal trend test revealed heterogeneous results both for the Belg and Kiremt seasons. In the Kiremt season, decline of rainfall was observed in five out of six stations, but only Dedo station has experienced a statistically significant decrease with $Z=2.42$ at 0.05 significance level ($P<0.05$). The remaining one station showed an increasing trend but not significant trend. However, during the Belg season, an increasing trend was observed in four out of six stations but the trend wasn't statistically significant for all stations. The remaining two stations showed a decreasing trend, but only one station (Dedo) showed a statistically significant decrease with $Z=-1.98$ at 0.05 significance level ($P<0.05$).

Table 4.3. Results of Mann-Kendall test for annual and seasonal Rainfall at six stations

Station Name	Mean Annual PCP	Annual		Kiremt		Belg	
		P-Value	Z-Value	P-Value	Z-Value	P-Value	Z-Value
Chira	1813.7	0.95	0.78639	0.570	0.1821	0.320	1.02952
Dedo	1686.1	0.00	**-2.4945**	0.001	**-2.42**	0.000	**-1.98293**
Gedo	933.5	0.65	-1.2267	0.394	-1.19581	0.955	-1.24816
Limugenet	2001.4	0.018	**2.21569**	0.118	-1.6147	0.094	0.79432
Sekoru	1374.6	0.29	-0.2178	0.069	-0.16987	0.670	0.13291
Yayaaottana	1009.9	0.35	-1.0520	0.798	-0.85111	0.244	1.1257

***Bold numbers indicate statistically significant trends at 0.05 level**

As shown in Figure 4.7 and Table 4.4, the trend analyzed result, which projected annual precipitation under SSP5-8.5 and SSP2-4.5 emission scenarios, shows significant increasing trends in the river basin over two future periods.

Table 4.4. Results of Mann-Kendall test for projected mean annual Rainfall

Time	P-Value	Sen's Slope	Z-Value	Minimum	Maximum	Mean	Std. deviation
RCP4.5_2020-2045	0.016	4.21	**2.709**	1139.80	1794.54	1403.40	163.16
RCP4.5_2046-2071	0.029	0.36	**1.950**	1266.02	1794.23	1478.90	124.10
RCP8.5_2020-2045	0.001	0.49	**3.596**	1197.85	1705.97	1418.67	143.17
RCP8.5_2046-2071	0.017	5.88	**3.45565**	1310.38	2174.73	1695.74	179.83

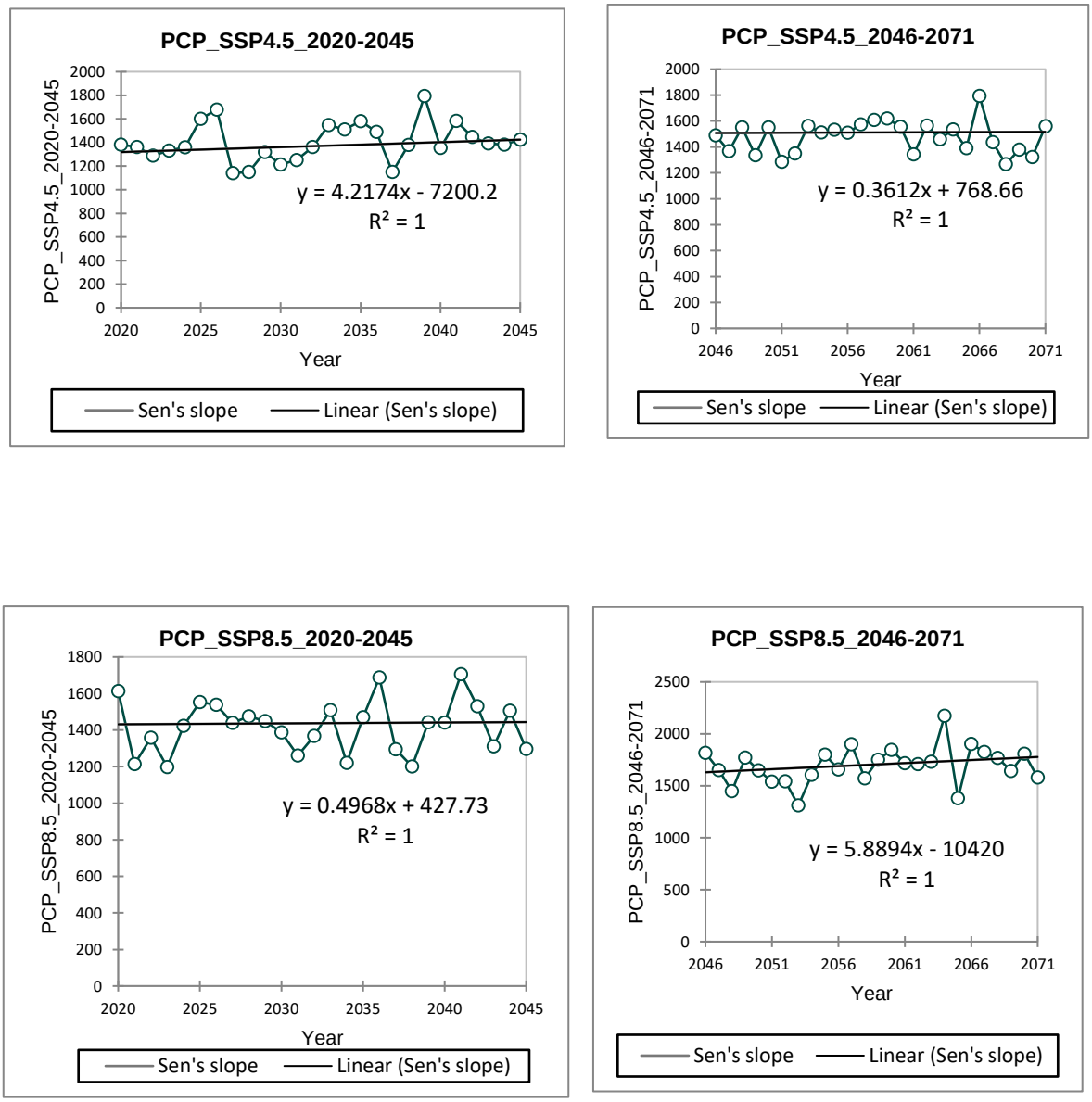

Figure 4.7. Projected annual mean precipitation trends under SSP2-4.5 and SSP5-8.5 for two future study periods (2020-2071) using a Mann Kendall test

Generally, the trends were not statistically significant at a monthly time scale for all of the investigated climate stations. However, there is an increase and decrease in the stations. The trend test of projected Kiremt season precipitation distributions under SSP2-4.5 emission scenarios in near future time period revealed significant increasing trend with Z=2.743 but, in mid future time period revealed insignificant increasing trend and SSP5-8.5 emission scenarios in two future study periods revealed insignificant increasing trend ($P<0.05$).

Table 4.5. Results of Mann-Kendall test for summer season projected Rainfall

	P-Value	Sen's Slope	Z-Value	Minimum	Maximum	Mean	Std. deviation
RCP4.5_2020-2045	0.043	5.15	**2.743**	546.9	898.3	697.6	92.6
RCP4.5_2046-2071	0.567	1.21	0.012	640.2	907.8	748.6	61.2
RCP8.5_2020-2045	0.146	2.41	0.661	546.1	871.8	703.3	63.6
RCP8.5_2046-2071	0.058	5.18	1.41756	703.3	1003.4	848.4	91.3

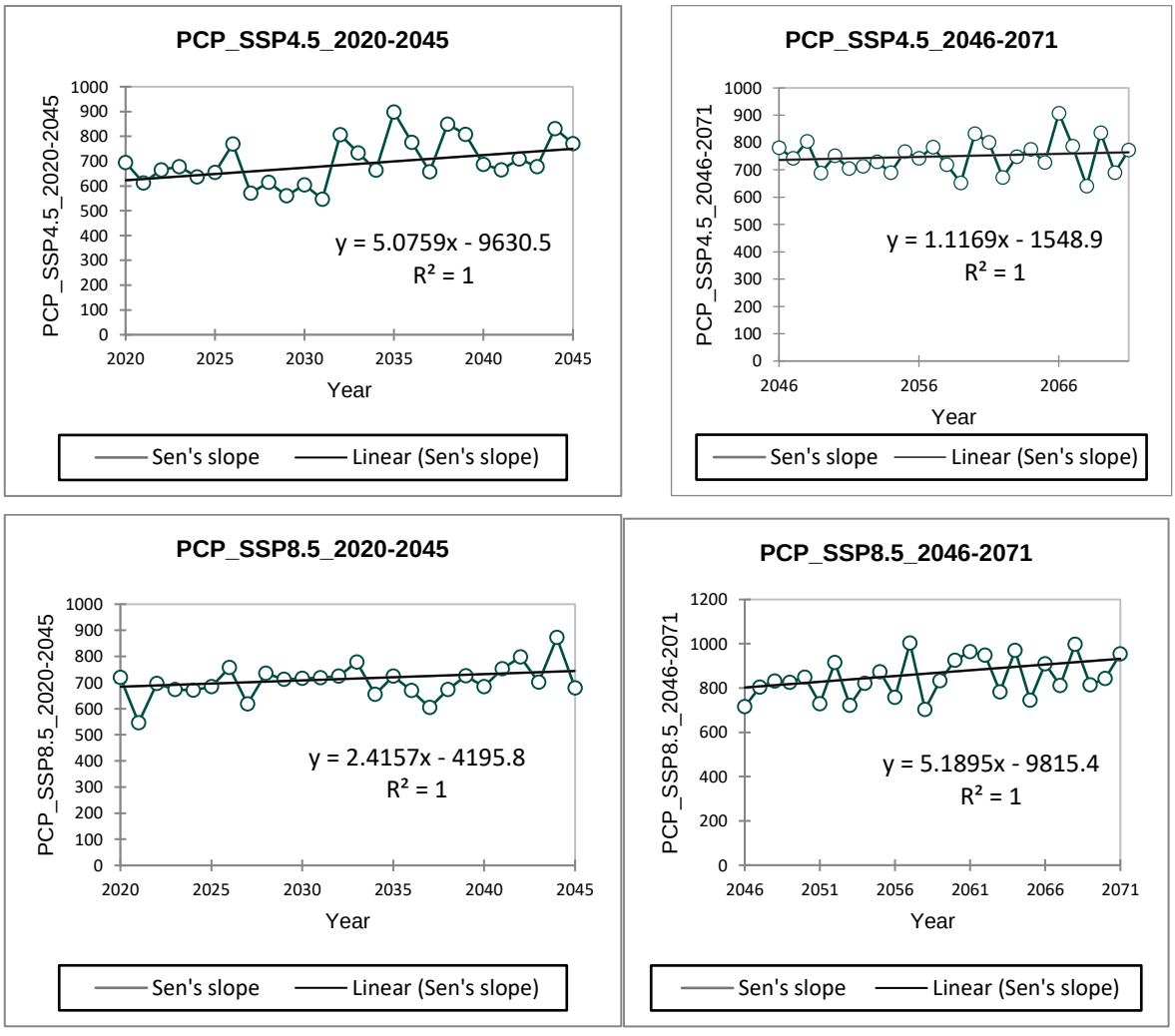

Figure 4.8. Projected annual mean summer season precipitation trends under SSP2-4.5 and SSP5-8.5 for two future study periods (2020-2071) using a Mann Kendall test

The trend test of projected Belg precipitation distributions under SSP2-4.5 shows insignificant decreasing trend for near future and significant increasing trend for mid future with Z=1.95 and SSP5-8.5 emission scenarios for mid future study periods revealed insignificant increasing trend (P>0.05) but, under SSP5-8.5 emission scenario for near future study period projected Belg precipitation showed significant increasing trend with Z=3.63.

Table 4.6. Results of Mann-Kendall test for spring season projected Rainfall

	P-Value	Sen's Slope	Z-Value	Minimum	Maximum	Mean	Std. deviation
RCP4.5_2020-2045	0.158	-3.81	-0.3448	166.8	476.3	310.1	84.9
RCP4.5_2046-2071	0.027	-1.00	**1.9552**	207.1	387.1	298.6	44.5
RCP8.5_2020-2045	0.0071	-4.53	**3.6387**	208.3	500.5	301.4	76.2
RCP8.5_2046-2071	0.895	-0.26	1.24922	212.4	481.1	318.1	79.6

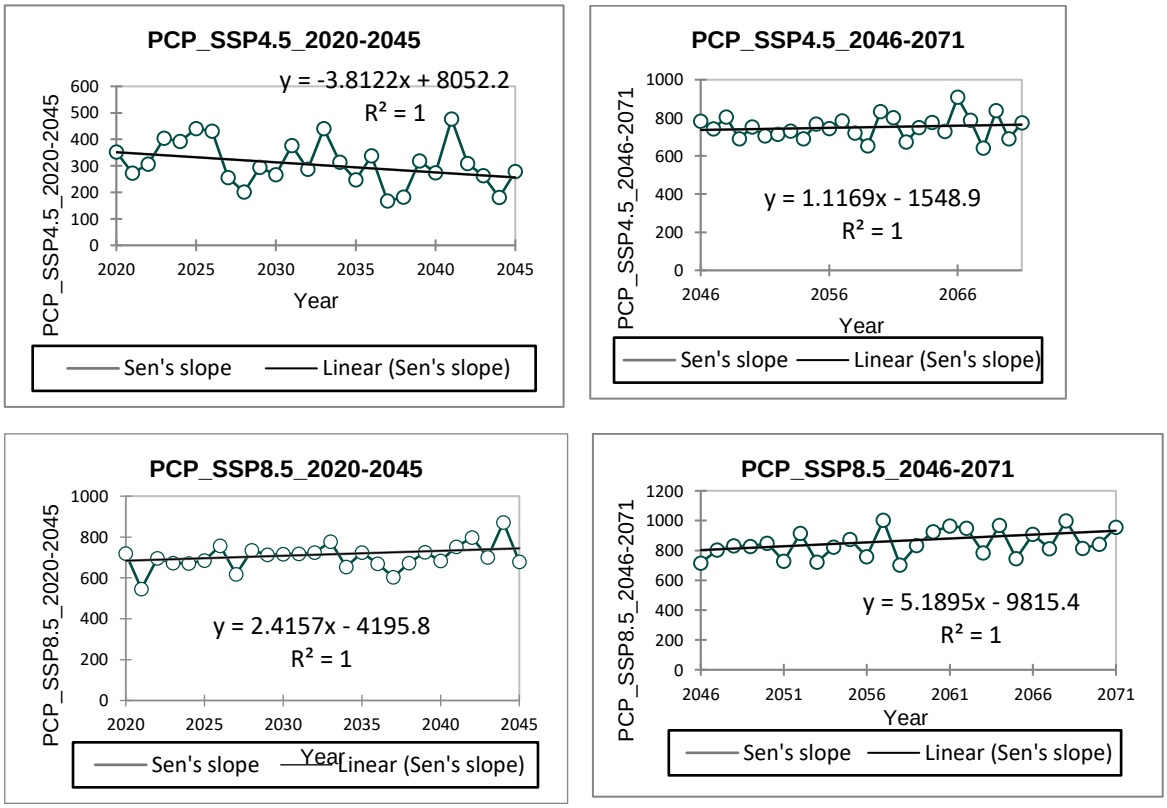

Figure 4.9. Projected annual mean spring season precipitation trends under SSP2-4.5 and SSP5-8.5 for two future study periods (2020-2071) using a Mann Kendall test

4.4. Projected Changes in Annual and Seasonal Temperature

Changes in temperature projections from downscaled Coupled Model Intercomparison Project 6 global climate model output data. Six averages of the bias-adjusted temperature output and each individual average revealed a greater predicted temperature change than the reference period, as indicated in Figures 4.10. According to the graph (Figure 4.10), the reference period's annual mean, maximum, and lowest temperatures were 19.01^{o}c, 25.62^{o}c, and 12.4^{o}c respectively. Evaluation and comparison with the reference period were done for the projected annual average maximum and minimum temperatures under the SSP2-4.5 and SSP5-8.5 emission scenarios. According to the results of the projected annual average temperature under the SSP2-4.5 and SSP5-8.5 emission scenarios, there is an increase in the river basin's temperature during the three future periods compared to the reference period (Figure4.3).

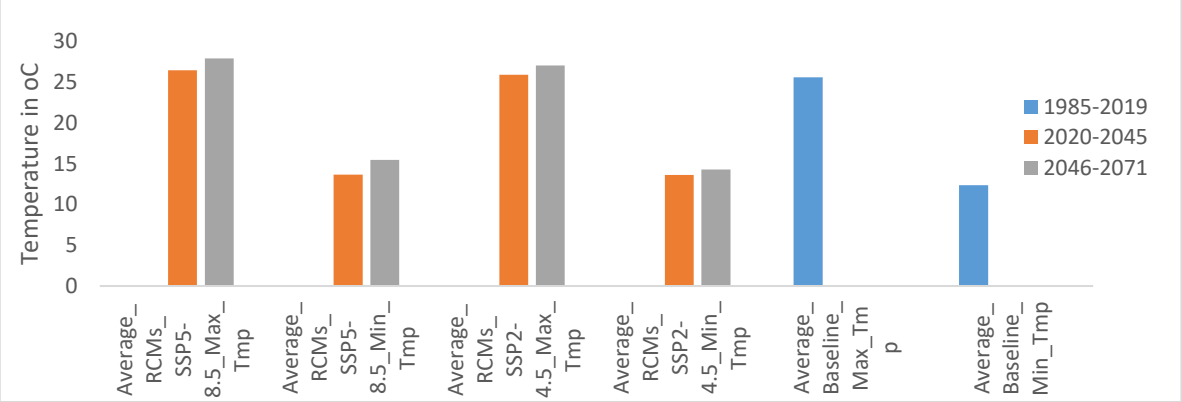

Figure 4.10. Changes in annual average maximum and minimum temperatures projected in the SSP2-4.5 and SSP5-8.5 emissions scenarios over the period (2020-2071) and observed over the period (1985-2019)

As shown in Figures 4.11 and 4.12, the trend analyzed result, which projected annual minimum and maximum temperatures under SSP5-8.5 and SSP2-4.5 emission scenarios, shows an increasing trends in the river basin over three future periods.

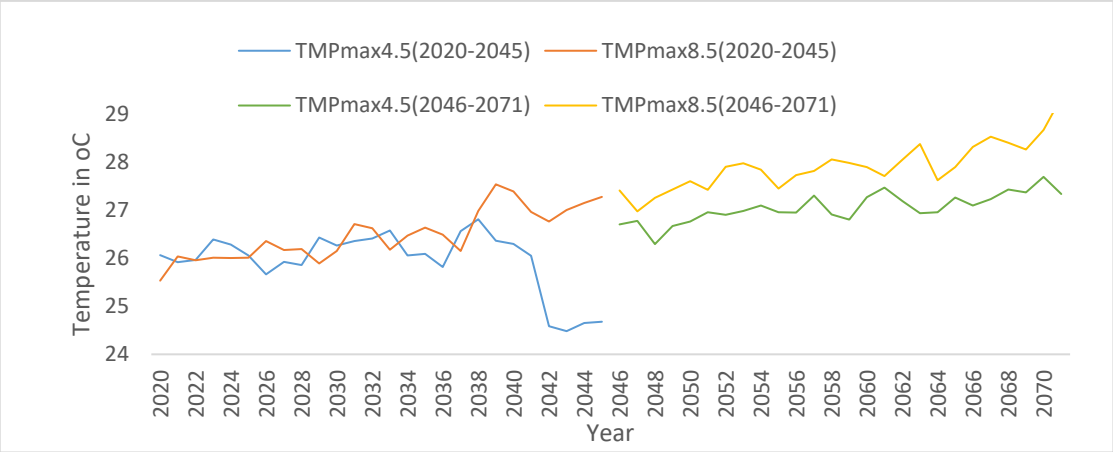

Figure 4.11. Projected change in annual maximum temperature under SSP2-4.5 and SSP5-8.5 emission scenarios during (2020-2071)

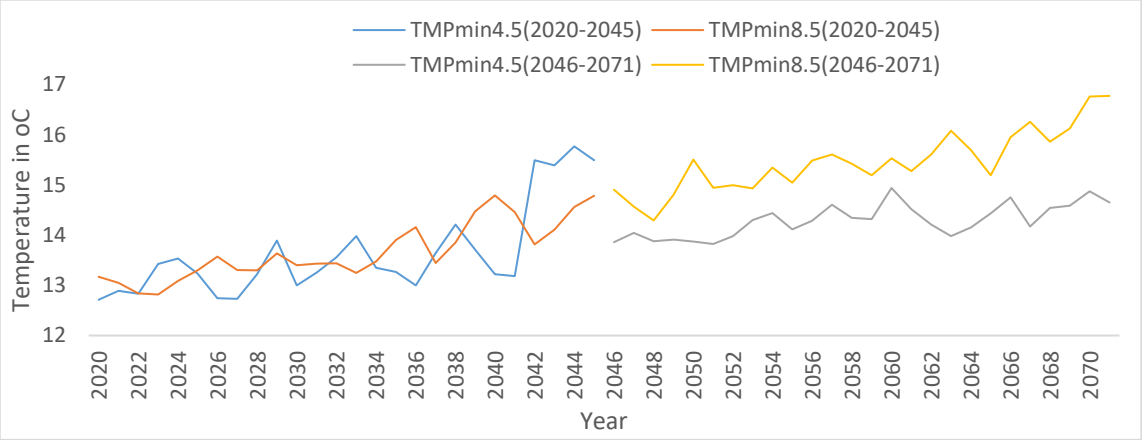

Figure 4.12. Projected change in annual minimum temperature under SSP2-4.5 and SSP5-8.5 emission scenarios during (2020-2071)

In near future time period, almost all the future projection of maximum temperature under SSP2-4.5 has shown increasing trend. But, there is a probability of those 4months Feb, Apr, Oct and Nov maximum temperature to be decreased by 0.12%, 0.13%, 0.05% and 0.19% respectively. In mid future time period the highest absolute mean monthly difference from the baseline temperature is found at the month of July. This shows a temperature increase by 2.78^{o}c (12.32%). In general, the annual maximum temperature may increase by 1.28% and 5.58% for near and mid future time period respectively. (Fig. 4.13)

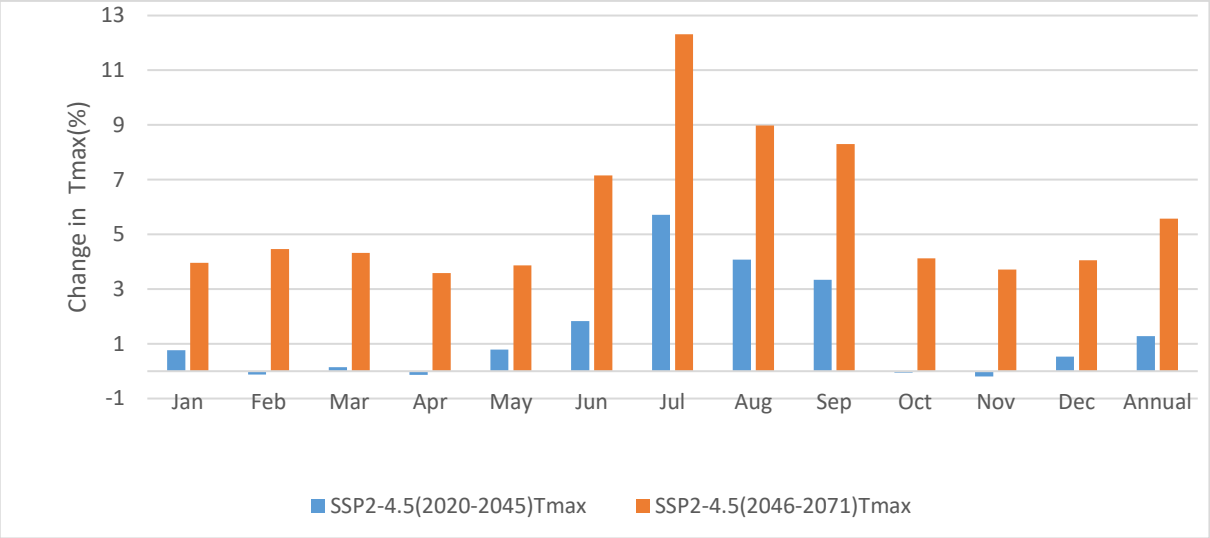

Figure 4.13. Mean monthly maximum temperature change under SSP2-4.5 scenario

In near future time period, all the future projection of maximum temperature under SSP5-8.5 has shown increasing trend. The highest temperature increment will be expected on July. The change may exceed 1.75^{o}c (7.77%). In mid future time period the highest absolute mean monthly difference from the baseline temperature is found at the month of July. This shows a temperature increase by 17.57 %(3.97^{o}c). In general the annual maximum temperature may increase by 3.37% and 8.97% for near and mid future time period respectively. (Fig.4.14)

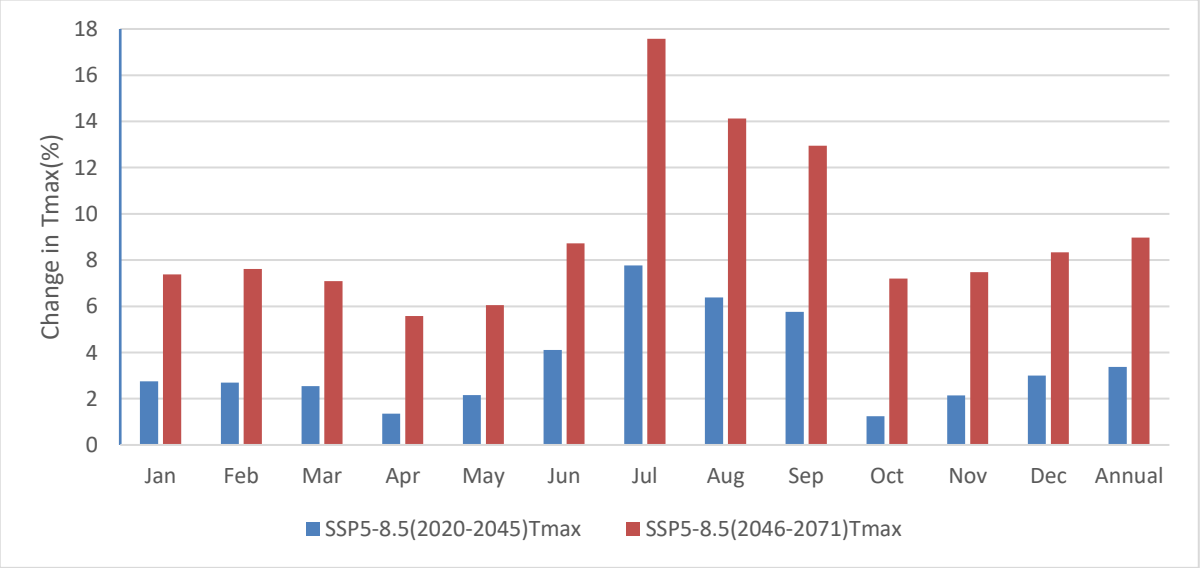

Figure 4.14. Mean monthly maximum temperature change under SSP5-8.5 scenario

Minimum temperature projection shows an increasing trend for both SSP2-4.5 scenario and SSP5-8.5 scenario. In near future time period (2020-2045) all the future projection of minimum temperature under SSP2-4.5 has shown increasing trend for all months. The highest increment of minimum temperature is expected to be during Jul and Sep. The change may exceed 2.04^{o}c (16.17%) and 2.05^{o}c (16.56%). And also the future projection of minimum temperature in 2046-2071 under SSP2-4.5 has shown increasing trend for all months. The highest increment is expected to be during Jul and Aug. This shows a temperature increase by 3.3^{o}c (26.15%) and 3^{o}c (23.94%) respectively. In general the annual minimum temperature projection under SSP2-4.5 scenario has revealed significant increase by 10.23 %(1.27^{o}c) and 15.46 %(1.92^{o}c) at near and mid time period respectively. (Fig. 4.15)

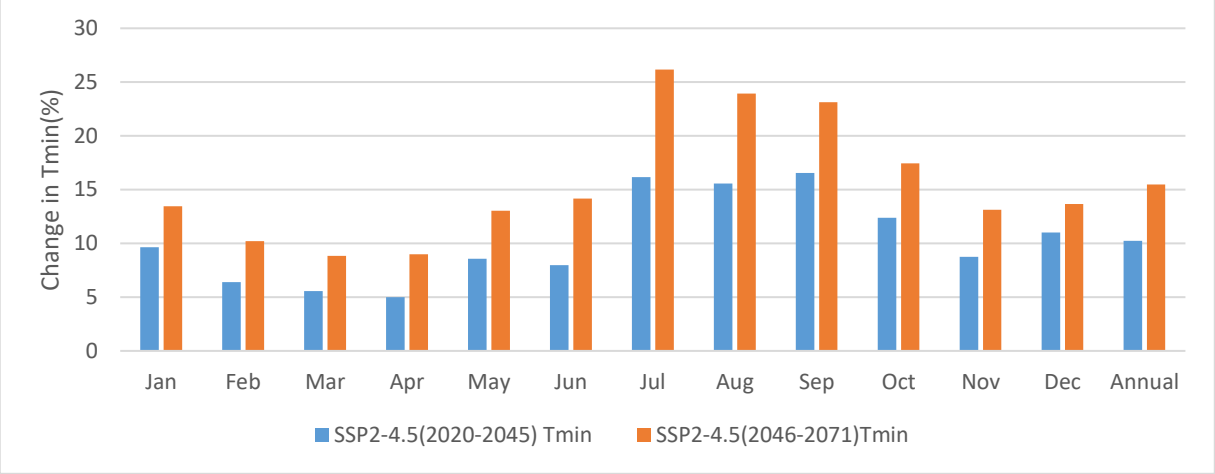

Figure 4.15. Mean monthly minimum temperature change under SSP2-4.5 scenario

Under SSP5-8.5 scenario in near future time period (2020-2045) all the future projection of minimum temperature has shown increasing trend for all months. The highest increment of minimum temperature is expected to be during Jul and Aug. This shows a temperature increase by 2.26^{o}c (17.94%) and 2.23^{o}c (17.75%) respectively. In mid future under SSP5-8.5 has shown increasing trend for all months. The highest increment is expected to be during Jul and Aug. This shows a temperature increase by 5.06^{o}c (40.16%) and 4.6^{o}c (36.7%) respectively. In general the annual minimum temperature projection under SSP5-8.5 scenario has revealed significant increase by 10.4 %(1.29^{o}c) and 24.96 %(3.09^{o}c) at near and mid time period respectively. (Fig.4.16)

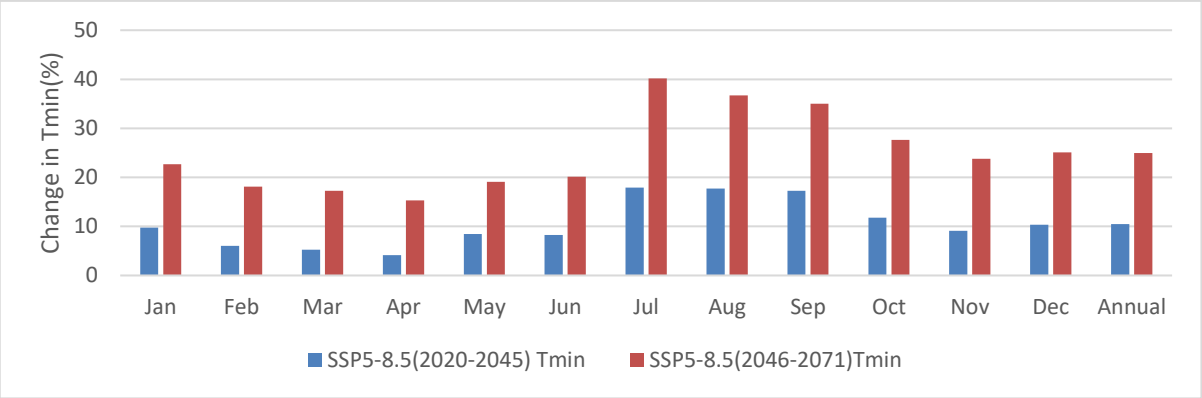

Figure 4.16. Mean monthly minimum temperature change under SSP5-8.5 scenario

Generally, the projected annual average minimum temperature under SSP2-4.5 emission scenarios increases the range between 1.2-1.9 ^{o}C while under SSP5-8.5 emission scenarios increase the range between 1.3-3.09 ^{o}C shown as (Figure 4.15 and 4.16). Also, the projected change in annual average maximum temperature under SSP2-4.5 emission scenarios increases the range between 0.3-1.43^{o}C while under SSP5-8.5 emission scenarios increase the range between 0.86-2.3^{o}C shown as (Figure 4.13 and 4.14). Temperature change under SSP5-8.5 emission scenarios is larger and more severe than under SSP2-4.5 emission scenarios, according to this study. This indicates that SSP5-8.5 has the largest carbon emission scenario compared to SSP2-4.5. The findings of this investigation corroborated those of a prior study (IPCC, 2014).

The changes in minimum and maximum temperatures for each month were examined. The results showed that under SSP2-4.5 and SSP5-8.5 emission scenarios, future minimum and maximum temperatures are expected to increase in comparison to reference periods. The mean monthly minimum temperature estimated under the SSP2-4.5 and SSP5-8.5 emission scenarios is lower during the two seasons (winter and spring), however, it is greater during the two wet. Season (summer and fall) (Figure 4.17)

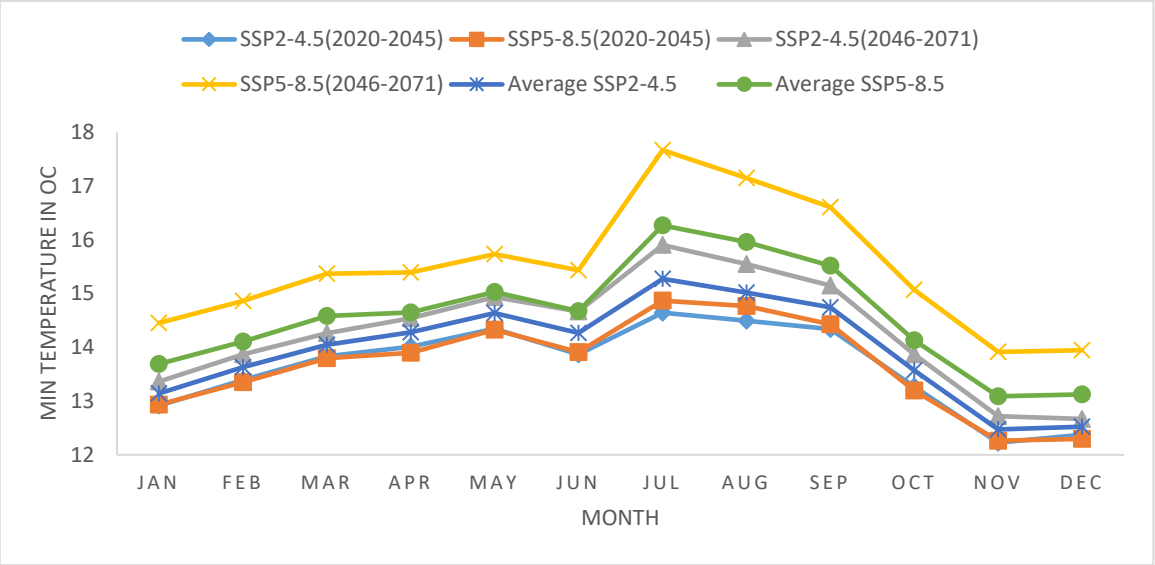

Figure 4.17. Projected monthly minimum temperature change under SSP2-4.5 and SSP5-8.5 emission scenarios over (2020–2071)

The mean monthly maximum temperature estimated under SSP2-4.5 and SSP5-8.5 emission scenarios is higher during the spring and winter seasons, or hot and dry months (Dec, Jan, Feb, Mar, Apr, and May), and lower during the two rainy seasons, summer and fall (Jun, Jul, Aug, Sep, Oct ,and Nov).Figure 4.18 depicts this.

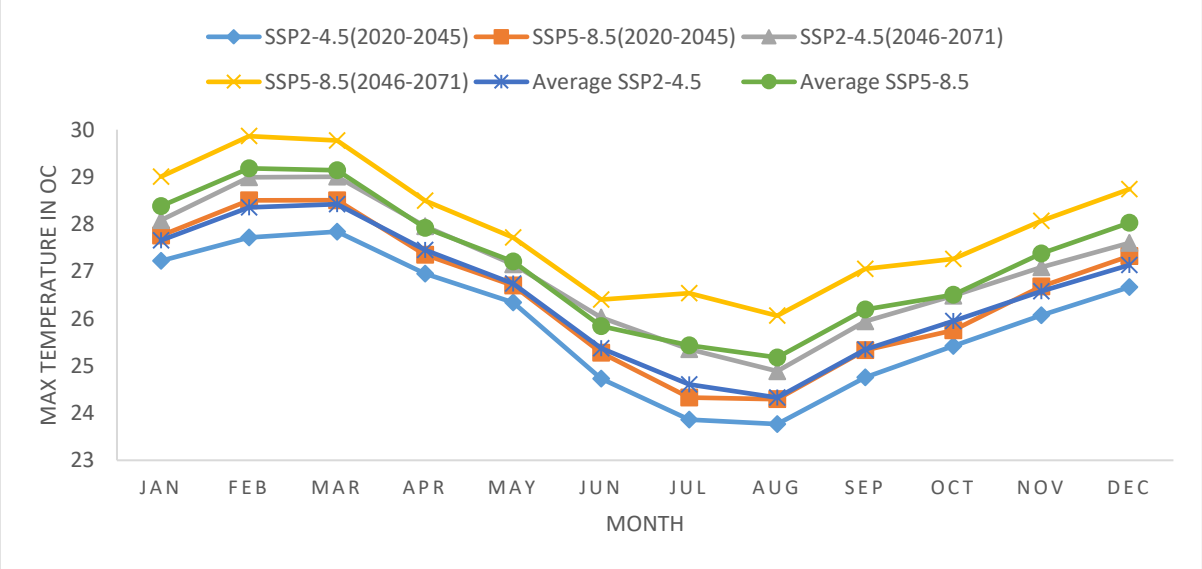

Figure 4.18. Projected monthly maximum temperature change under SSP2-4.5 and SSP5-8.5 emission scenarios over (2020–2071)

The increase in temperatures, according to (Eromo et al. 2016) and (Abdulahi et al. 2022) can lead to an increase in precipitation in certain areas, which is related to the length of the

seasonal distribution and the amount of precipitation. On the other hand, an increase in Temperature according to (Emiru et al. 2022) can lead to a decrease in precipitation, it is because of raise in temperature enhances evaporation, which reduces surface water and dries out soils and vegetation. This makes periods with low precipitation. High temperatures can improve the ability to increase evapotranspiration, lower soil moisture content, increase the number of days in which warm air holds more water vapor per year and increase water availability. This means that for the same quantity of precipitation, high amount of rain will reach river streams, enhancing streamflow. Rises in temperature, will have an impact on water availability. This is partly because as temperatures rise, larger evaporation rates are predicted. In the future, Upper Omo gibe River Basin is predicted to see higher temperatures and more water stress.

4.5. Trend Analysis of Annual and Seasonal Temperature

Based on the Mann Kendall trend test and trend Changes in annual and seasonal maximum and minimum temperatures were assessed. The results of the trend test revealed statistically significant positive increasing trends in the baseline and projected annual and seasonal (summer and spring) maximum and minimum temperatures. In the average annual temperature at six weather gauging stations in the upper Omo River Basin were analyzed. The annual average temperature change results showed an increasing trend at six meteorological gauging stations. (Fig. 4.19)

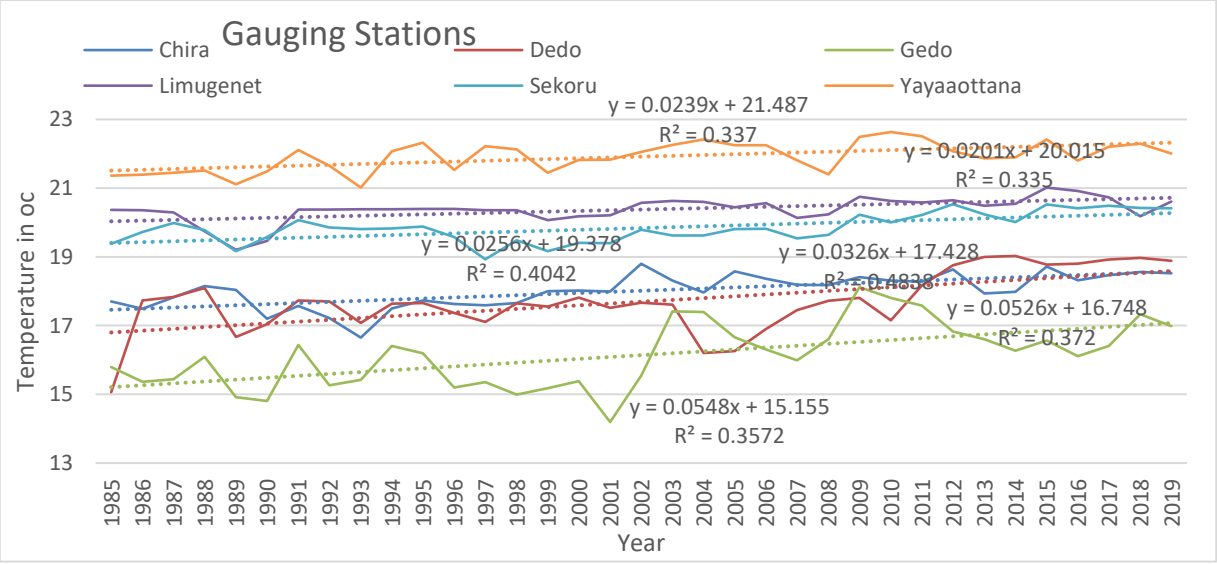

Figure 4.19. Annual average temperature changes in Upper Omo River Basin during (1985-2019)

In the Baseline period (1985–2019), the mean annual temperature for most stations showed significant increasing trend with P-value<0.05 and Z-value >1.96 but only Gedo station showed insignificant increasing trend with Z=1.08. The mean seasonal temperature (Kiremt) showed significant increasing trend for Gedo, Sekoru and Yayaaottana with Z-value=2.12, 1.97 and 2.40 respectively. And also the mean seasonal temperature (Belg) revealed both significant decreasing and increasing trend for all stations except Gedo station with P-value<0.05 and Z-value >1.96.(Table 4.7).

Table 4.7. Results of Mann-Kendall trend test for annual and seasonal mean Temperature at six stations

Station Name	Mean Annual TMP(^{o}c)	Annual		Summer		Spring	
		P-Value	Z-Value	P-Value	Z-Value	P-Value	Z-Value
Chira	23.9	0.000	**2.08115**	0.086	0.517	0.000	**-4.36397**
Dedo	23.5	0.001	**2.656**	0.006	0.784	0.001	**-2.46871**
Gedo	22.4	0.650	1.08895	0.023	**2.120**	0.691	-1.51825
Limugenet	27.2	0.001	**2.33601**	0.006	0.6797	0.002	**3.2177**
Sekoru	26.3	0.001	**1.96133**	<0.0001	**1.9726**	0.001	**2.722**
Yayaaottana	30.4	<0.0001	**1.9931**	0.023	**2.40511**	0.001	**1.97193**

The annual maximum temperature revealed significant increasing trend for all stations except Gedo station with Z>1.96, in contrast the annual minimum temperature for most stations showed significant decreasing trend except Yayaaottana and Sekoru with Z>1.96and P-value<0.05. (Table 4.7)

Table4.8. Results of Mann-Kendall trend test for annual max and min Temperature at six stations

Station	TMP	P-Value	Sen's Slope	Z-Value	Minimum	Maximum	Mean	Std. deviation
Chira	TMPmin	<0.0001	0.030	**-1.9817**	10.193	12.857	12.088	0.524
	TMPmax	0.000	0.035	**2.809**	22.760	25.470	23.941	0.580
Dedo	TMPmin	0.031	0.025	**-1.9846**	6.608	13.458	11.849	1.226
	TMPmax	0.001	0.068	**2.0725**	22.093	25.528	23.541	1.060
Gedo	TMPmin	<0.0001	0.092	**-2.2503**	6.333	13.421	9.920	1.437
	TMPmax	0.650	0.006	0.4634	21.169	24.441	22.362	0.848

Limugenet	TMPmin	0.000	0.010	**-1.9644**	12.372	14.232	13.593	0.373
	TMPmax	0.001	0.016	**2.1246**	26.037	27.913	27.162	0.393
Sekoru	TMPmin	0.007	0.030	-0.7674	11.990	14.274	13.426	0.592
	TMPmax	0.001	0.032	**1.9992**	24.638	27.267	26.252	0.524
Yayaaottana	TMPmin	0.570	0.006	-0.7728	12.147	14.443	13.387	0.524
	TMPmax	<0.0001	0.042	**2.5771**	29.229	31.723	30.447	0.615

The maximum seasonal temperature (Belg) for Chira, Dedo, Limugenet, Sekoru and Yayaaottana revealed significant increasing trend with Z=2.93, Z=2.54, Z= 2.58, Z=2.03 and Z=2.57 respectively, in contrast the minimum seasonal (Belg) temperature for most stations except Dedo and Yayaaottana showed significant decreasing trend with Z>1.96.

Table 4.9. Results of Mann-Kendall trend test for spring season max and min Temperature at six stations

Station	TMP	p-value	Sen's slope	Z-Value	Minimum	Maximum	Mean	Std. deviation
Chira	TMPmin	<0.0001	0.043	**-1.9806**	9.71	14.00	12.62	0.812
	TMPmax	0.000	0.048	**2.93807**	22.49	26.57	24.96	0.912
Dedo	TMPmin	0.334	0.014	-0.0606	5.02	13.54	12.01	1.455
	TMPmax	0.001	0.060	**2.54082**	21.67	26.16	24.21	1.098
Gedo	TMPmin	0.003	0.066	**-2.2776**	6.73	12.70	10.36	1.368
	TMPmax	0.691	0.008	0.46877	21.68	25.46	23.67	0.955
Limugenet	TMPmin	0.001	0.015	**-3.7081**	13.16	15.93	14.70	0.461
	TMPmax	0.002	0.023	**2.5855**	26.86	29.74	28.92	0.619
Sekoru	TMPmin	0.021	0.026	**-3.7412**	10.38	15.82	14.45	0.898
	TMPmax	0.001	0.029	**2.03099**	25.71	29.73	27.95	0.738
Yayaaottana	TMPmin	0.609	0.005	-0.6462	12.34	16.57	15.17	0.753
	TMPmax	0.001	0.051	**2.57733**	30.08	34.41	32.11	0.955

***Bold numbers indicate statistically significant trends at 0.05 level**

The maximum seasonal temperature (Kiremt) for Gedo, Sekoru and Yayaaottana stations revealed a significant increasing trend with Z-Value=3.35, Z-value=2.98 and Z-value=3.5 and P-value<0.05 respectively, in contrast the minimum seasonal (Kiremt) temperature for all stations showed significant decreasing trend except Sekoru and Yayaaottana with p-value<0.05 and Z-value>1.96.

Table 4.10. Results of Mann-Kendall trend test for summer season max and min Temperature at six stations

Variable	TMP	p-value	Sen's slope	Z-Value	Minimum	Maximum	Mean	Std. deviation
Chira	TMPmin	<0.0001	0.024	**-2.989**	9.682	12.858	12.118	0.708
	TMPmax	0.086	0.019	0.674	20.60	24.200	21.921	0.712
Dedo	TMPmin	0.011	0.030	**-3.055**	5.833	15.542	11.728	1.528
	TMPmax	0.006	0.082	0.728	19.94	25.692	22.242	1.634
Gedo	TMPmin	<0.0001	0.105	**-2.412**	5.688	14.585	9.627	1.681
	TMPmax	0.023	0.056	**3.354**	17.92	24.255	20.036	1.432
Limugenet	TMPmin	0.017	0.011	**-2.638**	13.18	14.672	14.184	0.373
	TMPmax	0.006	0.017	0.116	21.54	25.625	24.525	0.659
Sekoru	TMPmin	0.074	0.021	-0.780	11.95	14.681	13.351	0.617
	TMPmax	<0.0001	0.035	**2.983**	22.43	24.772	23.744	0.548
Yayaaottana	TMPmin	1.000	0.000	-0.503	13.61	16.077	14.983	0.518
	TMPmax	0.023	0.024	**3.521**	25.68	28.511	26.912	0.619

Based on the Mann Kendall trend test, the projections of mean Belg season temperatures based on the evaluated SSP2-4.5 and SSP5-8.5 emission scenario indicate a significant upward trend in the basin across the two future time periods as shown in Table 4.11.

Table4.11. Results of Mann-Kendall trend test for spring season projected mean Temperature

	P-Value	Sen's Slope	Z-Value
RCP4.5_2020-2045	**0.00478**	-3.812	**2.87884**
RCP4.5_2046-2071	**0.000213**	-1.003	**2.17463**
RCP8.5_2020-2045	**0.0000019**	-4.5392	**3.63512**
RCP8.5_2046-2071	**0.0000017**	-0.2642	**3.33932**

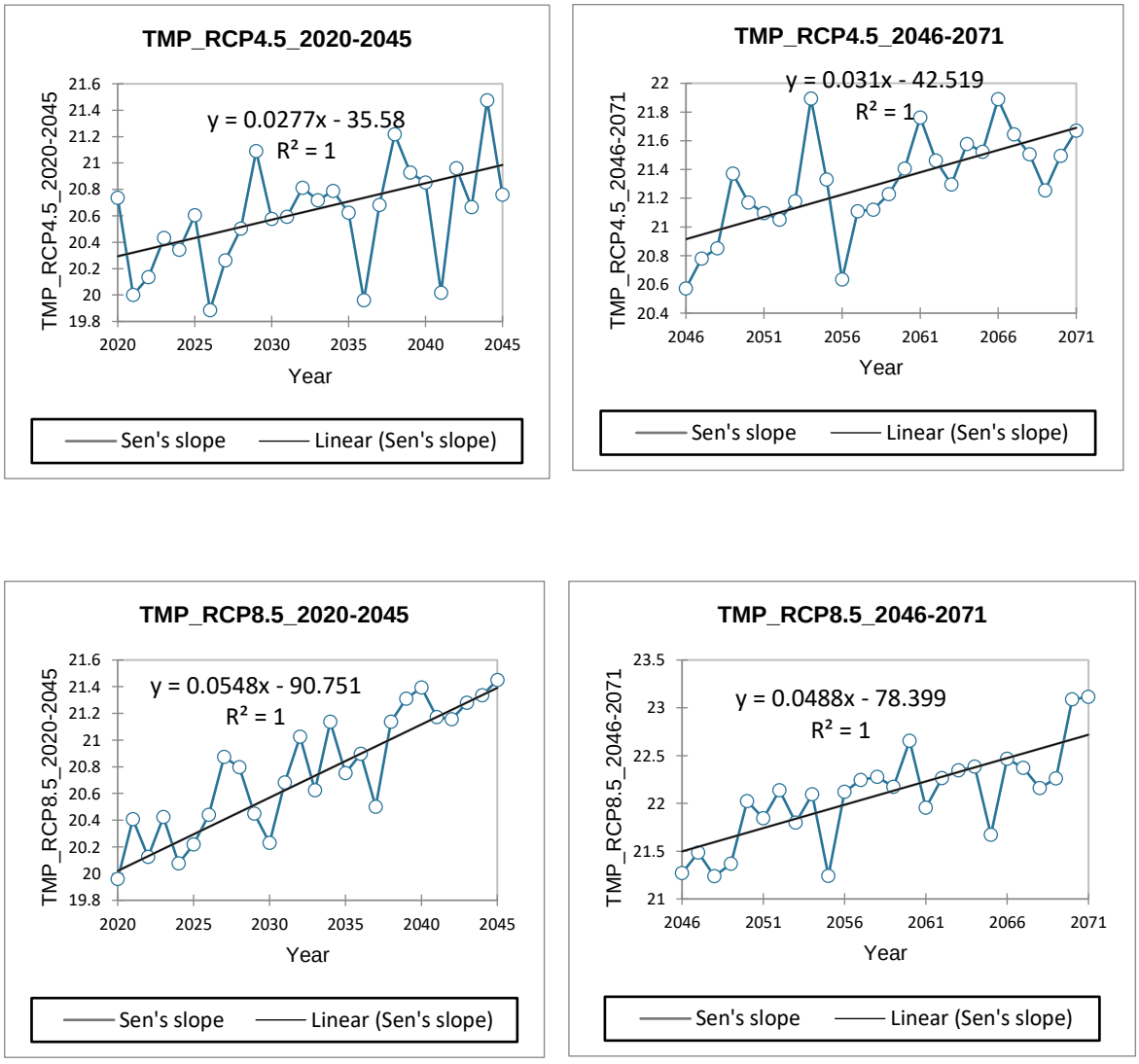

Figure 4.20. Spring season projected mean Belg season temperature trends under SSP2-4.5 and SSP5-8.5 for two future study periods (2020-2070) using a Mann Kendall test

Based on the Mann Kendall trend test, the projections of mean Kiremt season temperatures based on the evaluated SSP2-4.5 and SSP5-8.5 emission scenario indicate a significant upward trend in the basin across the two future time periods as shown in Figure4.21.

Table4.12. Results of Mann-Kendall trend test for summer season projected mean Temperature

	P-Value	Sen's Slope	Z-Value
RCP4.5_2020-2045	**0.00202**	5.1	**2.93008**
RCP4.5_2046-2071	**0.00416**	1.1	**2.20512**
RCP8.5_2020-2045	**0.00005**	2.4	**3.5941**
RCP8.5_2046-2071	**0.00003**	5.2	**3.31906**

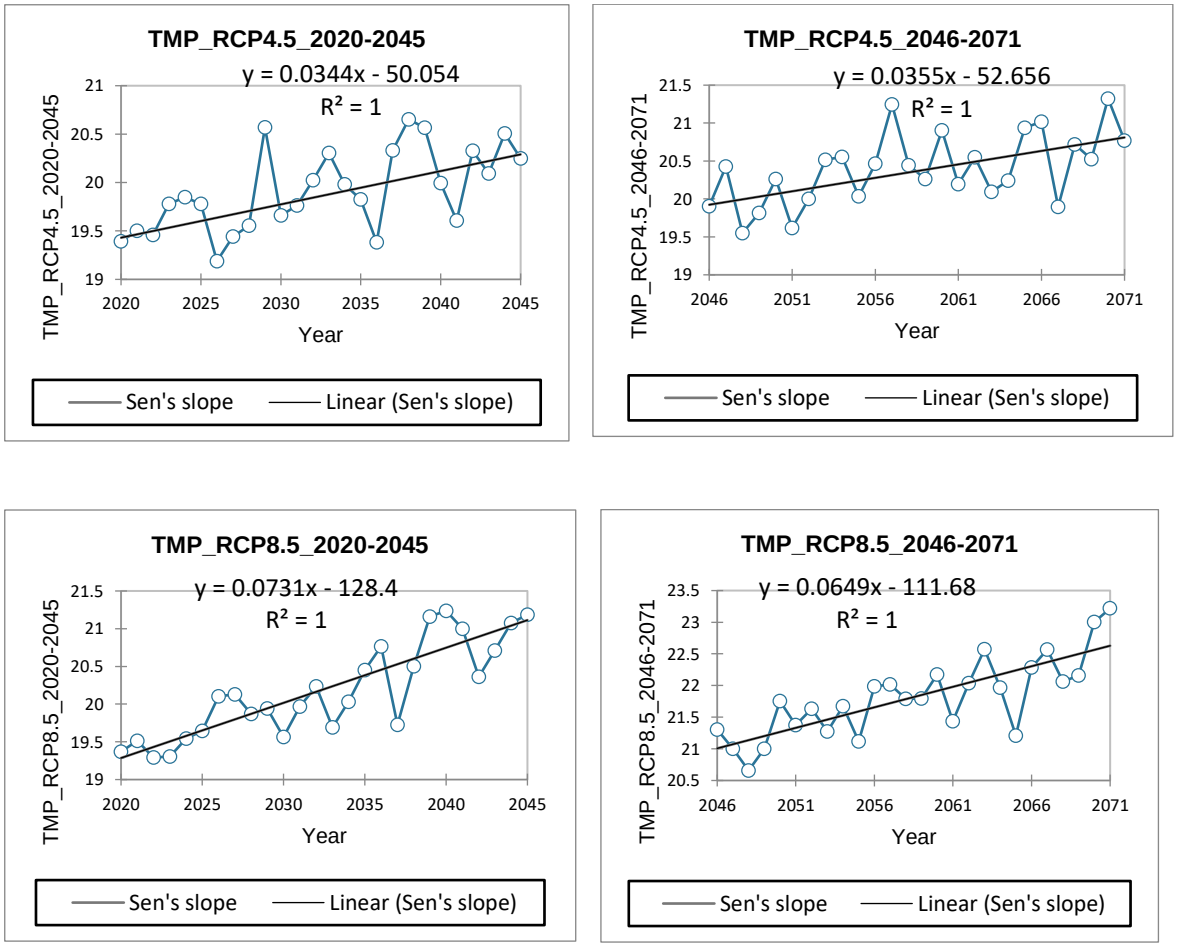

Figure 4.21. Summer season projected mean summer season temperature trends under SSP2-4.5 and SSP5-8.5 for two future study periods (2020-2071) using a Mann Kendall test

4.6. Impacts of Climate Change on Streamflow

4.6.1. Sensitivity Analysis, Calibration and Validation of the SWAT Model

The Rainfall-Runoff modelling was conducted using SWAT model. Firstly, the performance the model was evaluated by using hydrograph comparison at Abelti gauge station through calibration and validation. Calibration and validation aimed at the water balance and overall shape agreement of the observed discharge was determined using NSE and R^2. Flow calibration and validation conducted at a single location called Abelti gauge station due to lack of reliable upstream data were done by using hydro metrological data of 2000-2013 and 2014-2019 respectively and two years was kept as the warm up period. Model warm up period is important it is because of there is no information in the hydrologic model and the model was calibrated and validated using sensitive parameter response to streamflow amount and streamflow relevant parameters.

4.6.1.1. Sensitivity Analysis of Streamflow Parameters

The sensitivity analysis method combines Latin-Hypercube and One-factor-At-a-Time (LH OAT) sampling to provide a global sensitivity analysis for a large number of parameters with a small number of models runs. SWAT comprises 26 parameters for stream flow, however only seven parameters were chosen to have an impact on controlling the hydrological processes in the upper Omo river basin. The most sensitive SWAT hydrological model parameters that influence streamflow of upper Omo river basin and used in Calibration were; plant uptake compensation factor (EPCO), soil evaporation compensation factor (ESCO), threshold depth of water in the shallow aquifer required for return flow to occur (GWQMN), Ground water delay (GW_DELAY), maximum canopy storage (CANMX), SCS runoff curve number (CN2) and base flow alpha factor (ALPHA_BF). (Table 4.5)

The results of sensitivity Analysis determined that the most sensitive parameters were with base flow alpha factor (ALPHA_BF) with t-value of 7.68 and p-value of 0.00, SCS runoff curve number (CN2) with t-value of 2.85 and p-value of 0.01 and maximum canopy storage (CANMX) with t-value of 1.81 and p-value of 0.08. But, plant uptake compensation factor (EPCO) was the least sensitive parameter with t-value of 0.17 and p-value of 0.86. As a result, the findings were consistent with earlier study (Etefa et al. 2022) and were used as a basis for further calibration.

Table 4.13. List of Streamflow Parameters Name, Fitted value and Allowable range for Calibration and Validation

No	Parameter Name	Fitted Value	Range	t-value	p-value	Rank of Sensitivity
1	R__CN2.mgt	60.69	35-98	2.85	0.01	2
2	V__ALPHA_BF.gw	0.034	0-1	7.68	0.00	1
3	V__GW_DELAY.gw	35.41	0-500	1.40	0.17	4
4	V__GWQMN.gw	899	0-5000	-0.73	0.47	5
5	V__CANMX.hru	68.15	0-100	1.81	0.08	3
6	V__ESCO.bsn	0.69	0-1	0.62	0.54	6
7	R__EPCO.bsn	0.14	0-1	0.17	0.86	7

4.6.1.2. Flow Calibration at Abelti Gauge Station

Flow Calibration was done by using the observed daily Rainfall, daily Temperature and observed flow at Abelti gauging station. On monthly basis, **NSE=0.71** and **R^2=0.79** was obtained. (Table 4.6) These values demonstrate that the model has a very good capability to simulate the observed flow for both low flow and high flow periods.

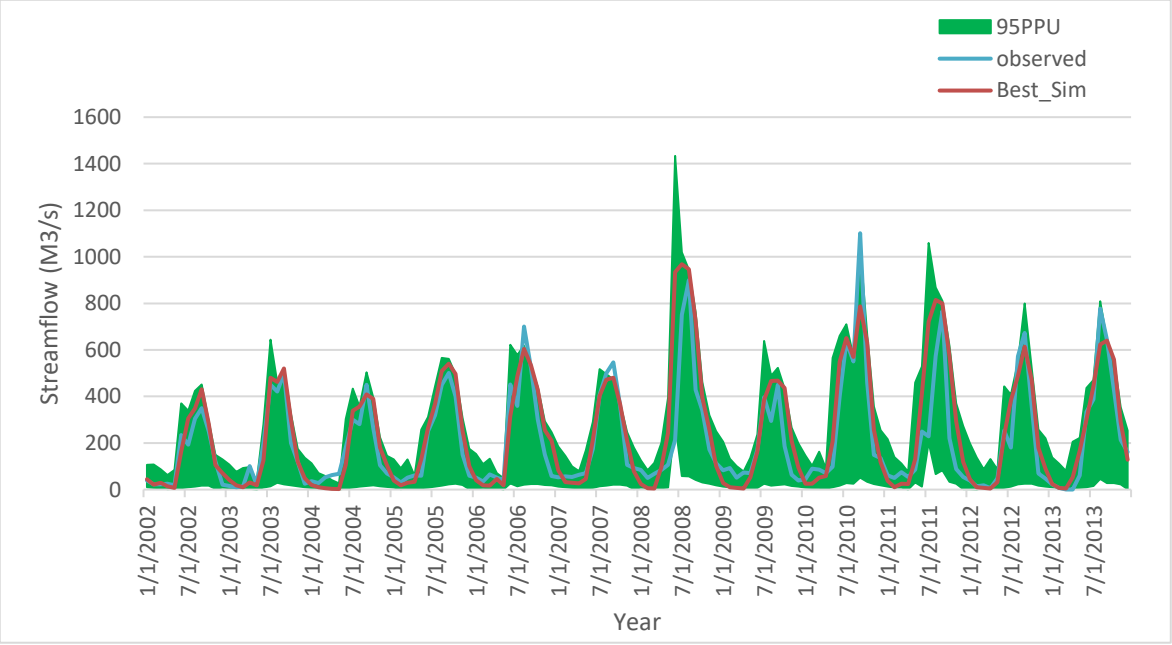

Figure 4.22. Hydrograph of the Model Calibration and Uncertainty Analysis Monthly Streamflow at Abelti Gauge Station.

4.6.1.3 Flow Validation at Abelti Gauge Station

Flow Validation was done by using the same efficiency evaluation techniques during flow calibration were implemented. On monthly basis, observed flow comparison against simulated flow resulted with a **NSE=0.85** and **R^2=0.86**. (Table 4.6)

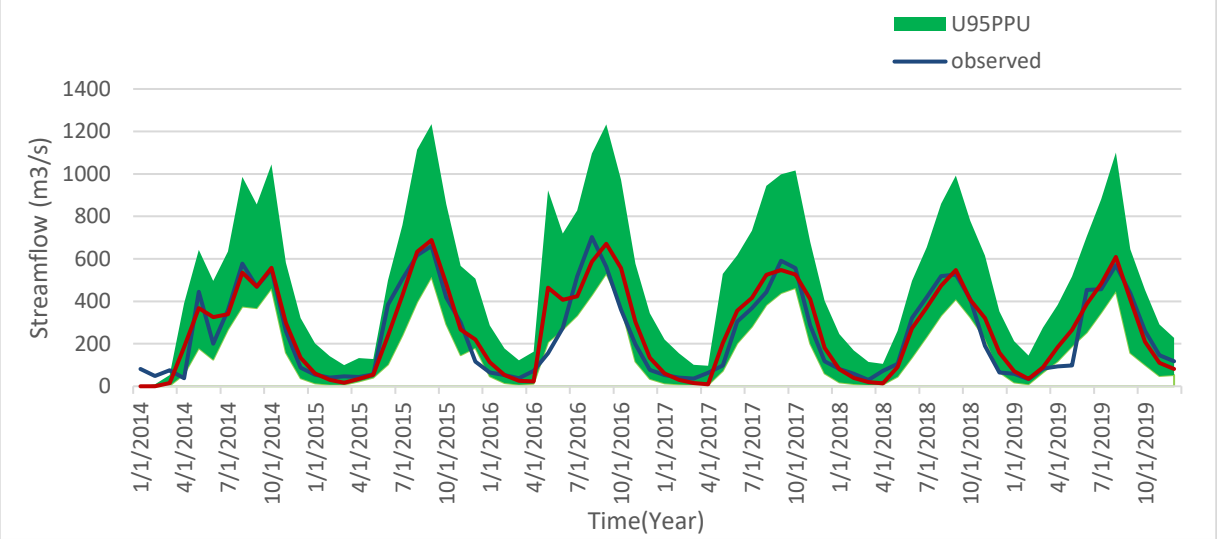

Figure 4.23. Hydrograph of the Model Validation and Uncertainty Analysis Monthly Streamflow at Abelti Gauge Station

Generally, the calibration and validation results show good shape agreement between the observed and simulated flow at Abelti gauge station.

Table 4.14. Model performance assessment and statistical measures of criteria

Performance	NSE	R^2
Very Good	0.75<NSE<1	0.75<R^2<1
Good	0.65<NSE<0.75	0.65<R^2<0.75
Satisfactory	0.5<NSE<0.65	0.5<R^2<0.65
Unsatisfactory	NSE<0.5	R^2<0.5

Source (Moriasi et al. 2015)

Table 4.15. Statistical Performance Indicators of Model Calibration and Validation

	R^2	NSE	Performance
Calibration (2000-2013)	0.79	0.71	Good
Validation (2014-2019)	0.86	0.85	Very Good

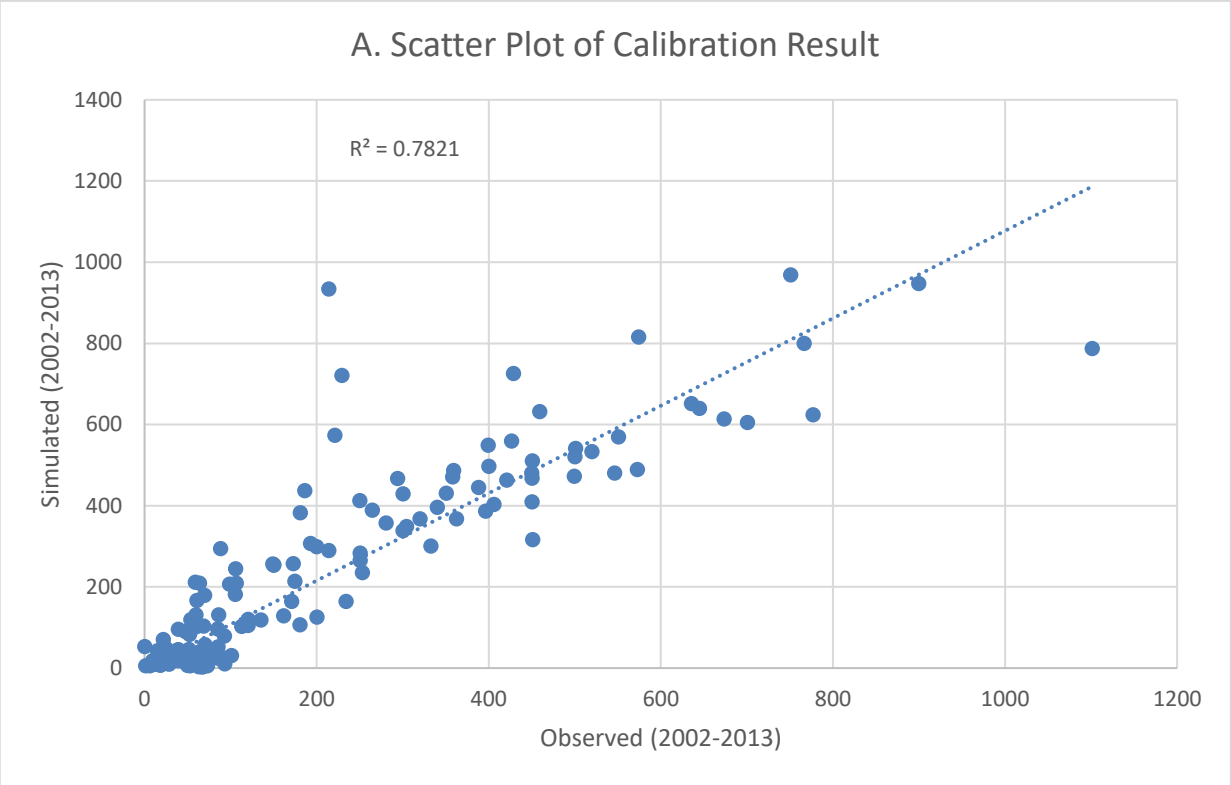

Figure 4.24. Scatter Plot of Calibration Result

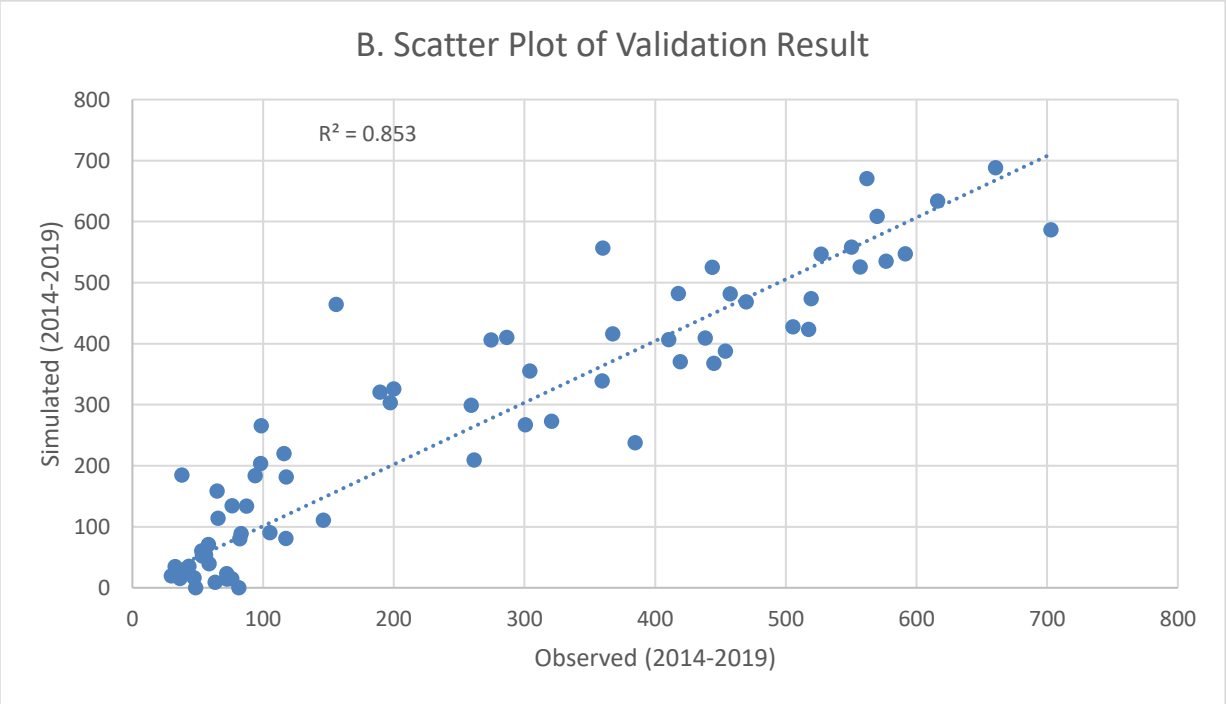

Figure 4.25. Scatter Plot of Validation Result

4.6.2. Impacts of Climate Change on Future Annual, Monthly and Seasonal Streamflow

The impacts of climate change on Annual, Monthly and Seasonal basis of streamflow data was analyzed. The results for the analysis were determined in this section. Changes in streamflow magnitude due to the future impacts of precipitation and temperature were predicted. Therefore, if change in any one of these characteristics is observed, there is a wide probability that the streamflow volume may change. Assessed mean annual, total annual, monthly mean and seasonal mean streamflow under SSP2-4.5 and SSP5-8.5 emission scenarios showed a significant reduction in the future for all study periods (2020-2045 and 2046-2071) compared to the baseline period (2002-2019).

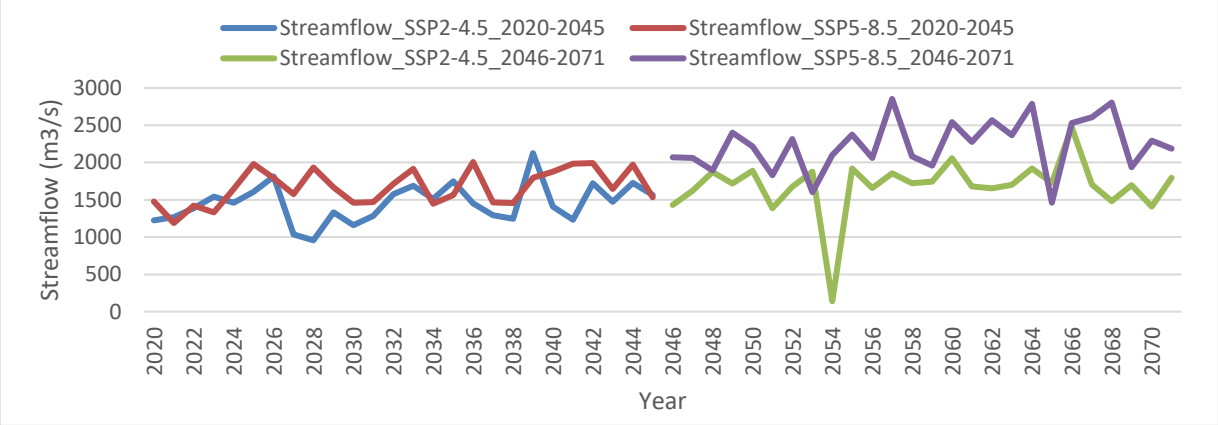

Figure 4.26. Projected annual streamflow change under SSP5-8.5 and SSP2-4.5 emission scenarios over (2020–2071).

Precipitation, minimum and maximum temperature were the climate change drivers considered for the impact assessment. The annual and seasonal streamflow of the river basin is projected to be the lowest for 2020-2045 compared to midterm (2046-2071). Decrease in annual and seasonal streamflow is a result of increase in temperature and decrease in precipitation during hot and dry seasons for two future study periods relative to baseline period. Predicted monthly average streamflow change during rainy season (summer and irregular rain) decreases range from 43.68-52.65% under the SSP2-4.5 emission scenarios in mid and near future respectively, while 26.91–45.36 % under the SSP5-8.5 emission scenarios in mid and near future respectively. Predicted monthly average streamflow change during the dry season (autumn and winter) decrease range 45.61–55.58% under the SSP2-4.5 scenario in mid and near future respectively and 29.87–39.75% under the SSP5-8.5 emission scenarios in mid and near future respectively. (Figure 4.29 and Figure 4.30)

Table 4.16. Annual Streamflow projected

Years	Simulated Average Annual Streamflow in (m3/s)	Annual Mean Streamflow Percentage Change (%)
PR_ Baseline period 1985-2019	249.979	
PR_SSP2-4.5_2020-2045	121.301	-51.47%
PR_SSP2-4.5_2046-2071	145.379	-43.82%
PR_SSP5-8.5_2020-2045	138.811	-44.47%
PR_SSP5-8.5_2046-2071	186.435	-25.42%

Table 4.17. Seasonal Streamflow Projected

Years	Dry Season Mean Monthly Streamflow (m3/s)	Dry Season Mean Monthly Streamflow Percentage Change (%)	Rainy Season Mean Monthly Streamflow (m3/s)	Rainy Season Mean Monthly Streamflow Percentage Change (%)
PR_ Baseline period 1985-2019	213.9		478.7	
PR_SSP2-4.5_2020-2045	95.01	-55.58%	226.6	-52.65%
PR_SSP2-4.5_2046-2071	116.3	-45.61%	269.6	-43.68%
PR_SSP5-8.5_2020-2045	128.8	-39.75%	261.6	-45.36%
PR_SSP5-8.5_2046-2071	150.1	-29.87%	349.9	-26.91%

According to the SSP2-4.5 emission scenarios predicted the highest monthly average streamflow decrease by 145.4 m3/s in mid future (2046-2071) and 121.3m3/s in near future (2020-2045), while under SSP5-8.5 emission scenarios the highest monthly average streamflow decreases to be 186.4 m3/s in mid future and 138.8 m3/s in near future compared to reference period (2000-2019) (Table 4.16).

In 2020, the SSP2-4.5 scenario showed a monthly mean streamflow significant decrease in all months except February and March, It decreases up to 62.3%. And also, it shows a

significant increase in two months up to 25.47%. On the same fashion SSP5-8.5 scenario shows a monthly significant decrease up to 55.17% in all months except February and percentage increment up to 19.37% in February.

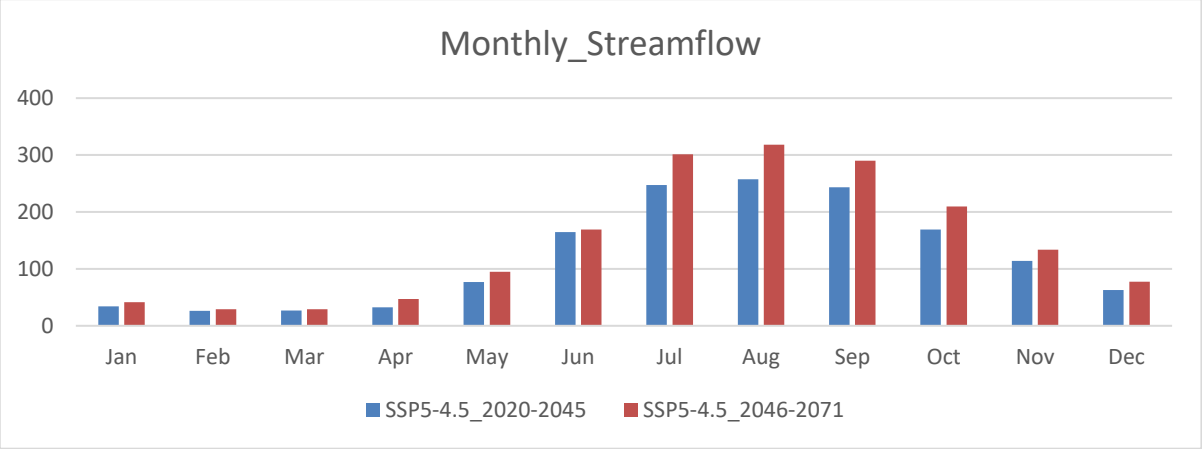

Figure.4.27. Projected monthly streamflow change under SSP2-4.5 emission scenarios over (2020–2071).

In 2046, the SSP2-4.5 scenario showed a monthly mean Streamflow significant decrease up to 53.24% in all months except in February and March and monthly mean precipitation significant increase reach up to 41.36% in Feb. And also, SSP5-8.5 scenario shows a monthly significant decrease up to 37.23% in different months except in Jan, Feb and Mar and percentage increment up to 59.85% in Jan, Feb and Mar.

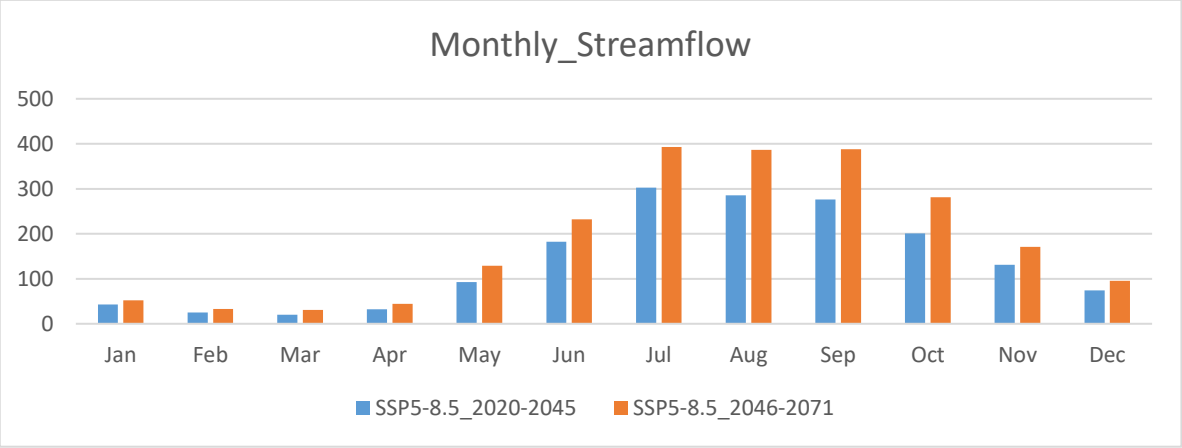

Figure.4.28. Projected monthly streamflow change under SSP5-8.5 emission scenarios over (2020–2071).

In general, for near term the annual streamflow decrease significantly by 51.47% and 44.47% for SSP2-4.5 and SSP5-8.5 respectively. For midterm the annual precipitation decrease significantly by 41.84% and 25.42% for SSP2-4.5 and SSP5-8.5 respectively.

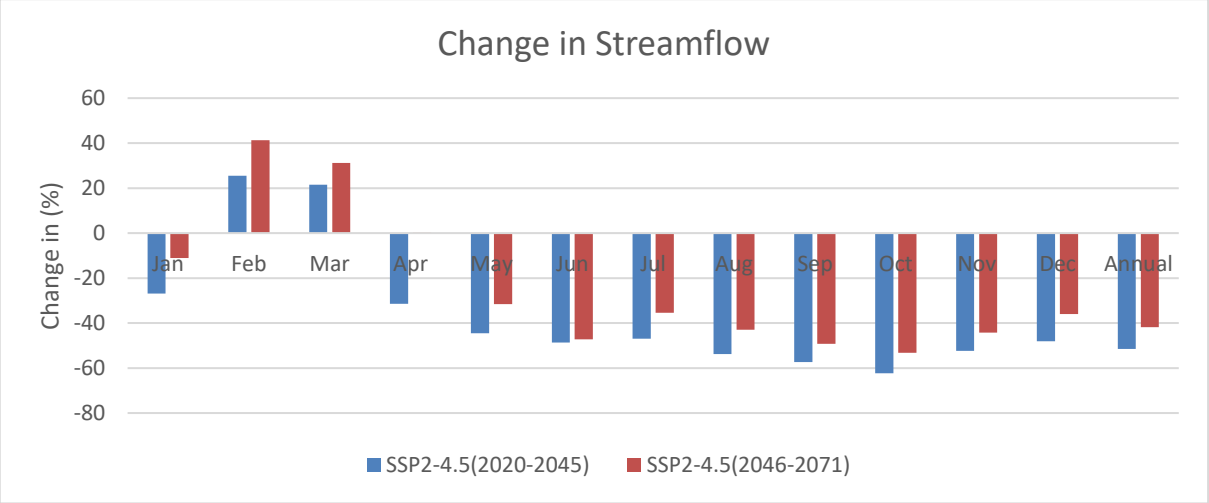

Figure 4.29. Mean monthly Streamflow change under SSP2-4.5 scenario

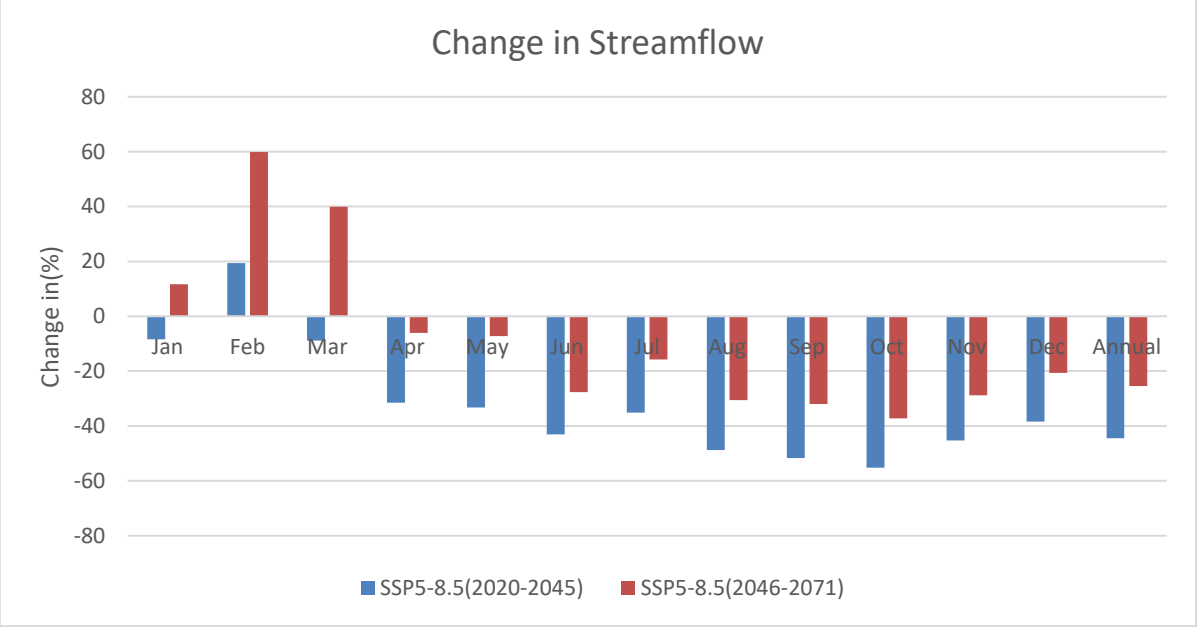

Figure 4.30. Mean monthly Streamflow change under SSP5-8.5 scenario

The results of this research determined that the streamflow in the river basin will decrease in the future. The previous studies that supports this research's results are determined below; As (Wudeneh et al. 2021) stated that an increase in Temperature and decrease in Precipitation will lead to a decrease in Streamflow that, shows there is an interaction between

climate change and streamflow change. The streamflow projections indicate large (seasonal, long-term mean and extreme) streamflow decreases for all major rivers in Ethiopia and increases in the equatorial parts of the region.(Hirpa et al. 2019) Streamflow change is highly dependent on precipitation change, as precipitation increases streamflow will also increase for both SSP2-4.5 and SSP5-8.5 scenario. (Abdulahi et al. 2022)

The reduction of annual average streamflow is highly dependent on climate change variables (temperature and precipitation). As annual average temperature increases, the rate of evapotranspiration increases. The rate of evaporation increases because there is a higher amount of energy available to convert liquid water to water vapor and transpiration increases because at warmer temperature plants open up their stomata and release more water vapor, which lowers soil moisture content and can reduce runoff ratios. That means less rain will make it to the streams and there will be less streamflow for the same amount of precipitation. As annual precipitation decreases, the amount of rain will be decreased. When rainfall is less, less water will be drained in to surrounding streams and rivers and it will lead to slow runoff causing the volume of water in a river channel to decrease.

The reduction of streamflow in rainy season is lower than that of dry season for both SSP2-4.5 and SSP5-8.5 in near and mid future it's because of precipitation is expected to be higher (high RF) in rainy seasons so that higher precipitation will lead to high amount of flow of streams and low amount of reduction of streamflow. On the other hand, in dry seasons the amount of precipitation will be lower so it will lead to decrement in flow of streams and rivers. The previous study investigated by (Wudeneh et al. 2021) supports this result. The reduction of streamflow is indirectly related with temperature amount, as temperature increases the magnitude of streamflow will be decreased this is because of the increment of temperature will lead to dry environment. So, dry seasons or dry environment will lead to the decrement of flow of streams. According to the results mentioned above, the combined effects of rising temperatures and falling precipitation will have an impact on streamflow. The results of this investigation show that streamflow is extremely responsive to temperature and precipitation.

5. Summary and Conclusion

5.1 Summary

This study predicted the potential impacts of climate change on streamflow in the Upper Omo river basin. The study used statistically downscaled and bias corrected ensemble mean of five GCM precipitation, maximum temperature and minimum temperature for Upper Omo river basin under SSP2-4.5 and SSP5-8.5 were used for near(2020-2045) and mid(2046-2071) future and fed them in to the validated SWAT model to simulate future changes in streamflow due to change of climate. The Mann Kendall trend test was used to determine whether a change is statistically significant and to detect trends of the baseline line period and future periods of projected temperature, and precipitation.

The results of the trend test revealed significant decreasing trends in the baseline and projected annual and seasonal (Kiremt and Belg) precipitation. The results of the trend test revealed statistically significant positive increasing trends in the baseline and projected annual and seasonal (summer and spring) maximum and minimum temperatures.

The future precipitation projection did not manifest the same increase or decrease all over the time horizons. However, future projection has shown considerable change. Annual precipitation amounts were projected under SSP2-4.5 and SSP5-8.5 emission scenarios for two future study periods. The trend test results for projected annual precipitation under SSP2-4.5 and SSP5-8.5 emission scenarios for near study period show a significantly decreasing trend and an increasing trend for mid future. The average annual precipitation over the study area is projected to decrease by 3.6 and 4.5% under SSP2-4.5 and SSP5-8.5 scenarios, respectively, for the period of 2020–2045. Similarly, for the period of 2046–2071, the average annual precipitation is projected to increase by 0.6 and 13.3% under SSP2-4.5 and SSP5-8.5 scenarios, respectively.

Projected annual minimum and maximum temperatures under SSP5-8.5 and SSP2-4.5 emission scenarios, shows a significant increasing trends in the river basin over three future periods. The projected annual average minimum temperature under SSP2-4.5 emission scenarios increases the range between 1.2-1.9 ^{o}c while under SSP5-8.5 emission scenarios increase the range between 1.3-3.09 ^{o}c. Also, the projected change in annual average maximum temperature under SSP2-4.5 emission scenarios increases the range between 0.3-1.43^{o}c while under SSP5-8.5 emission scenarios increase the range between 0.86-2.3^{o}c.

Temperature change under SSP5-8.5 emission scenarios is larger and more severe than under SSP2-4.5 emission scenarios, according to this study. This indicates that SSP5-8.5 has the largest carbon emission scenario compared to SSP2-4.5. The findings of this investigation corroborated those of a prior study (IPCC, 2014).

The result of hydrological model calibration and validation indicates that the SWAT model simulates the streamflow considerably good for the study area. The model performance criterion which is used to evaluate the model result indicates that the NSE and R^2 are 0.71, 0.79 and 0.85, 0.86 during calibration and validation period respectively.

Assessed annual mean, total annual, monthly mean and seasonal mean streamflow under SSP2-4.5 and SSP5-8.5 emission scenarios showed a reduction in the future for all study periods (2020-2045 and 2046-2071). The annual and seasonal streamflow of the river basin is projected to be the lowest for 2020-2045 compared to midterm (2046-2071). According to the SSP2-4.5 emission scenarios predicted the highest monthly average streamflow decrease by 145.4 m3/s in mid future (2046-2071) and 121.3m3/s in near future (2020-2045), while under SSP5-8.5 emission scenarios the highest monthly average streamflow decreases to be 186.4 m3/s in mid future and 138.8 m3/s in near future. Predicted annual average streamflow change decrease range 43.82–51.47% under the SSP2-4.5 emission scenarios in mid and near future respectively, while under the SSP5-8.5 emission scenarios decrease range 25.42–44.47% in mid and near future respectively.

The reduction of annual average streamflow is highly dependent on climate change variables (temperature and precipitation). As annual average temperature increases, the rate of evapotranspiration increases. The rate of evaporation increases because there is a higher amount of energy available to convert liquid water to water vapor and transpiration increases because at warmer temperature plants open up their stomata and release more water vapor, which lowers soil moisture content and can reduce runoff ratios. That means less rain will make it to the streams and there will be less streamflow for the same amount of precipitation. And also, as temperatures rise, glaciers and snowpack are melting earlier in the year, leading to reduced streamflow. As annual precipitation decreases, the amount of rain will be decreased. When rainfall is less, less water will be drained in to surrounding streams and rivers and it will lead to slow runoff causing the volume of water in a river channel to decrease.

The impacts of climate change on streamflow are multifaceted, affecting water availability, ecological health, and societal well-being. Recognizing these impacts and implementing effective adaptation and mitigation measures are crucial for ensuring the resilience of freshwater systems and minimizing the adverse consequences on both nature and human communities.

5.2 Conclusion

Generally, the projections for future stream flow suggest that both combined scenarios have a significant impact on stream flow. In the Upper Omo river basin, future climate change is the major driver of decreased stream flow. However, despite higher precipitation under the SSP5-8.5 scenario in the mid-future, mean annual stream flow is expected to decrease due to increases in maximum and minimum temperature, which cause more evaporation and infiltration. Therefore, changes in temperature have a significant impact on stream flow. The results of the simulations indicate that climate change can be effective in reducing future water-related risks in the Upper Omo river basin. By considering future changes in the regional hydrological cycle, these measures can be helpful for regional decision-makers and other stakeholders in effectively planning and managing soil and water resources.

5.3 Recommendation

Depending on the results of the study the following recommendation were given:

- This study was done in insufficient availability of data on the upper Omo basin, which reduces the accuracy of the results developed. Hence the results of this study should be taken as a starting point for further studies especially on upper Omo river basin.
- The result of this study is based on only five GCMs and two emission scenarios. However, it is often recommended to apply different GCMs and emission scenarios so as to make comparison between different models as well as to explore a wide range of climate change scenarios that would result in different hydrological impacts. Hence this work should be extended in the future by including different GCMs and emission scenario.
- The impact of climate change on stream flow was assessed in this study, implying that land use or land cover will remain the same in the future. Regardless, land use or land cover in the basin is changing as a result of natural and human activities. So, further studies are recommended that include both climate and land use/land cover change.

- This study shows there will be a decrease in the availability of water for streamflow; hence, mitigation strategies, adaptation measures, and management options should be developed to reduce this impact, including improved water management strategies and increased investment in climate-resilient infrastructure.
- Ensure efficient management of reservoirs to maximize water availability. Consider adopting advanced water management techniques such as demand forecasting, real-time monitoring, and adaptive release policies. This can help balance water supply and environmental requirements.

Reference

Abdo, K. S., B. M. Fiseha, T. H.M. Rientjes, A. S.M. Gieske, and A. T. Haile. 2009. "Assessment of Climate Change Impacts on the Hydrology of Gilgel Abay Catchment in Lake Tana Basin, Ethiopia." Hydrological Processes 23 (26): 3661–69. https://doi.org/10.1002/hyp.7363.

Abdulahi, Salih Duri, Brook Abate, Arus Edo Harka, and Sead Burhan Husen. 2022. "Response of Climate Change Impact on Streamflow: The Case of the Upper Awash Sub-Basin, Ethiopia." Journal of Water and Climate Change 13 (2): 607–28. https://doi.org/10.2166/wcc.2021.251.

Adams, Richard M. 2014. "CLIMATE CHANGE AND WATER RESOURCES : POTENTIAL IMPACTS AND CLIMATE CHANGE AND WATER RESOURCES : POTENTIAL IMPACTS AND IMPLICATIONS by Professor , Department of Agricultural and Resource Economics Oregon State University Corvallis , OR 97331 and Dannele E," no. January 2006.

Akoko, George, Tu Hoang Le, Takashi Gomi, and Tasuku Kato. 2021. "A Review of SWAT Model Application in Africa."

Anh, Quan Tran, and Kenji Taniguchi. 2018. "Coupling Dynamical and Statistical Downscaling for High-Resolution Rainfall Forecasting : Case Study of the Red River."

Atinafu, Dereje. 2015. "SURFACE WATER POTENTIAL ASSESSMENT AND DEMAND SCEINARIO ANALYSIS IN OMO GIBE RIVER BASIN Addis Ababa University," 100.

Bishaw, Yemsrach. 2012. "Evaluation of Climate Change Impact on Omo-Gibe Basin, Ethiopia."

Brekke, Levi D., Julie E. Kiang, J. Rolf Olsen, Roger S. Pulwarty, David A. Raff, D. Phil Turnipseed, Robert S. Webb, and Kathleen D. White. 2009. "Climate Change and Water Resources Management: A Federal Perspective." US Geological Survey Circular, no. 1331: 1–76. https://doi.org/10.3133/cir1331.

Brooks, Nick, Simon Anderson, Jessica Ayers, Ian Burton, and Ian Tellam. 2011. IIED Working Paper: Tracking Adaptation and Measuring Development. Change.

Burn, Donald H., Omar I. Abdul Aziz, and Alain Pietroniro. 2004. "A Comparison of Trends in Hydrological Variables for Two Watersheds in the Mackenzie River Basin." Canadian Water Resources Journal 29 (4): 283–98. https://doi.org/10.4296/cwrj283.

Chen, Jie, Franois P. Brissette, Annie Poulin, and Robert Leconte. 2011. "Overall Uncertainty Study of the Hydrological Impacts of Climate Change for a Canadian Watershed." Water Resources Research 47 (12): 1–16. https://doi.org/10.1029/2011WR010602.

Copernicus. 2019. "What Is Bias Correction ?," 1.

Dai, Aiguo. 2011. "Characteristics and Trends in Various Forms of the Palmer Drought Severity Index during 1900-2008." Journal of Geophysical Research Atmospheres 116 (12). https://doi.org/10.1029/2010JD015541.

Das, Biswajit, Sanjay Jain, Surjeet Singh, and Praveen Thakur. 2019. "Evaluation of Multisite Performance of SWAT Model in the Gomti River." Applied Water Science 9 (5): 1–10. https://doi.org/10.1007/s13201-019-1013-x.

Desalegn Jaweso, Brook Abate, Andreas Bauwe and Bernd Lennartz. 2019. "Hydro-Meteorological Trends in the Upper Omo-Ghibe River Basin, Ethiopia," 1–18.

Emiru, Nega Chalie, John Walker Recha, Julian R Thompson, Abrham Belay, Ermias Aynekulu, Alen Manyevere, Teferi D Demissie, et al. 2022. "Impact of Climate Change on the Hydrology of the Upper Awash River Basin , Ethiopia."

Eromo, Shiferaw, Chaemiso Adane, Abebe Santosh, and Murlidhar Pingale. 2016. "Assessment of the Impact of Climate Change on Surface Hydrological Processes Using SWAT : A Case Study of Omo-Gibe River Basin , Ethiopia." Modeling Earth Systems and Environment 2 (4): 1–15. https://doi.org/10.1007/s40808-016-0257-9.

Ganasri, B P. 2015. “A Review on Hydrological Models ENGINEERING (ICWRCOE 2015) A Review on Hydrological Models,” no. December. https://doi.org/10.1016/j.aqpro.2015.02.126.

Goosse, Hugues. 2019. “Description of the Climate System and Its Components.” Climate System Dynamics and Modelling, no. 2007: 1–29. https://doi.org/10.1017/cbo9781316018682.002.

Hargreaves, George H., and Richard G. Allen. 2003. “History and Evaluation of Hargreaves Evapotranspiration Equation.” Journal of Irrigation and Drainage Engineering 129 (1): 53–63. https://doi.org/10.1061/(asce)0733-9437(2003)129:1(53).

Hewitson, Bruce, and Robert G Crane. 1996. “Climate Downscaling : Techniques and Application,” no. January 2014. https://doi.org/10.3354/cr007085.

Hirpa, Feyera A, Lorenzo Alfieri, Thomas Lees, Jian Peng, Ellen Dyer, and Simon J Dadson. 2019. “Streamflow Response to Climate Change in the Greater Horn of Africa,” 341–63.

Jain, Sharad K. 2012. “Downscaling Methods in Climate Change Studies,” 1–18.

Jarraud, M., and A. Steiner. 2012. Summary for Policymakers. Managing the Risks of Extreme Events and Disasters to Advance Climate Change Adaptation: Special Report of the Intergovernmental Panel on Climate Change. Vol. 9781107025. https://doi.org/10.1017/CBO9781139177245.003.

Jaweso, Dessalegn, Brook Abate, Andreas Bauwe, and Bernd Lennartz. 2019. “Hydro-Meteorological Trends in the Upper Omo-Ghibe River Basin, Ethiopia.” Water (Switzerland) 11 (9): 1–18. https://doi.org/10.3390/w11091951.

Jena, Pravat, Sarita Azad, and Madhavan Nair Rajeevan. 2015. “Statistical Selection of the Optimum Models in the CMIP5 Dataset for Climate Change Projections of Indian Monsoon Rainfall,” 858–75. https://doi.org/10.3390/cli3040858.

Jha, Manoj, Jeffrey G. Arnold, Philip W. Gassman, Filippo Giorgi, and Roy R. Gu. 2006. "Climate Change Sensitivity Assessment on Upper Mississippi River Basin Streamflows Using SWAT." Journal of the American Water Resources Association 42 (4): 997–1015. https://doi.org/10.1111/j.1752-1688.2006.tb04510.x.

Kang, Bo-seong, Sung-kee Yang, and Myung-soo Kang. 2019. "A Comparative Analysis of the Accuracy of Areal Precipitation According to the Rainfall Analysis Method of Mountainous Streams" 28 (October): 841–49.

Kassie, Menale, Moti Jaleta, and Alessandra Mattei. 2014. "Evaluating the Impact of Improved Maize Varieties on Food Security in Rural Tanzania: Evidence from a Continuous Treatment Approach." Food Security 6 (2): 217–30. https://doi.org/10.1007/s12571-014-0332-x.

Kattsov, Vladimir, Russian Federation, Chris Reason, South Africa, Alessandro Anav Uk, Timothy Andrews Uk, Johanna Baehr, et al. 2013. "Evaluation of Climate Models." Climate Change 2013 the Physical Science Basis: Working Group I Contribution to the Fifth Assessment Report of the Intergovernmental Panel on Climate Change 9781107057: 741–866. https://doi.org/10.1017/CBO9781107415324.020.

Kidmose, J., J. C. Refsgaard, L. Troldborg, L. P. Seaby, and M. M. Escrivà. 2013. "Climate Change Impact on Groundwater Levels: Ensemble Modelling of Extreme Values." Hydrology and Earth System Sciences 17 (4): 1619–34. https://doi.org/10.5194/hess-17-1619-2013.

Knutti, Reto, and Gabriele C. Hegerl. 2008. "The Equilibrium Sensitivity of the Earth's Temperature to Radiation Changes." Nature Geoscience 1 (11): 735–43. https://doi.org/10.1038/ngeo337.

Kumar, Rohitashw, and Harender Raj Gautam. 2014. "Climate Change and Its Impact on Agricultural Productivity in India." Journal of Climatology & Weather Forecasting 2 (1): 1–4. https://doi.org/10.4172/2332-2594.1000109.

Lai, Ang Ting, I. Ching Lin, Yu Wen Yang, and Mei Feng Wu. 2012. “Climate Change and Human Health.” Journal of Internal Medicine of Taiwan 23 (5): 343–50. https://doi.org/10.6314/JIMT.2012.23(5).05.

Lenderink, van Ulden, van den Hurk, and Keller. 2007. “A Study on Combining Global and Regional Climate Model Results for Generating Climate Scenarios of Temperature and Precipitation for the Netherlands.” Climate Dynamics 29 (2–3): 157–76. https://doi.org/10.1007/s00382-007-0227-z.

Masamba, Musiba. 2018. “The Role of Models in Climate Change Studies,” no. April.

Melkamu, Teshome Ayana, Wagesho Amencho Negash, and Kemal Mohammed Abdella. 2017. “Assessment of the Impacts of Climate Change on Gibe-III Reservoir Using Reliability, Resilience and Vulnerability (RRV) Indices.” Scientific & Engineering Research 8 (10): 1606–28.

Mendelsohn, Robert. 2007. “Measuring Climate Impacts with Cross-Sectional Analysis.” Climatic Change 81 (1): 1–7. https://doi.org/10.1007/s10584-005-9007-0.

Miller, Paul, and Thomas C. Piechota. 2008. “Regional Analysis of Trend and Step Changes Observed in Hydroclimatic Variables around the Colorado River Basin.” Journal of Hydrometeorology 9 (5): 1020–34. https://doi.org/10.1175/2008JHM988.1.

Moriasi, D. N., M. W. Gitau, N. Pai, and P. Daggupati. 2015. “Hydrologic and Water Quality Models: Performance Measures and Evaluation Criteria.” Transactions of the ASABE 58 (6): 1763–85. https://doi.org/10.13031/trans.58.10715.

Muluneh, Alemayehu, Chamo Sub-basins View, and James Hutton. 2019. “Stream Flow Response to Climate Change on Tikur Wuha Catchment, Rift Valley of Ethiopia.” Journal of Environment and Earth Science, no. August 2019. https://doi.org/10.7176/jees/9-8-01.

Panhalkar, S S. 2014. “Hydrological Modeling Using SWAT Model and Geoinformatic Techniques.” THE EGYPTIAN JOURNAL OF REMOTE SENSING AND SPACE. https://doi.org/10.1016/j.ejrs.2014.03.001.

Priestely, C. H. B., and R. J. Taylor. 1972. “On the Assessment of Surface Heat Flux and Evaporation Using Large-Scale Parameters.” Monthly Weather Review 100 (2): 81–92. https://doi.org/10.1175/1520-0493(1972)100<0081:otaosh>2.3.co;2.

Qian, Yun, and Yongxin Zhang. 2006. “2: Regional Climate Models.”

R.J. STOUFFER, V. EYRING, G.A. MEEHL, S.BONY, C. SENIOR, B. STEVENS, AND K.E. TAYLOR. 2017. “CMIP5 SCIENTIFIC GAPS AND RECOMMENDATIONS FOR CMIP6,” no. January: 95–105. https://doi.org/10.1175/BAMS-D-15-00013.1.

Rathjens, Hendrik, Katrin Bieger, Raghavan Srinivasan, and Jeffrey G Arnold. 2016. “CMhyd User Manual Documentation for Preparing Simulated Climate Change Data for Hydrologic Impact Studies,” p.16p.

Richard Jones, David Hassell, Debbie Hudson, Simon Wilson, Geoff Jenkins and John Mitchell. 2003. “Climate Change Scenarios,” no. December.

NEITSCH, ARNOLD, KINIRY, WILLIAMS. 2005. “SOIL AND WATER ASSESSMENT TOOL DOCUMENTATION.”

NEITSCH, ARNOLD, KINIRY, WILLIAMS et.al. 2002. “Soil and Water Assessment Tool Theoretical Documentation” 13 (04): 52–55. https://doi.org/10.1055/s-0029-1192096.

Schnarr, Sylwia Trzaska and Emilie. 2014. “A REVIEW OF DOWNSCALING METHODS FOR CLIMATE CHANGE PROJECTIONS,” no. September.

Shang, H., J. Yan, M. Gebremichael, and S. M. Ayalew. 2011. “Trend Analysis of Extreme Precipitation in the Northwestern Highlands of Ethiopia with a Case Study of Debre Markos.” Hydrology and Earth System Sciences 15 (6): 1937–44. https://doi.org/10.5194/hess-15-1937-2011.

Singh, Vijay P. 2018. “Hydrologic Modeling: Progress and Future Directions.” Geoscience Letters 5 (1). https://doi.org/10.1186/s40562-018-0113-z.

Stocker, Thomas. 2011. “Introduction to Climate Modelling.” Advances in Geophysical and Environmental Mechanics and Mathematics, 1–170.

Sun, Jinqiu, Haofang Yan, and Zhenxin Bao. 2022. “Investigating Impacts of Climate Change on Runoff from the Qinhuai River by Using the SWAT Model and CMIP6 Scenarios.”

carter, Leemans, Lal, Whetton. 2015. “Climate Scenario Development.”

Tadesse, Etefa Tilahun and Minda. 2022. “Most Sensitive Parameters of Soil and Water Assessment Tool (SWAT) Hydrological Model : A Review,” 4–9. https://doi.org/10.33552/AOMB.2022.03.000558.

Teshome, Helen, Kindie Tesfaye, Nigussie Dechassa, Tamado Tana, and Matthew Huber. 2022. “Analysis of Past and Projected Trends of Rainfall and Temperature Parameters in Eastern and Western Hararghe Zones, Ethiopia.” Atmosphere 13 (1). https://doi.org/10.3390/atmos13010067.

Tigabu, Tibebe B., Paul D. Wagner, Georg Hörmann, Jens Kiesel, and Nicola Fohrer. 2021. “Climate Change Impacts on the Water and Groundwater Resources of the Lake Tana Basin, Ethiopia.” Journal of Water and Climate Change 12 (5): 1544–63. https://doi.org/10.2166/wcc.2020.126.

Trenberth, Kevin E. 2012. “Framing the Way to Relate Climate Extremes to Climate Change.” Climatic Change 115 (2): 283–90. https://doi.org/10.1007/s10584-012-0441-5.

Trzaska, S, and E Schnarr. 2014. “A Review of Downscaling Methods for Climate Change Projections.” United States Agency for International Development by Tetra Tech ARD, no. September: 1–42.

United Nations Development Program, United Nations Economic Commission for Africa, African Development Bank and African Union. 2022. “2020 Africa Sustainable Development Report: Towards Recovery and Sustainable Development in the Decade of Action,” 116. https://www.undp.org/sites/g/files/zskgke326/files/migration/africa/RBA---ASDR-2020---updated---03032022.pdf.

WaleWorqlul, Abeyou, Yihun Dile Taddele, Essayas Kaba Ayana, Jaehak Jeong, Anwar Assefa Adem, and Thomas Gerik. 2018. “Impact of Climate Change on Streamflow Hydrology in Headwater Catchments of the Upper Blue Nile Basin, Ethiopia.” Water (Switzerland) 10 (2). https://doi.org/10.3390/w10020120.

Walthall, Charles L., Christoper J. CJ Anderson, Lance Baumgard H., Eugene Es Takle, Lois Wright-Morton, J Hatfield, P Backlund, et al. 2013. “Climate Change and Agriculture in the United States: Effects and Adaptation.” USDA Technical Bulletin 1935 1: 186 pages.

Williams, Paul D. 2009. “Rapid Climate Change: An Overview for Economists.” International Journal of Green Economics 3 (1): 63–76. https://doi.org/10.1504/IJGE.2009.026492.

Wu, Jia, Zhenyu Han, Rouke Li, Ying Xu, and Ying Shi. 2021. “Changes of Extreme Climate Events and Related Risk Exposures in Huang-Huai-Hai River Basin under 1.5–2°C Global Warming Targets Based on High Resolution Combined Dynamical and Statistical Downscaling Dataset.” International Journal of Climatology 41 (2): 1383–1401. https://doi.org/10.1002/joc.6820.

Wudeneh Temesgen, Alemsged Tamiru and Tom Rientjes. 2021. “Impact of Climate Change on the Stream Fl Ow of the Arjo-Didessa Catchment under RCP Scenarios Wudeneh Temesgen Bekele, Alemseged Tamiru Haile and Tom Rientjes,” 2325–37. https://doi.org/10.2166/wcc.2021.307.

Zeman, Christian, and Christoph Schär. 2021. “An Ensemble-Based Statistical Methodology to Detect Differences in Weather and Climate Model Executables,” no. September: 1–29.

APENDICES

Appendix Figure 1: Observed and Simulated Mean Monthly Hydrograph during Calibration Period

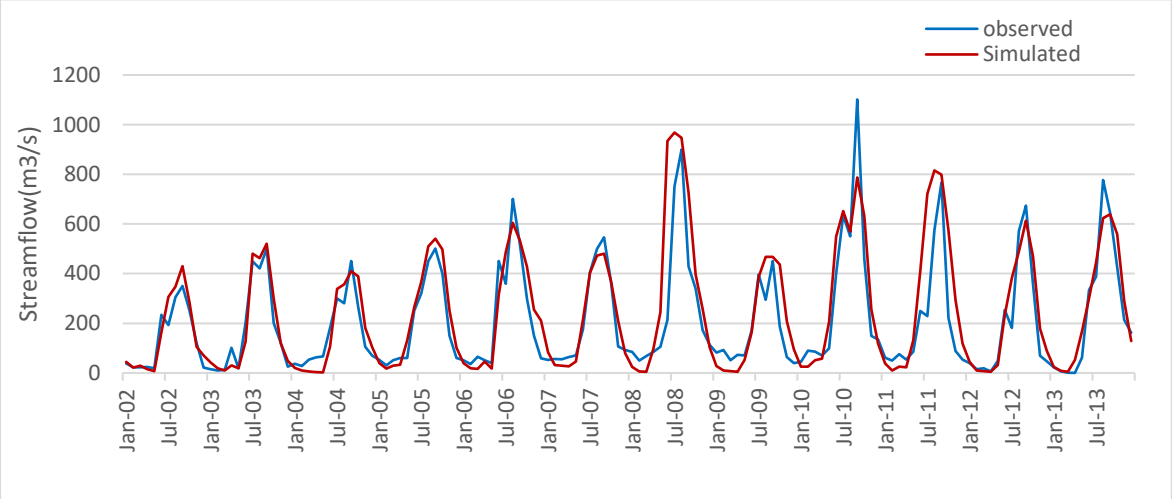

Appendix Figure 2: Observed and Simulated Mean Monthly Hydrograph during Validation Period